STABILITY ASSESSMENT OF MAN-MADE SLOPES A CASE STUDY IN YEN BAI

TRAN THE VIET
MAR, 2011

SUPERVISORS:
Dr. D. Alkema
Dr. H.R.G.K. Hack

ADVISOR:
Ms. Nguyen Thi Hai Van

SLOPE STABILITY ASSESSMENT OF MAN-MADE SLOPES A CASE STUDY IN YEN BAI

TRAN THE VIET

Enschede, The Netherlands, 03, 2011

Thesis submitted to the Faculty of Geo-Information Science and Earth Observation of the University of Twente in partial fulfilment of the requirements for the degree of Master of Science in Geo-information Science and Earth Observation.
Specialization: Applied Earth Sciences

SUPERVISORS:
Dr. D. Alkema
Dr. H.R.G.K. Hack

THESIS ASSESSMENT BOARD:
Prof. Dr. V.G. Jetten (Chair)
Dr. L.P.H. van Beek (External Examiner, Department of Physical Geography, Utrecht University)

ABSTRACT

Man-made slope failures which have caused more and more serious losses and damages to people and properties are one of major concerns in most of urbanized mountainous areas in Vietnam. In those regions, excavation of hill slopes has been seen very common to create space for building and road construction.

Yen Bai city, a case study area located in northern Vietnam, is now undergoing a rapid urbanization. Most slopes have been excavated with limited studies by the local citizens. The cuts made are often very steep (65^0 to 75^0), with the dimensions of 15-20 m width and 10-20 m height. Those slopes are therefore at high risk of failure to the entities nearby the slopes.

The main purpose of this research is to evaluate the future stability of man-made slopes under the influence of weathering processes in tropical region, specifically in Yen Bai city. Three slopes were selected for the investigation, which are satisfied the flowing criteria: field work accessibility, different ages (2, 25 and 31 years), similar geotechnical and groundwater conditions (all three are parts of the same hill, formed on Ngoi Chi formation), identical slope aspect (North-West) and land cover (plantation with 50% coverage, mix of acacia and bushes). To approach the main purpose, two types of analyses were used: 1) Assessing the differences in several relevant geo-mechanical and hydrological soil properties among selected slopes of different ages, and 2) Assessing the consequences of these differences on the stability of these slopes using deterministic slope stability methods. GEO-STUDIO 2004 v6.22 was the main software used for slope stability analysis. In addition to available data (topography, geology, rainfall), field observation, field tests and laboratory tests were carried out in order to collect necessary data for the research.

The results show that: 1) The soil profiles of three selected slopes are composed of residual soil on top (0.9 - 1.2 m) and completely weathered layer underneath (3.5 – 4.5 m), which are similar to soil profiles in other tropical hills; 2) The physico-mechanical and engineering properties of the soil are changed over soil depth and lifetime of the slope; 3) In the relationship with the age of cut-slopes, the shear strength of soil in those slopes is gradually decreased, while the effective internal friction is inversely proportional to time; 4) Factor of safety (FoS) reaches a critical value of 1 when cut-slopes with angle of 65^0 is 52 years old, those of 70^0 are 48 years old and those of 75^0 are 44 years old; 5) When the rain intensity is higher than the saturated hydraulic conductivity of the top soil, the rainfall duration will be the main effect to the FoS values of the slope; (6) The main causes of man-made slope failures are combination of nature (weathering, cracking) and human activities (load surcharge on top, excavation of slope-side).

The final conclusion is drawn that: located in the tropical climate region, strongly influenced by weathering process, all man-made slopes with angles of $65\text{-}75^0$ will be sooner or later failed. Thus, more attention on thorough studies on cut-slopes, and strict regulations for excavating slopes and constructing houses must be required.

ACKNOWLEDGEMENTS

There are many people I am deeply indebted for their help and assistance throughout my study. First of all, I would like to give my sincere thanks to ITC for the funding and facilities that enable my study. I thank very much Dr. Trinh Minh Thu and Dr. Le Thi Chau Ha from Hanoi Water Resources University for giving me the opportunity to study at ITC; I would like to express my sincere gratitude to my supervisors Dr. Dinand Alkema and Dr. Robert Hack for their scientific guidance. I am also very grateful to Prof. Victor Jetten, Dr. David Rosister, and Dr. Mark van der Meijde for their useful instruction within and outside of this research. I also express my thanks to my advisor Nguyen Thi Hai Van for sharing her research and many valuable data. I greatly appreciate GITHRA project for supporting me all necessary field equipment. I would like to give many thanks to Dr. Le Quoc Hung and his colleagues from the Vietnam Institute of Geosciences and Mineral Resources, to the local authorities and people of Yen Bai city for their assistance and provision of important information during my field work. I am thankful to Mr. Pham Huy Dung for assisting me with soil sample tests at WRU's laboratory. I will never forget all nice moments with my Vietnamese friends, thanks for sharing all the experience, knowledge, fun, together dinners, coffee, lunch and other breaks. Many thanks give to my classmates at the Applied Earth Science course: Darwin, Haydar, Stef, etc. I enjoyed the good time for studying with you at ITC. Finally, I give special thanks to my family for never-ending support.
And many others I cannot name here…

Thank all of you for everything!

TABLE OF CONTENTS

LIST OF FIGURES

LIST OF TABLES

1. INTRODUCTION

1.1. Background

Over the last two decades, Vietnam has been endangered by a large number of landslides which have caused severe losses and damages to people and assets at the mountain foot (Tran. & Shaw., 2007; Few & Tran, 2010) . Investigations by Doan (2004), Nguyen (2009), and Saint-Macary et al. (2010) have shown that most landslides are the results of combination between hydro-meteorological phenomena (typhoon, heavy rains) and human activities (cultivation, urbanization, road widening, etc.)

Yen Bai is a young city which is experiencing a rapid urbanization. Many new highways are being built and widened to serve for the demand of the economy. As many benefits can be received from living close to main roads. These days, more and more people try to settle along road-sides for living and doing businesses (Figure 1-1). To do so, most families from other regions with hand tools cut deep into the foot-hills with arbitrary slope angles just to have sufficient area for their houses. And soon, these roads become busy business streets that rest in front of the hills and run along the roads. However, in these houses, majority citizens only care about their front site that facing the road but not the side behind. The cuts made were often very steep (65^0 to 75^0), with the dimension of 15m to 20m depth and 15m height. Thus, in a random way, many slopes that stand vertically with high risk of failure have been created.

Situated in the North of Vietnam, Yen Bai is influenced by tropical climate with high temperatures and humidity around the year. It is one of the areas that have highest average annual rainfall in Vietnam (nearly 2500 mm). This is a perfect environment for weathering. In addition, the city also suffers strongly from ancient tectonic activities, with the formation and existence of the Northwest – Southeast and Northeast-Southwest fault systems; the rocks that lie on this tectonic zone are under a great influence of physical and chemical weathering processes (Doan, 2004). Therefore the soils are loose, crinkle, and crumble (Figure 1-2) which is a good condition for the development of landslides in the rainy seasons (Doan, 2004). Thus, excavating a slope without considering the influence of future weathering in combination with other critical conditions is dangerous. This explains why every year in this area especially in rainy seasons, the records of damage due to slope failures become longer and longer. Hence, a study on the change of the physical and mechanical parameters of cut slope's material subjected to time and the weather influences and its consequences on the stability of slope is necessary. This would help engineers to evaluate the stability of present slopes as well as to prevent failures that may occur in the future.

Figure 1-1: Slope cuts to create space in Yen Bai

Figure 1-2: Weathering productions of rocks in Yen Bai

1.2. The problem statement

Yen Bai city is characterized by hilly topography formed by tropical residual soils. The research site is dominated by rocks in Ngoi Chi formation: (AR-nc1) and (AR-nc2). According to the study of Doan (2004) and Nguyen (2009), the final weathering productions of these formations are soils that are loose, crinkle and crumble with a high content of clay. With a thickness of the weathering crust ranging from 3m to 10m, when the rocks and indurated soils degrade over time into that final production, this would become a good environment to develop slope failure especially when they are cut steeply or subjected to critical condition such as heavy rain. Experiences in Yen Bai also show that, most slope failures recorded occurred in the top soil layers where the soils are totally weathered as a result of steep slope cuts.

In the study area, most man-made slopes are cut spontaneously by citizens themselves to create space for settling and housing. The aim to have a land for living is more important than the new formed slope behind. Therefore the slope angles were chosen by experience, without using any standards or precise calculations and most of them are likely to be too steep. These slopes may stand stably at the present but since the weathering processes still have influence on the slope's material, failures can happen at any time.

Most of slopes in Yen Bai are covered by tropical residual soil; the water table is expected to be deep under the surface. Hence the upper soil layers are in unsaturated state. Negative pore water pressures are believed to play an important role in increasing the stability of unsaturated slopes. However, due to the lack of knowledge and equipment while dealing with unsaturated soils, all present calculations of slope stability are based on the theory of saturated soil mechanics. It gives overdesigned and thus costly designs.

A study must be done for a clearly understanding about the degradation of geotechnical characteristics as well as the unsaturated behaviour of tropical soils and rocks on cut slopes (man- made slopes) in the study area especially along heavily weathered steep cut slopes.

1.3. Research objective

The general objective of this study is to evaluate the future stability of man-made slopes under the influence of weathering processes in tropical region. In specific, it studies how the engineering characteristics of soil and rock evolve subjected to time and how these changes influence the stability of on selected man-made slopes in the study area. The research objective is arranged into several sub-objectives as follow:

1.3.1. Specific objective 1

To evaluate the influence of weathering on the physico-mechanical properties of soils and rocks on the selected slopes subjected to time. This objective is further divided into several sub-objectives:

- Getting to know some main engineering characteristics of soils and rocks in tropical region
- Find out the influence of weathering on the changing of soil and rock characteristics in general and to the soil and rock shear strength in specific and from that predict the future decay of the weathered soil masses.
- Assess the stability of man-made slopes in the research site and define the relationship between the factors of safety subjected to time.

1.3.2. Specific objective 2

To assess the stability of a selected man-made slope for various rainfall scenarios:

- Based on the collected data about rainfall in the studied area to find some rainfall events in the past that resulted in severe landslides. The needed data is the rainfall intensity and duration
- Assess the stability of slopes under these critical conditions.

1.3.3. Specific objective 3

To propose designed recommendations and stabilized methodologies for the stability of man-made slopes in the study area

1.4. Research questions

These following research questions are defined to meet these above objectives:

1.4.1. For specific objective 1

- What do the soil profiles of the selected slope look like?
- How significant does the weathering processes affect physico-mechanical properties and engineering properties of soil on the selected slope in the study area? How can they be quantified? Which parameter being influenced the most?
- What is the relationship between the shear strength of soil and rock in the study area subjected to time? What are the factors of safety (FoS) of the study slopes? How do they change subjected to time? When will the study slopes fail down under the same rate of weathering?

1.4.2. For specific objective 2

- What is the critical rainfall in the study area for the current physic-mechanical properties of the slope materials?
- What are the values of FoS when the influence of these critical rainfall are taken into account?

1.4.3. For specific objective 3

- What are the main causes that lead to slope failures in the study area?
- What recommendations for slope stabilization can be used?

1.5. Hypothesis

Due to weathering processes, the physio-mechanical properties decay over time which will result eventually in a reduction of the Factor of Safety. In man-made slopes this may result in failure with catastrophic consequences.

1.6. The study area

1.6.1. Geographical location

Located in the transition between the North-western, Viet Bac and Northern midland, Yen Bai city is the capital of Yen Bai province. It lies between latitudes 21^0 40’ to 21^0 46’ North and longitudes 104^0 50’ 08’ to 104^0 58’ 15” East (Figure 1-3). The city is situated at the transition of highlands and midlands in the East of Hoang Lien Mountains with an area of about 108 km^2 (Ha, 2009).

Being a young city that belonged to Yen Bai province, at the present time Yen Bai city has 17 administrative units including 7 wards: Yen Thinh, Yen Ninh, Minh Tan, Nguyen Thai Hoc, Dong Tam, Nguyen Phuc, Hong Ha and 10 communes: Minh Bao, Nam Cuong, Tuy Loc, Tan Thinh, Van Phu, Van Tien, Phuc Loc, Au Lau, Gioi Phien, Hop Minh.

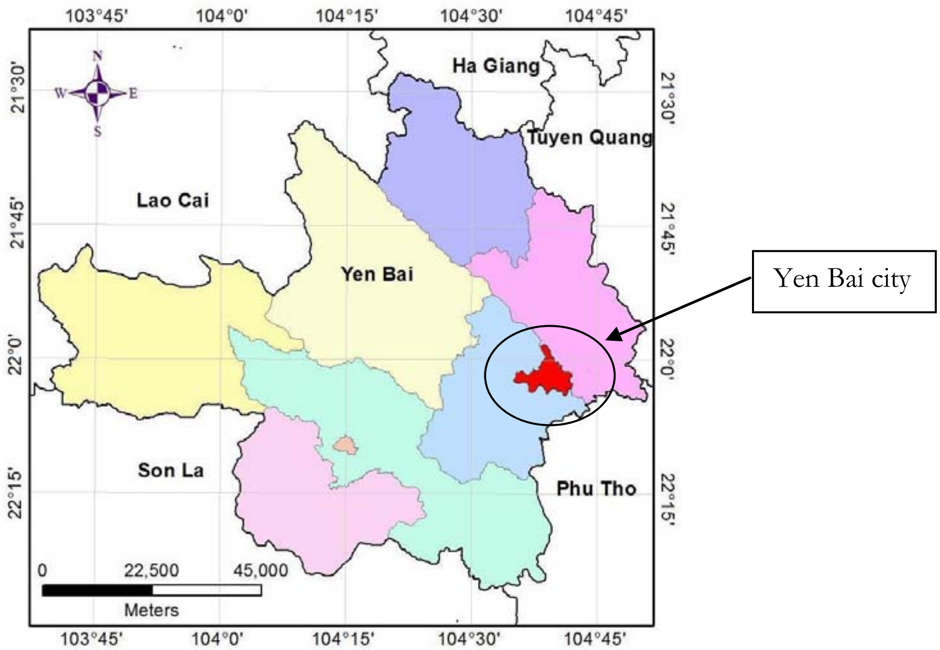

Figure 1-3: The geographical location of Yen Bai city
(Source: Vietnam Institute of Geosciences and Mineral Resources)

1.6.2. Topography

Yen Bai city is located in the low land part of Yen Bai province – Vietnam. According to Vinh et al. (2005), the city's topography is dominated by three types of terrains, see (Figure 1-4).

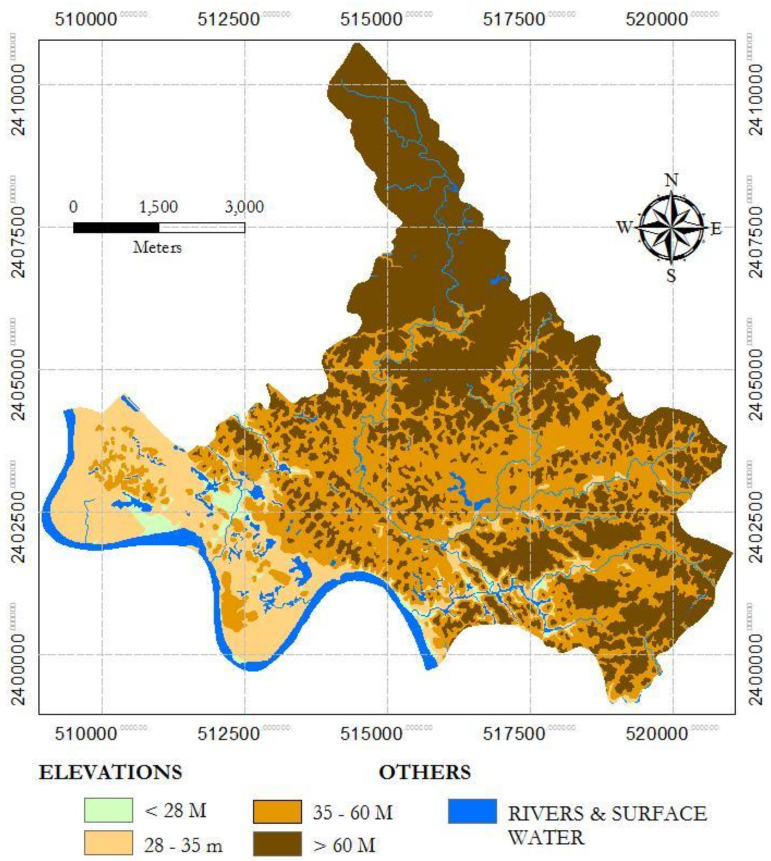

Figure 1- 4: Topological map of Yen Bai City
(Source: Vietnam Institute of Geosciences and Mineral Resources)

1. Hills occupy most part of the city with the average elevation of more than 60m, composed of several ranges of hills and mountains with Northwest-Southeast direction and fairly steep slopes.
2. Valleys distribute alternately among the hilly terrains, prolonging with the stream valleys and having the elevations from 28-35m
3. Alluvial plains and fans consist of a number of fields situated at the hill and mountain bases, along the two sides of the Hong River, with the average elevation of 28-50m

1.6.3. Geology

Figure 1-5 is the geological map within Yen Bai city scale. This map was built based on the raw data from the Vietnamese Institute of Geosciences and Mineral Resources (VIGMR), such as a geological information regions map, a fault map and a river system map. According to The book of Vietnamese Geology – Northern Part by (Truong et al., 1979), the geological map 1/50.000 scale Doan Hung – Yen Binh sheet group by (Hoang & Le, 1997); and the geological map 1/200.000 by (Vinh, et al., 2005). Yen Bai city was formed by the following stratigraphic units, as described in the next section:

1.6.3.1. Strata (Stratum)

QUATERNARY SYSTEM
Distributed along the two banks of Hong River round Thac Ba Lake and in some small stream valleys, it is composed of soft sediments, pebble, granule, clayey sand, and organic materials. This system includes: Upper Pleistocene sediment (aQ_{III}), lower – middle Holocene sediment (aQ_{IV}^{1-2} , aQ_{IV}^{2}), upper Holocene sediment ($aapQ_{IV}^{3}$).

NEOGEN SYSTEM
Distributed along the two sides of the Red River, it is composed of conglomerate, gravel stones, clay-shale, coaly-shale and coal-lenses. Representing for NEOGEN system in Yen Bai city is Co Phuc Formation (N_1^3cp).

ARCHEAN ERATHEM, Song Hong Group (AR-sh)

a. Nui Voi Formation (AR-nv)

In the study area, there is only Allomember 2 ($AR\text{-}nv^2$), it is distributed in the North of the city, along the Northwest – Southeast strike as an anticlinal core in Minh Quan mountain at the elevation of 497m. Its main components including: orthoclase, quartz, plagioclase. Thickness: 540-850m.

b. Ngoi Chi Formation (AR-nc)

This Formation is composed of quartz, silimanite, biotite and garnet. Its strike is commonly Northwest – Southeast, rocks were fold and tectonically strongly broken. Ngoi Chi formation has been classified into two allomembers following upward order: Allomember 1 ($AR\text{-}nc^1$) and Allomember 2 ($AR\text{-}nc^2$).

1.6.3.2. Magma

The intrusive magma formations over the study area are intrusions and vein belt of Cam An (vPR1ca) and Tan Huong (vEth) complex, formed small masses and scattered around the area.

- Cam An Complex: Including phase 1 (vPR1ca) and phase 2 (vPR2ca). This complex composes of plagioclase, pyroxene, brown hornblende, andesine, diopsite, and garnet.
- Tan Huong Complex: Also includes two phases: phase 1(vE1th) and phase 2 (vE2th). Its main mineral components: kali feldspar, plagioclase, biotite, garnet, orthoclase, oligoclase, quatz, garnet, sometimes a little mount of biotite or muscovite.

1.6.3.3. Faults

In this city, there are Northwest – Southeast fault systems, including:

- Red River fault system: This fault dips toward Northeast with the inclined plane are 70^0. The vertical slip is 1.8km – 2.2km, belongs to reverse fault type. The past activities of the Red River fault generated a number of fracture zones and made the rock and soil weathered, very vulnerable to landslides.

- Go Xoan - Go Chua fault systems: Parallel to Hong River fault and together with it forms a boundary between Neogen sediments and Ngoi Chi formation.

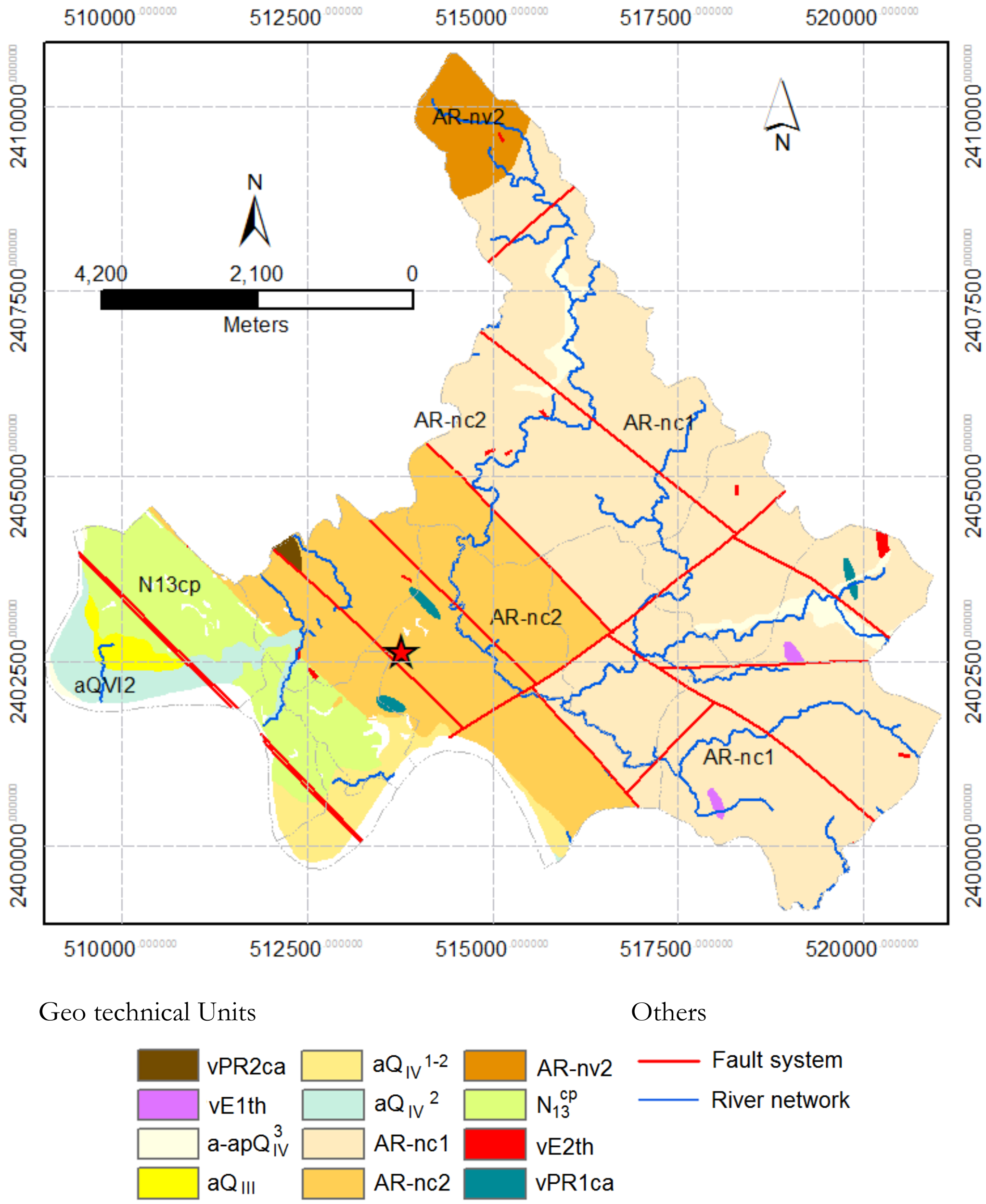

Figure 1-5: Geological map of Yen Bai city

(Source: Vietnam Institute of Geosciences and Mineral Resources)

1.6.4. Meteo – Hydrology

Located in tropical monsoon region, Yen Bai's climate is influenced by the topographical features. Its average temperature is 22^0 – 23^0 C; fluctuating between 20.5^0 and 27.5^0. Rainy season often starts from May until October. This city receives an average from 1.500 mm – 2.200 mm of annual rainfall with the maximum daily rainfall of 349 mm (6 Sep 1973) (Nguyen (manager), 2009). Figure 1.6 shows the average daily rainfall in 12 months of year from 1960 to 2009 in Yen Bai.

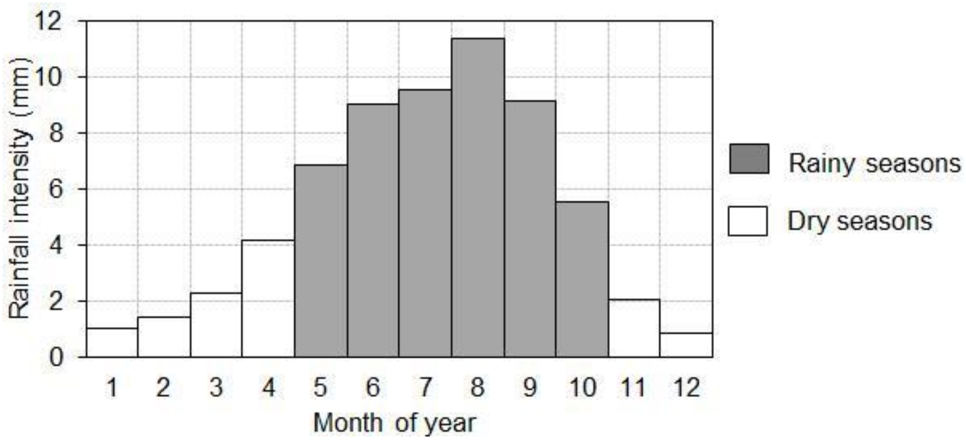

Figure 1-6: The average daily rainfall in 12 months of year from 1960 to 2009 in Yen Bai
(The Hydro Meteorological Data Centre (HMDC)

2. LITERATURE REVIEW

2.1. Introduction

Weathering and especially future weathering after construction of a slope is a main cause for failure of a slope during its engineering life-time (Hack & Price, 1997). In the design of a slope, the future degradation of the rock mass due to weathering is of major importance (Hack, 1998). The problem of infrastructure works that become unsafe with time due to decay of rock and soil masses in artificial and natural slopes is a well-known feature in every part of the world. Some road cuts stand up for a century with sometimes even no apparent loss of safety, whereas some will already show failures during construction. Some will fail after one year, some after ten. The question is: why this difference? (Huisman, 2006).

Making quantitative predictions about the future evolution of natural slopes has a great meaning in engineering practice. Slopes subject to weathering may undergo a series of landslides, occurring at different times, which cause the progressive retrogression of the slope front (Utili, 2004). Rock masses undergo degradation of their geotechnical properties in time due to weathering and erosion. Knowledge of the degradation of the properties, in particular in engineering time, is useful in the design and construction of safe slopes (Chapagain, 2001).
In the first part of this chapter, some basic background about the nature of weathering will be presented, and then an overview of slope stability calculation is given.

2.2. Weathering

2.2.1. Definition of weathering

The definition of weathering has appeared long time ago, and it has been improved over time. Polynov (1937, cited in Ollier, 1969, p. 1) defined weathering as: 'Weathering is the change of rocks from the massive to the clastic state'. This definition is too general and does not clearly show the nature of weathering. Later on, Reiche (1950, cited in Ollier, 1969, p.1) gave out a more detailed one: 'Weathering is the response of materials which were in equilibrium within the lithosphere to conditions at or near its contact with the atmosphere, the hydrosphere, and perhaps still more importantly, the biosphere'. There is no reason to assume that the starting products of weathering were ever in equilibrium with the lithosphere – some rocks may never have attained perfect equilibrium (Abramson et al., 2002). As an improvement of Reiche's definition, according to Ollier (1969): 'Weathering is the breakdown and alteration of materials near the earth surface to products that are more in equilibrium with newly imposed physic-chemical conditions. And closer to the present time, Selby & Hodder (1993), based on the old studies, provided perhaps the most adequate one: 'Weathering is the process of alteration and breakdown of soil and rock materials at and near the earth's surface by physical, chemical and biotic processes', this definition has shown three main factors that contribute to weathering processes including: physics, chemistry and biology. These factors will be mentioned more detailed below:

2.2.2. Types of weathering

As said by Huat, et al. (2004): Weathering consists of chemical weathering operating through chemical decomposition, physical weathering involving physical disintegration and biological weathering caused by chemical or physical changes through the agency of biological organism. The first two processes are quite different as disintegration involves no chemical reactions but these processes often operate simultaneously abetting each other as in the case of the physical disintegration of a larger rock into smaller parts whereby increasing the total surface area and accelerating chemical decomposition (Huat, et al., 2004).

2.2.2.1. Physical weathering

Physical or mechanical weathering is the physical disintegration of a rock into smaller fragments. The different types of physical weathering include frost wedging, exfoliation, thermal expansion and contraction and abrasion (Huat, et al., 2004).

a. Frost wedging: occurs when water freezes and expands in cracks in rocks. The expansion causes the rocks to come apart causing them to break up.
b. Wetting and drying: this is also known as slaking. Slaking occurs when the accumulated layers of water molecules in the mineral grains of a rock due to their increasing thickness push the rock grains apart with great tensional stress.
c. Thermal expansion and contraction: as heating causes rock to expand and cooling results in contraction, the repeated expansion and contraction of different minerals at different rates causes stresses along mineral boundaries leading to breakdown of the rock.
d. Mechanical exfoliation: this happens when the rock breaks into flat sheets along joints that parallel the ground surface as the rock is uncovered. This phenomenon is due to the expansion of rock due to pressure release caused by the removal of overlying rock by erosion. This is also called unloading.
e. Abrasion: this is the physical grinding down of rock fragments. It occurs when two rock surfaces come in contact with mechanical wearing or grinding of their surfaces.

2.2.2.2. Chemical weathering

According to Huat et al. (2004): Chemical weathering involves the chemical dissolution or alteration of the chemical and mineralogical composition of minerals. It involves the breakdown of minerals into new compounds by the action of chemical agents (e.g. acid in the air, in rain, etc.). The rock forming minerals are vulnerable to attack by water, oxygen and carbon dioxide at the new surface environment they are exposed to, and tend to undergo chemical changes to form new stable minerals. Gidigasu (1976, cited in Huat, 2004, p.12) concluded the main sequence of the chemical weathering process is as follows:

a. First, the rock structure is made weaker by the selective attack on the constituent minerals in igneous and metamorphic rocks, by a more general attack on calcareous rocks and by an attack on the cements of some sedimentary rocks.
b. Second, stresses are created within a rock by causing varying expansion of certain minerals.
c. Third, compounds are produced which can be removed in solution, leaving behind residual deposits. These include residual decomposition products e.g. clay minerals.
d. Chemical weathering is dependent on the amount of surface area, temperature and the availability of chemically active fluids. Smaller sized particles weather more rapidly due to a larger surface area. Figure2-1 illustrates how as the particles get smaller, its total surface area available for chemical weathering increases.

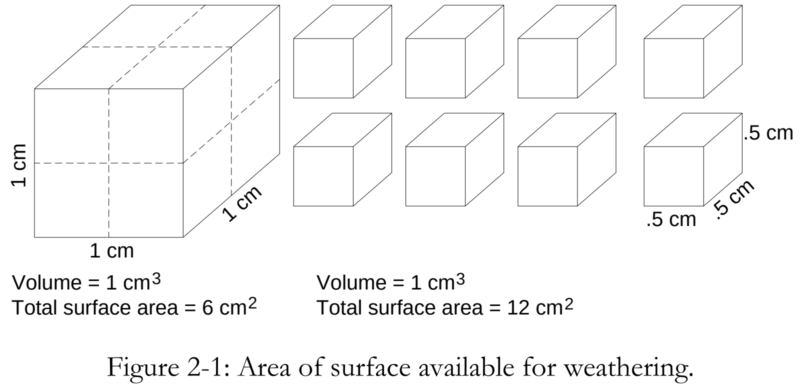

Figure 2-1: Area of surface available for weathering.
(Source: Ritter, 2009)

The presence of water and dissolved materials like ammonia, oxygen, carbonic acid, chlorides, sulphates and other materials cause chemical weathering. An increase in temperature increases the effectiveness of carbonic acid and oxygen as shown, for example, in humid climates where the intensity of the chemical weathering processes increases on account of the higher temperature. The maximum intensity of chemical weathering processes of rocks, consequently, occurs in the tropical regions (Jumikis, 1984). A number of different processes cause chemical weathering. The most common ones are hydrolysis, oxidation, reduction, hydration, carbonation and solution. These processes are described in Table 2-1.

Table 2-1: Common chemical processes

Process	Description
Solution	Decomposition of minerals involving water as a solvent and in rainwater aided by carbonic acid (H_2CO_3) formed due the presence of CO_2.
Oxidation	The combination with oxygen, the most common oxidizing agent, to form oxides and hydroxides or any other reaction which causes the loss of an electron that results in an increase in the positive charge.
Hydration	Hydration involves the absorption of water into the mineral causing the expansion of the mineral leading to eventual weakening.
Hydrolysis	Reaction of water directly with minerals where metal cations, replaced by hydrogen (H^+) ions, combine with hydroxyl (OH^-) ions.
Carbonation	The carbon dioxide (CO_2) dissolves in water to form carbonic acid (H_2CO_3) that reacts with minerals to e.g. dissolve calcite into bicarbonate ions and calcium.
Leaching	This involves the migration of ions by dissolution into water. The mobility of ions depends upon their ionic potential. For example, Ca, Mg, Na, K are easily leached by moving water, Fe is more resistant, Si is difficult to leach while Al is almost immobile

Source: Huat, et al. (2004)

2.2.2.3. Biological weathering

According to the study of (Huat, et al., 2004): biological weathering involves the disintegration of rock by biological organisms which act both as chemical and/or physical agents of weathering. These organisms release acids that react with rocks or mechanically break them up. A wide range of organisms ranging from microorganisms to plants and animals can cause weathering. Some of the more important processes are:

a. Rock fracture because of animal burrowing or the pressure from growing roots.
b. Movement and mixing of materials by movement of soil organisms
c. Carbon dioxide produced by organism respiration mixing with water forming carbonic acid augments simple chemical processes like solution.
d. Organic substances called chelates produced by organisms decompose minerals and rocks by the removal of metallic cations.
e. The moisture regime in soils influenced by organisms induces weathering as water is a necessary component in weathering processes.

2.2.3. Conditions controlling weathering in artificial slopes

According to Bland and Rolls (1998), conditions controlling weathering in artificial slopes fall into three categories:

2.2.3.1. Internal

They are the rock and soil material and mass properties such as porosity, permeability, discontinuities, and material composition. The style and rate of weathering is very much controlled by the porosity and permeability of the rock, which governs the ease with which water can enter and weathering products be removed. Some granular sediment have such a high porosity that practically every mineral grain is exposed to weathering; some massive igneous rocks have no inter-granular porosity at all, and can only weather at the surface and along a few widely spaced joints (Ollier, 1969).

2.2.3.2. External

Parameters related to the weathering environment such as climate, topography, chemistry of weathering solutions, hydrology, and vegetation.

a. Hydrology: Water is vitally concerned in weathering. It is one of the major reactants, the solvent in which many reactions take place, the transporting agent for many weathering products, and by its presence or absence largely controls the separation of oxidizing and reducing conditions (Ollier, 1969).
b. Climate: The chief climatic controls are related to water and temperature. Water involves the total amount of precipitation, intensity of rain, proportion of precipitation that forms run-off, and the precipitation- evaporation ration, amongst others. Temperature involves mean temperature, temperature range, and fluctuations about freezing point amongst others. Many other factors such as cloud cover, relative humidity, drying winds and climatic changeability may also be important locally (Ollier, 1969).

2.2.3.3. Geotechnical

Slope design parameters such as aspect, slope angle, height, method of excavation, and drainage measures.

2.2.4. Classification for weathering profiles

The weathering profile reflects the state of weathering along the soil profile or vertical soil section from the bedrock (unaltered parent rock) to the ground surface. It consists of material that shows progressive stages of transformation or 'grading' from fresh rock to completely weathered material towards the ground surface (Huat, et al., 2004). A proposed classification for weathering profiles over igneous, sedimentary or metamorphic rocks was given in Table 2-2 by MrLean and Gribble (2005).

Table 2-2: Classification of the weathering profile

Term	Grade	Description
Fresh	I	No visible sign of rock material weathering; perhaps slight discoloration on major discontinuity surfaces
Slightly weathered	II	Discoloration indicates weathering of rock material and discontinuity surfaces; all the rock material may be discolored by weathering
Moderately weathered	III	Less than half of the rock material is decomposed and/or disintegrated to a soil; fresh or discolored rock is present either as a continuous framework or as core-stones
Highly weathered	IV	More than half of the rock material is decomposed and/or disintegrated to a soil; fresh or discolored rock is present either as a discontinuous framework or as core-stones
Completely weathered	V	All rock material is decomposed and/or disintegrated to soil; the original mass structure is still largely intact
Residual soil	VI	All rock material is converted to soil; the mass structure and material fabric are destroyed; there is a large change in volume, but the soil has not been significantly transported

Source: MrLean & Gribble (2005)

2.3. Shear strength and slope stability

2.3.1. Saturated and unsaturated soils

The soil is supposed to be in saturated state when all the void spaces between the particles are filled with water. When a proportion of the void space is filled with air, the soil is in unsaturated state. According to Fredlund and Rahardjo (1987), saturated soil mechanics principles can be applied when the degree of saturation of a soil is greater than about 85%. However, when the degree of saturation is less than 85%, it becomes necessary to apply unsaturated soil mechanics principles.

For simplicity, the world of soil mechanics is divided by the water table. Below the water table, soil behaviour is governed by effective stress $(\sigma - u_w)$, whereas the unsaturated soil above the water table is governed by two independent stress variables: the net normal stress $(\sigma - u_a)$ and matric suction $(u_a - u_w)$ (D. G. Fredlund & Morgenstern, 1977). While a saturated soil possesses positive pore-water pressures, unsaturated soil is characterized by negative pore-water pressure (Wolfsohn & Fredlund, 1994).

Due to the fact that the soils are subjected to different types of pore-water pressure, the stresses that develop in each zone also differ. Figure 2-2 shows this difference.

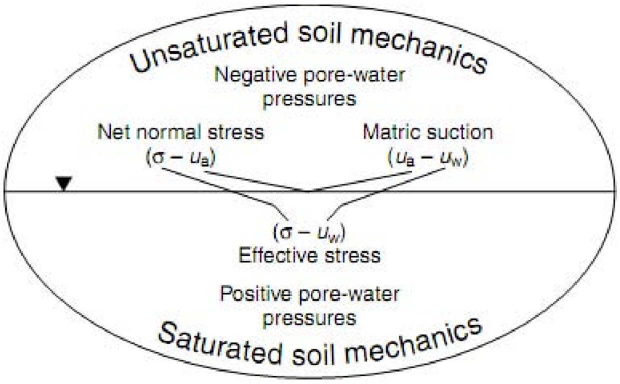

Figure 2-2: A visualization aid for the generalized world of soil mechanics
(Source: D. G. Fredlund, 1996)

2.3.2. Shear strength of unsaturated soils

Many geotechnical problems such as bearing capacity, lateral earth pressures, and slope stability are related to the shear strength of a soil (D. G. Fredlund & Rahardjo, 1993). Holtz and Kovacs (1981) defined the shear strength of a soil as the ultimate or maximum shear stress the soil can withstand. In saturated soil, the shear strength can be explained using Mohr-Coulomb failure criterion and the effective stress concept (Terzaghi et al., 1996).

$$\tau_{ff} = c' + (\sigma_f - u_w)_f \tan\phi' \qquad \text{(Eq.2.1)}$$

where

τ_{ff} = shear stress on the failure plane at failure
c' = effective cohesion, which is the shear strength intercept when the effective normal stress is equal to zero
$(\sigma_f - u_w)_f$ = effective normal stress on the failure plane at failure
σ_{ff} = total normal stress on the failure plane at failure
u_{wf} = pore-water pressure at failure
ϕ' = effective angle of internal friction.

Equation (2.1) characterizes a line which is called a failure envelope (Figure 2-3)

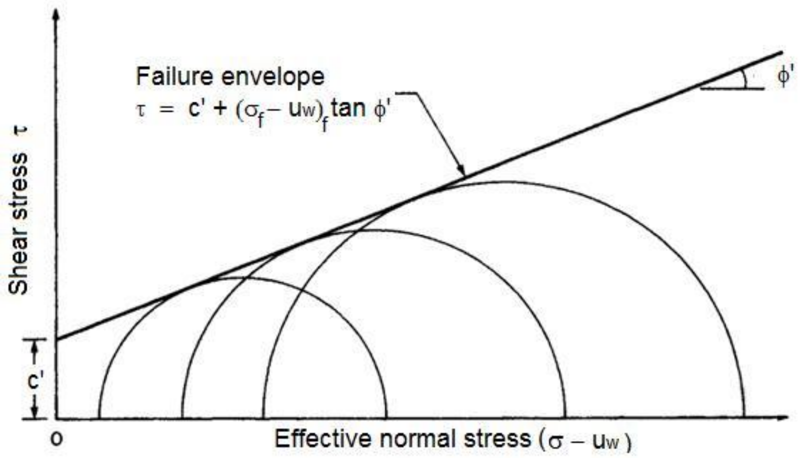

Figure 2-3: Mohr-Coulomb failure envelope for a saturated soil
(Source: Terzaghi, et al., 1996)

Fredlund and Rahardjo (1993) proposed an equation which interprets the shear strength of unsaturated soils in terms of two independent stress-state variables, $(\sigma - u_a)$ and $(u_a - u_w)$:

$$\tau_{ff} = c' + (\sigma_f - u_a)_f \tan\phi' + (u_a - u_w)_f \tan\phi^b \qquad \text{(Eq.2.2)}$$

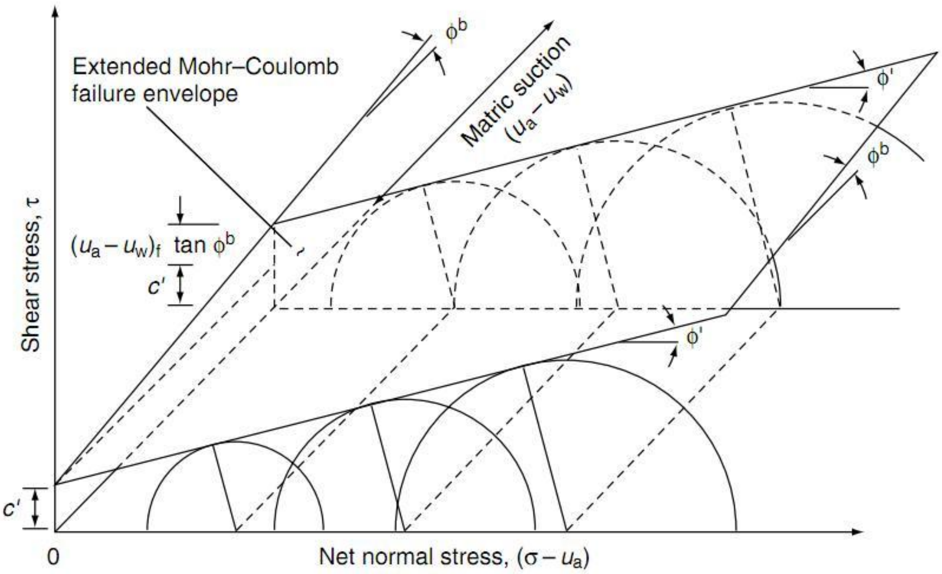

Figure 2-4: Extended Mohr–Coulomb failure envelope for unsaturated soils
(Source: D. G. Fredlund & Rahardjo, 1993)

where τ_{ff} is the shear stress on the failure plane at failure, c' is the intercept of the extended Mohr-Coulomb failure envelope on the shear stress axis where the net normal stress and the matric suction at failure are equal to zero. It is also referred to as effective cohesion, $(\sigma_f - u_a)_f$ is the net normal stress state on the failure plane at failure, u_{af} is the pore-air pressure on the failure plane at failure, ϕ' is the angle of internal friction associated with the net normal stress state variable $(u_a - u_w)_f$ is the matric suction on the failure plane at failure, and ϕ^b is the angle indicating the rate of increase in shear strength relative to the matric suction, $(u_a - u_w)_f$. According to Krahn (2004b), in capillary zone where the soil is saturated, but the pore-water pressure is under tension, ϕ^b = ϕ'. As the soil desaturates, ϕ^b decreases.

When the soil is saturated, all voids are filled with water, $u_a = u_w = u$ and (Eq.2.2) will be back to (Eq.2.1)

2.4. Slope stability assessment method

The main objective of this study is to assess the influence of weathering processes on the changing of soil and rock engineering characteristics, then assessing the effect of this change on the selected slope stability. Therefore, researching all slope stability calculation methods is not the purpose. Here, the simplified Bishop's method for unsaturated soils would be used for slope stability calculating. However, before going deeper into this method, some relevant background of unsaturated soil mechanics will be presented.

2.4.1. Factor of Safety (FoS)

The factor of safely for slope stability analysis is usually defined as the ration of the ultimate shear strength divided by the maximum mobilized shear stress at incipient failure. There are several ways in formulating the factor of safety FoS. The most common formulation for FoS assumes the FoS to be constant along the slip surface, and it is defined with respect to the force or moment equilibrium (Cheng & Lau, 2008)

a. Moment equilibrium: generally used for the analysis of rotational landslides. Considering a slip surface, the factor of safety F_m defined with respect to moment is given by:

$$F_m = \frac{M_r}{M_d} \qquad \text{(Eq.2.3)}$$

where M_r is the sum of the resisting moments and M_d is the sum of the driving moment.

b. Force equilibrium: generally applied to translational or rotational failures composed of planar or polygonal slip surfaces. The factor of safety F_f defined with respect to force is given by:

$$F_f = \frac{F_r}{F_d} \qquad \text{(Ep.2.4)}$$

where F_f is the sum of the resisting forces and F_d is the sum of the driving forces.

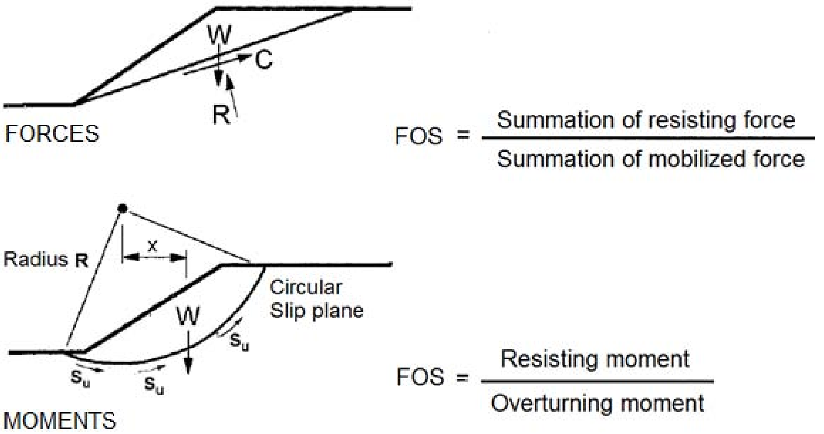

Figure 2-5: Two approaches of defining the factor of safety (FoS)
(Source: (Abramson, et al., 2002)

In the analysis of slope stability, it is very essential for engineer to provide a reasonable FoS which satisfies not only the safety but also the economic conditions. From this point of view, Liu and Evett (2005) gave out a table that shows significant values of FoS for design (Table 2.3)

Table 2-3: Significance of factor of safety, FoS for design

Safety Factor	Significance
Less than 1.0	Failure
1.0 – 1.2	Questionable safety
1.3 – 1.4	Satisfactory for cuts, fills, questionable for dams
1.5 – 1.75	Safe for dams

Source: Liu & Evett (2005)

2.4.2. Method of slices

The method of slices is used by most computer programs, as it can readily accommodate complex slope geometries, variable soil conditions, and the influence of external boundary loads (Abramson, et al., 2002). The principle of this method is the unstable soil mass above the slip surface is subdivided into a number of vertical slices (Figure 2-6) and individual slice would be treated as a unique sliding block. The actual number of slices used depends on the slope geometry and soil profile (Duncan & Wright, 2005).

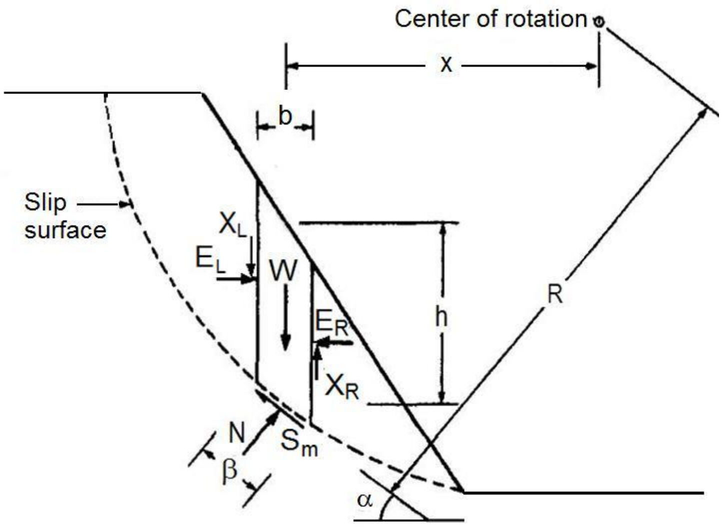

Figure 2-6: Circular slip surface with overlying soil mass subdivided into vertical slice
(Source: Fredlund & Rahardjo, 1993)

The forces acting on each slice for a general slope problem are defined as follows:

W = the total weight of the slice

N = the total normal force on the base on the slice

S_m = the Shear force mobilized on the base of each slice

E = the horizontal interslice normal forces (the “L” and “R” subscripts designate the left and right sides of the slice, respectively)

X = the vertical interslice shear forces (the “L” and “R” subscripts designate the left and right sides of the slice, respectively)

R = the radius for a circular slip surface or the moment arm that associated with the mobilized shear force, S_m for any shape of slip surface,

x = the horizontal distance from the centre line of each slice to the centre of rotation

f = the perpendicular offset of the normal force from the centre of rotation

h = the vertical distance from the centre of the base of each slice to the uppermost line in the geometry (i.e., generally ground surface)

α = the angle between the tangent to the centre of the base of each slice and the horizontal

β = sloping distance across the base of a slice

(Source: Fredlund & Rahardjo, 1993)

2.4.3. Bishop’s simplified method for unsaturated slopes

The Bishop method is one of the most popular slope stability analysis methods and is used worldwide. This method of slices satisfies only the moment equilibrium and it applies only for a circular failure surface (Cheng & Lau, 2008). The key point of this method is that it neglects the interslice shear forces and thus assumes that a normal or horizontal force adequately defines the interslice forces ($X_L = X_R = 0$) (Krahn, 2004b) (Figure 2-7). When the slip surface is assumed to has circular shape, the normal force on the base of each slice is derived by summing forces in a vertical direction then combining with the failure criteria (Eq.2.5) (see Figure 2-6)

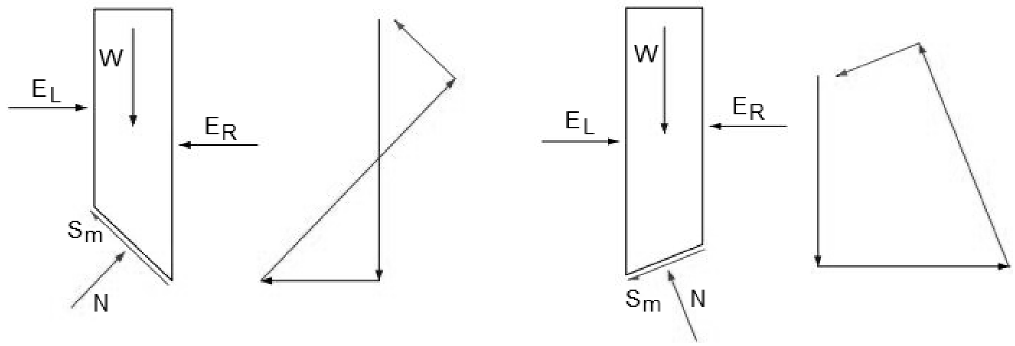

Figure 2-7: Force polygon for the Bishop's simplified method
(Source: Krahn, 2004b)

$$N = \frac{W - \frac{c'\beta\sin\alpha}{F} + u_a \frac{\beta\sin\alpha}{F}\left(\tan\Phi' - \tan\Phi^b\right) + u_w \frac{\beta\sin\alpha}{F}\tan\Phi^b}{m_\alpha} \quad \text{(Eq.2.5)}$$

The factor of safety is derived from the summation of moments about a common point.

$$F_m = \frac{\Sigma\left[c'\beta R + \left\{N - u_w\beta\frac{\tan\phi^b}{\tan\phi'} - u_a\beta\left(1 - \frac{\tan\phi^b}{\tan\phi'}\right)\right\} R\tan\phi'\right]}{\Sigma W_x - \Sigma Nf} \quad \text{(Eq.2.6)}$$

Equation (Eq.2.5) shows that the base normal force is a function of the factor of safety. This in turn makes the FoS equation nonlinear (that is, FoS appears on both sides of the equation) and an iterative procedure is consequently required to compute the FoS (Krahn, 2004b).

In summary, the Bishop's simplified method uses moment equilibrium for FoS and the vertical force equilibrium to calculate the total normal force N on the base on the slice. During equation construction, the vertical interslice forces are neglected. This method is applied mostly with circular shear surfaces.

2.5. Slope stabilization

According to Abramson, et al. (2002). Slope stabilization methods generally reduce driving forces, increase resisting forces, or both. In practice, many methods have been applied in slope stabilization:

1. Driving forces can be reduced by:
   - Excavate material from unstable group
   - Reduce the hydrostatic pressures acting on the unstable zone.
2. Resisting forces can be increased by:
   - Drainage that increase the shear strength of the ground
   - Elimination of weak strata or other potential failure zones
   - Building of retaining structures or other supports
   - Provision of in situ reinforcement of the ground
   - Chemical treatment (hardening of soils) to increase shear strength of the ground

3. METHODOLOGY AND DATA COLLECTION

3.1. Research methodology

In order to reach the objectives and to answer the research questions, this study focussed on two types of analyses: 1) Assessing the difference in a number of relevant geo-mechanical and hydrological soil properties between selected slopes of different ages, and 2) to assess the consequences of these differences on the stability of these slopes using deterministic slope stability methods. Ultimately, this should result in an estimation of the stability of cut-slopes over their engineering lifetime.

Figure 3-1 gives a conceptual overview of the work that was carried out. In sequential order, three steps can be identified: Data collection, data analysis and slope stability assessment. In this process, the data collection will be presented in the Section 3.3.

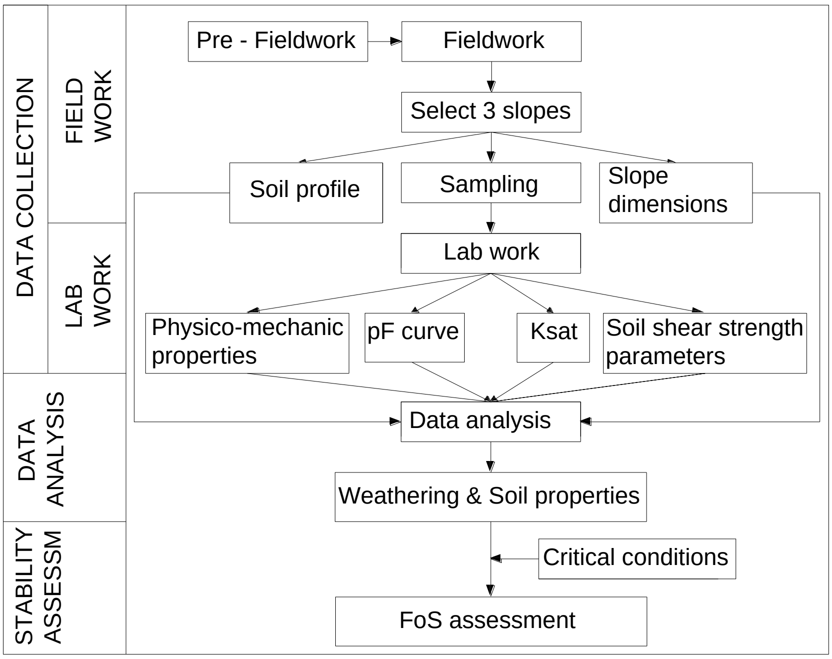

Figure 3-1: The research detailed process

3.1.1. Weathering evaluation

The data that need to be used as input for the evaluation is a series of some main soil engineering properties from (nearly) identical man-made slopes that only differ in their date of excavation. Basically, data from three different times should be considered and the larger the range of time is; the more appropriate the results for weathering assessment become. In this study we identified different cut-slopes (three as a minimum) with different exposure times but with some certain common conditions that make the comparisons between their engineering properties possible.
The certain common conditions include:

- Internal conditions:
  - Formed by the same parent bedrocks
  - Having similar groundwater condition
- External conditions:
  - Identical land cover

- Having similar slope & aspect.

In this study, three selected cut-slopes that were excavated at different times: 1) 31 years ago (S_1979), 2) 25 years ago (S_1985) and 3) 2 years ago (S_2008). All these slopes were part of the same hill side which was formed by the same geotechnical units (See Figures 3-2 and 3.7). Thus, the final data extracted from these slopes can be considered as the time-series data of one slope at three different exposure times.

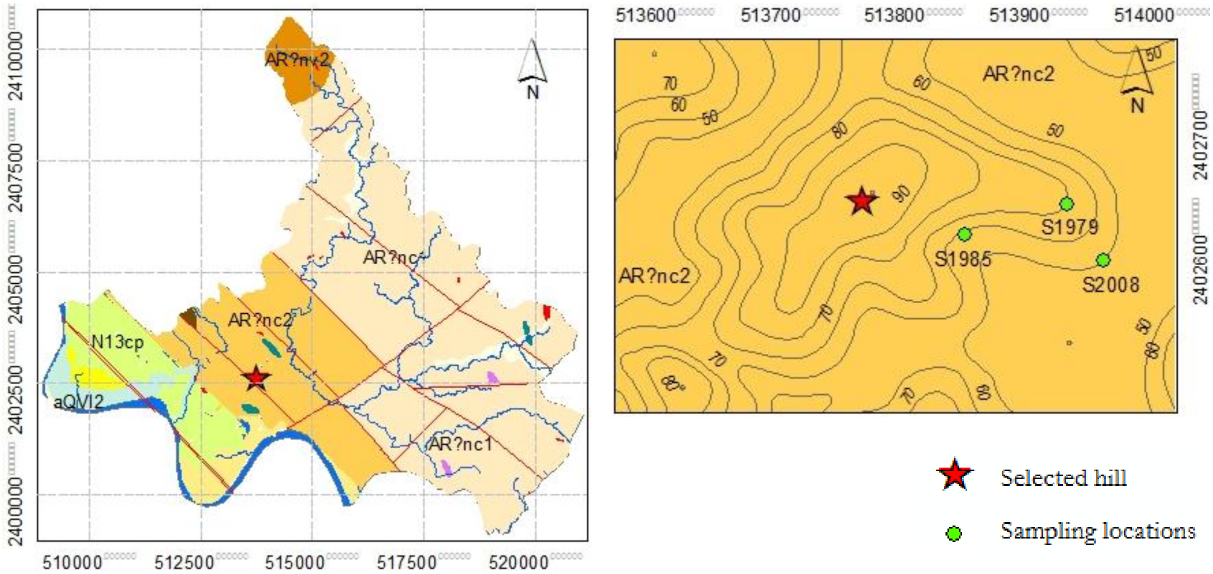

Figure 3-2: Sampling locations on the geological map

3.1.1.1. Data needed for weathering evaluation

Most of the data will be collected by doing fieldwork and soil testing in the laboratory. All samples from each soil layer for testing must be taken from the same depth. This study aims to evaluate some main engineering parameters of soil:

- Grain size distribution
- Void ratio
- Atterberg limits
- Soil-water characteristic curves (SWCC)
- Coefficient of permeability
- Saturated soil shear strength parameters from direct shear tests
- Soil shear strength results from penetrometer and vane shear tests.

3.1.1.2. Method of evaluation

The evaluation job aims to fulfil two tasks:

1. Analysis of all the measured main soil engineering parameters to find their trend subjected to time.

- Soil index properties: Particle size distribution, void ratio, porosity and Atterberg limits.
- Engineering properties: Soil-water characteristic curves; coefficient of permeability; shear strength parameters (cohesion and angle of internal friction).
- This study assumed that the degradation of soil dimensional engineering parameters under the influence of weathering processes follows a linear regression equation (see Figure 3-3)

$$Y = F(X) = A.X + B \qquad \text{(Eq. 3.1)}$$

where y = dependent variables at y axis
X= independent variables at x axis (time axis)
A = slope of the regression line
B = the intercept

2. Find out an average increasing rate (IR) or decreasing rate (DR) of this changing (weathering rate) To find a comparable changing rate, two specific different times which is one year difference on the trend-line need to be access (Figure 3-3).

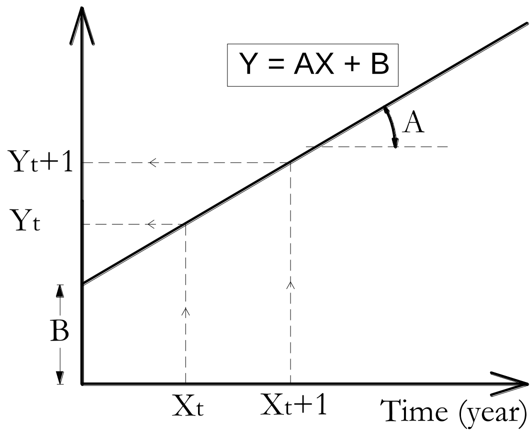

Figure 3-3: Weathering linear regression equations in case of increasing rate

Equation (3-2) will give out the rate of weathering for each soil's engineering parameters.

$$\text{IR or DR} = \frac{|Y_{t+1} - Y_t|}{Y_t} 100\% \qquad \text{(Eq.3.2)}$$

For each soil dimensional parameter, using equation Eq.3.2 based on the data extracted from equation Eq.3.1 which is defined from the results of field data analysis in Chapter 4, the values of IR or IR can be calculated at any required time.

3.1.2. Slope stability calculation

In this study, the GEO-STUDIO 2004 v6.22 is used for slope stability analysis. This is a suite of geotechnical software developed by GEO-SLOPE International Canada; it is considered to be the most powerful software and widely used in many countries in the world nowadays. The suite includes seven modules (Geo-slope INTERNATIONAL, 2008c).

- SEEP/W for groundwater seepage analysis
- SLOPE/W for slope stability analysis
- SIGMA/W for stress-deformation analysis
- QUAKE/W for dynamic earthquake analysis
- TEMP/W for geothermal
- CTRAN/W for contaminant transport
- VADOSE/W for vadose zone & covers

In this study, only the first two modules: SEEP/W and SLOPE/W were used and the behaviour of study slopes during

3.1.2.1. SEEP/W

SEEP/W is a finite element software product for analysing groundwater seepage and excess pore-water pressure dissipation problems within porous materials. The software can model both saturated and unsaturated flow (Geo-Slope INTERNATIONAL, 2008a). The use of SEEP/W in this research is to calculate the initial conditions of pore-water pressure of the selected slope. The results then will be integrated to SLOPE/W for slope stability analysis.

The principle of SEEW/W finite element is based on the Darcy's law and the rule that the sum of the rates of change of flows in the x- and y- directions plus the external applied flux is equal to the rate of change of the volumetric water content with respect to time (Krahn, 2004a).

$$\frac{\partial}{\partial x}\left(k_x \frac{\partial H}{\partial x}\right) + \frac{\partial}{\partial y}\left(k_y \frac{\partial H}{\partial y}\right) + Q = \frac{\partial \theta}{\partial t} \qquad \text{(Eq.3.3)}$$

where:

H	=	the total head,
k_x	=	the hydraulic conductivity in the x-direction,
k_y	=	the hydraulic conductivity in the y-direction,
Q	=	the applied boundary flux,
θ	=	the volumetric water content, and
t	=	time.

The total hydraulic head, H, is defined as:

$$H = \frac{u_w}{\gamma_w} + y \qquad \text{(Eq.3.4)}$$

where:

u_w	=	the pore-water pressure,
γ_w	=	the unit weight of water, and
y	=	the elevation.

Under steady-state conditions, the flux entering and leaving an element volume is the same at all times. It means the right side would equal to zero and Eq.3.3 now becomes:

$$\frac{\partial}{\partial x}\left(k_x \frac{\partial H}{\partial x}\right) + \frac{\partial}{\partial y}\left(k_y \frac{\partial H}{\partial y}\right) + Q = 0 \qquad \text{(Eq.3.5)}$$

So, two types of flow can be modelled in SEEP/W: 1) steady state flow where the flow rate of the fluid do not changes over time, ($\partial\theta/\partial t = 0$) and 2) transient flow referred to the condition where the flow rate of the fluid changes over time ($\partial\theta/\partial t \neq 0$).

To solve a problem in unsaturated flow, SEEP/W uses two functions:

1. Hydraulic conductivity function
2. Soil-water characteristic function

The magnitude of the maximum negative pore-water pressure is dependent on the shape of the hydraulic conductivity function and, to a lesser extent, on the rate of infiltration. The capability of the soil to store water under changes in pore-water pressures is represented by the soil-water characteristic function (Gui & Han, 2008).

The hydraulic boundaries for seepage analysis in this case are rainfall conditions. For seepage analysis in this case; there are three types of rainfall boundary: average daily rainfall in dry seasons, average daily rainfall in wet seasons and critical rainfalls.

Like other finite element software, these below steps must be done to solve a geotechnical problem in SEEP/W:

1. Sketch the problem: The cross-section of the problem is sketched base on the (X, Y) coordinates in this step. The more accuracy the sketch is, the more reliable the later results.
2. Specify the analysis type: there are two types of seepage analysis: 1) a steady-state analysis (non-time dependent analysis) and 2) transient seepage analysis (time dependent analysis).
3. Define the material properties: The numbers of defined materials depend of the number of soil layers that are taken into account. For a steady-state analysis, a hydraulic conductivity function which defines the relation between pore-water pressure and hydraulic conductivity must be declared. This function is used to define the hydraulic properties of the material. For a transient analysis, except from the hydraulic conductivity function, a volumetric water content function also has to declared to describe how the water contents change with different pressures in the soil as there is no fixed water content in time and space (Krahn, 2004a).

4. Generate the mesh of finite elements (cover the slope profile model): the mesh will cover the sketch to define the flow area.
5. Specify boundary conditions: the boundary conditions, in principle, are the driving force that creates the difference in hydraulic conditions between different locations within the model, and this causes seepage flow. In SEEP/W, the boundary conditions can be specified as total head (H), total nodal flow or flux (Q), or flow per unit length along the side of an element (q). In this research, the rainfall is considered as flow per unit length.
6. Solve the problem and view its results

Figure 3-4 illustrates a completed seepage model with the mesh of finite elements and assigned boundary conditions.

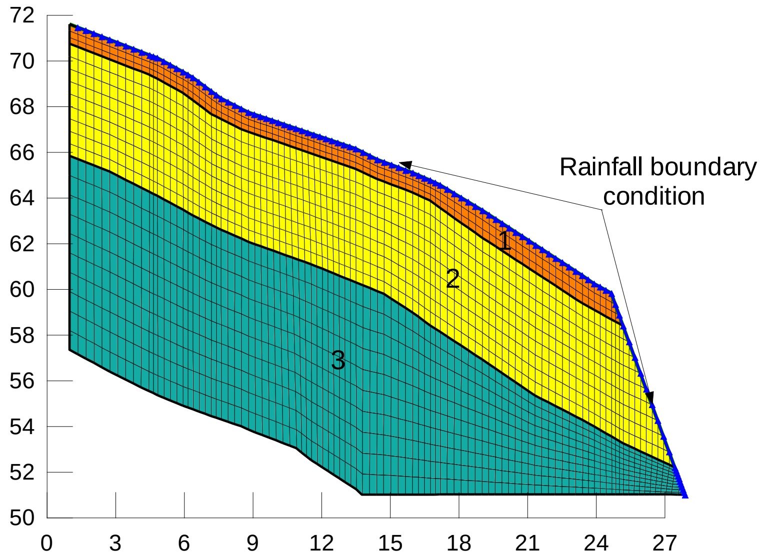

Figure 3-4: The seepage model with finite elements & assigned boundary condition of the selected slope

3.1.2.2. SLOPE/W

SLOPE/W is the leading slope stability software product for computing the factor of safety of slopes using the principles of the limit equilibrium methods (Geo-Slope INTERNATIONAL, 2008b). In a specific case, SLOPE/W can integrate with SEEP/W to solve a stability problem that takes the ground seepage and pore-water pressure into account. Within the module, eleven solution techniques for the method of slices have been developed. Basically, all are very similar. The differences between these methods are what equations of statics are included and satisfied, which interslide forces are included and what is the assumed relationship between the interslice shear and normal forces (Krahn, 2004b). In Figure 3-5 is a typical sliding mass discretized into slices and the possible forces on the slice. On the slice base and on the slice sides are the normal and shear forces.

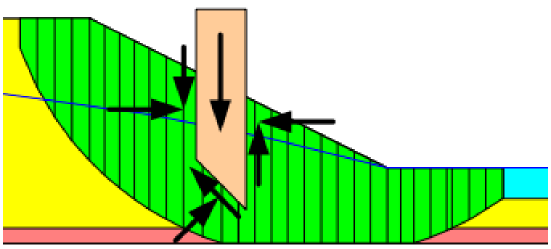

Figure 3-5: Slice discretization and slice forces in a sliding mass

Table 3-1 is the list of methods available in SLOPE/W. It also implies equations of statics which suit for each method. Table 3-2 summaries the interslice force characteristics for each suitable method

Table 3-1: Equations of Statics Satisfied

Method	Moment Equilibrium	Force Equilibrium
Ordinary or Fellenius	Yes	No
Bishop's Simplified	Yes	No
Janbu's Simplified	No	Yes
Spencer	Yes	Yes
Morgenstern-Price	Yes	Yes
Corps of Engineers-1	No	Yes
Corps of Engineers-2	No	Yes
Lowe-Karafiath	No	Yes
Janbu Generalized	Yes (by slice)	Yes
Sarma-Vertical slices	Yes	Yes

Source: Krahn (2004b)

Table 3-2: Interslice force characteristics and relationships

Method	Interslice Normal (E)	Interslice Shear (X)	Inclination of X/E resultant, and X-E Relationship
Ordinary or Fellenius	No	No	No interslice forces
Bishop's Simplified	Yes	No	Horizontal
Janbu's Simplified	Yes	No	Horizontal
Spencer	Yes	Yes	Constant
Morgenstern-Price	Yes	Yes	Variable; user function
Corps of Engineers-1	Yes	Yes	Inclination of a line from crest
Corps of Engineers-2	Yes	Yes	Inclination of ground surface at top of slice
Lowe-Karafiath	Yes	Yes	Average of ground surface and slice base inclination
Janbu Generalized	Yes	Yes	Applied line of thrust and moment equilibrium of slice
Sarma-Vertical slices	Yes	Yes	X = C + E tan

Source: Krahn (2004b)

The stability calculations in this research were carried out based on the Bishop simplified method (see Section 2.4.3) combined with pore-water analysis done in SEEP/W.
Data required for slope stability analysis using SLOPE/W are:

1. Unit weight below groundwater table: α_s
2. Unit weight above groundwater table: α_w
3. Unsaturated shear strength parameters of soil including: Effective internal friction φ' and effective cohesion c'
4. The angle defining the increase in shear strength due to the negative pore-water pressures ^{b}. According to (Krahn, 2004b), in SLOPE/W, ^{b} is treated as a constant value. For practical problems, ^{b} can be taken to be about (1/2)φ'. In SLOPW/W, if ^{b}is undefined (zero), any negative pore-water pressure is ignored. If ^{b}is a non-zero specified value, an extra strength component dependent on the suction is added to the slice base shear strength.

Basically, the most realistic position of the critical slip surface will be computed when effective strength parameters are used together with realistic pore-water pressures (Geo-Slope INTERNATIONAL, 2008b). Therefore, in a slope stability problem, specifying pore-water pressures play an important role.

SLOPE/W is fully integrated with the finite element products available in GeoStudio. Thus, with the same cross-section, when a computation with SEEP/W was done, using integrated function from SEEP/W to SLOPE/W would help to reduce the work. Following this approach, two steps were executed: firstly, the infiltration and the ground water flow were analysed to achieve the pore-water pressure distribution within the slope; secondly, the stability of the slope was analysed using the pore-water pressure profile obtained from previous step. The procedure involves the following steps:

1. Integrate the computed SEEP/W modal to the new SLOPE/W problem. Follow this way, the finite element mesh also being imported to SLOPE/W.
2. Specifying the pore-pressure conditions: the pore-water pressures were modelled in SEEP/W and then integrated with SLOPE/W.
3. Define soil properties: each soil layer was defined with its unit weight, shear strength parameters including effective cohesion c', effective internal friction φ' and also the value of ^{b}.
4. Defining the slip surface: The option "Grid and Radius" was chose to define the circular slip surface (see Section 2.4.3)
5. Draw the grid and radius for circular slips. The trial slip surface is a portion of a circle that cuts through the slope. A circle can be defined by specifying the x-y coordinate of the centre and the radius. A wide variation of trial slip surfaces can be specified with a defined grid of circle centres and a range of defined radii. In SLOPE/W, this procedure is called the Grid and Radius method (Krahn, 2004b). Figure 3-6 illustrates the a SLOPE/W model in the final step before solving
6. Solve & view the results.

Figure 3-6 shows a completed stability model using Grid and Radius slip surface option

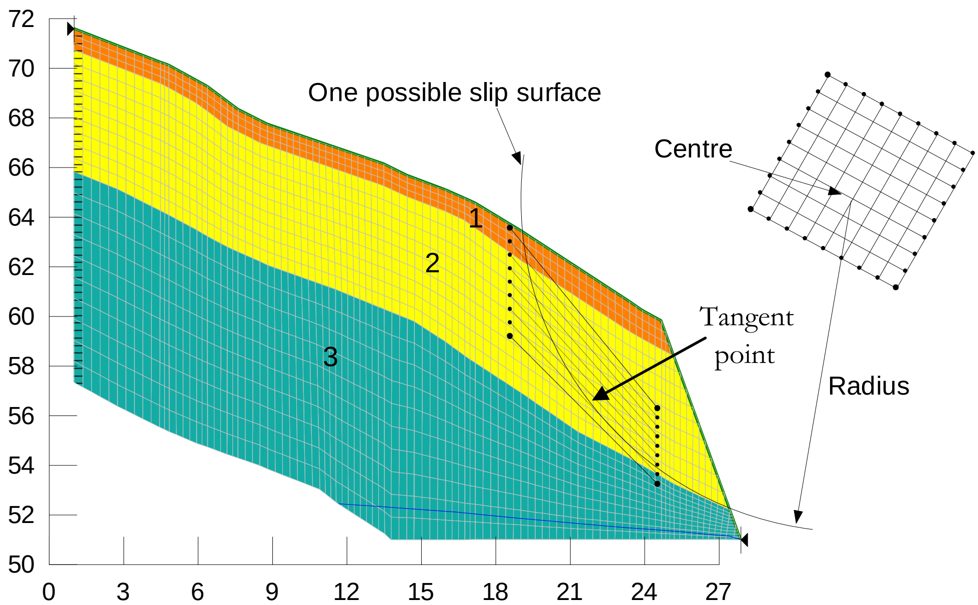

Figure 3-6: A completed stability model using Grid & Radius slip surface option

3.2. Scenario cases in slope stability

As outlined in Section 3.1, calculations of the stability of slopes in this study aim to solve two purposes:

1. To evaluate the influence of the degradation of soil engineering properties due to weathering processes to the stability of cut-slopes.
2. To assess the stability study slopes under critical rainfall conditions.

To meet the above purposes, the stability of a 2, 25 and 31 years old slope were accessed by GEO-STUDIO 2004. Three cases of slope angles which are 65^0, 70^0 and 75^0 corresponding to the range of inclination angles of cut-slopes these observed from the field were considered. For the first purpose, average daily rainfall in rainy seasons was considered. For the second purpose, two critical rainfall conditions corresponding to the rainfall events happened in 2006 and 2008 were considered. The reason for choosing these rainfalls will be explain on Section 5.2.5.

3.3. Data collection

3.3.1. Pre-Fieldwork data

The data that is already available from old works or related projects. Most available existing data is from the Vietnam Institute of Geosciences and Mineral Resources (VIGMR).

3.3.1.1. Maps

The maps that are necessary for this study including: a digital elevation model (DEM) and a geological map. Among them, The DEM was built from a 10m contour map, taken from the topo-map (created in 2002, scale 1: 10.000), and then it was classified into three levels of elevation corresponding to the three main types of terrain in the study area: Hills (> 60m), valleys (28 – 35m) and alluvial plains & fans (28 – 50m) (Vinh, et al., 2005). Figure 1-4 shows the classified DEM with an additional river map, an administrative map and a road network map. The geological map (Figure 1-5) is in a scale of 1: 10000 was created in 2008. All available maps were listed in Table 3-3.

Table 3-3: Collected maps in the study area

Available Maps	Type	Date	Scale	Source
Contours 10m	Vector	2002	1: 10,000	VIGMR
River network	Vector	2002	1: 10,000	VIGMR
Road network	Vector	2002	1: 10,000	VIGMR
Topography	Vector	2002	1:10,000	VIGMR
Administrative boundaries	Vector	2002	1: 10,000	VIGMR
Geological map	Vector	2008	1: 10,000	VIGMR

3.3.1.2. Rainfall and other related data

The collected rainfall data was provided by The Hydro Meteorological Data Centre (HMDC) including:

- Average daily rainfall from 1960 to 2009
- Average hourly rainfall from 2000 to 2009
- Records about old landslides and their damages were provided by VIGMR and the Authorities of Yen Bai city communities.

3.3.2. Fieldwork data

In order to cover the methodology as outlined in Section 3.1, going on fieldwork is required to collected unavailable data. The fieldwork processes are delineated below

3.3.2.1. Locate the research sites (sampling locations)

Base on the conditions for choosing the research sites, three selected slopes are all located on a hill that belongs to Ngoi Chi formation (AR-nc^2) (Figure: 3-2). The detailed description of these slopes is as below

1. Slope 1 (S2008): Located about 3.5m above the foothill, this two years old cut was done in 2008 for create more living space. It runs along the foothill around 360m long and 4 - 15m high. At the sampling location, the height of the slope is about 6m with the slope angle is 70 degree. On the surface of the slope, there is a thin moss layer but it is not so difficult to differentiate separate soil and rock layers from the top to the bottom.
2. Slope 2 (S1985): Located on the middle of the hill, this slope was cut to create space to build a tank of water. The owner wanted to take advantage of the height of this location to distribute water to the surrounding area. This is cut is smaller than slope 1. At the sampling location it is about 4.5m height and 120m wide.

3. Slope 3 (S1979): Located on the highest position in compare to other formers. The slope was created in 1979. Its first purpose to cut was to create land for a graveyard for the family's ancestor. However, then it was changed into land for cultivation. For this purpose, only the top soil (1 - 1.5m) was removed and the slope still keeps its natural slope angle (around 30^0 to 35^0).

The sketch of three selected slopes is illustrated on Figure 3-7

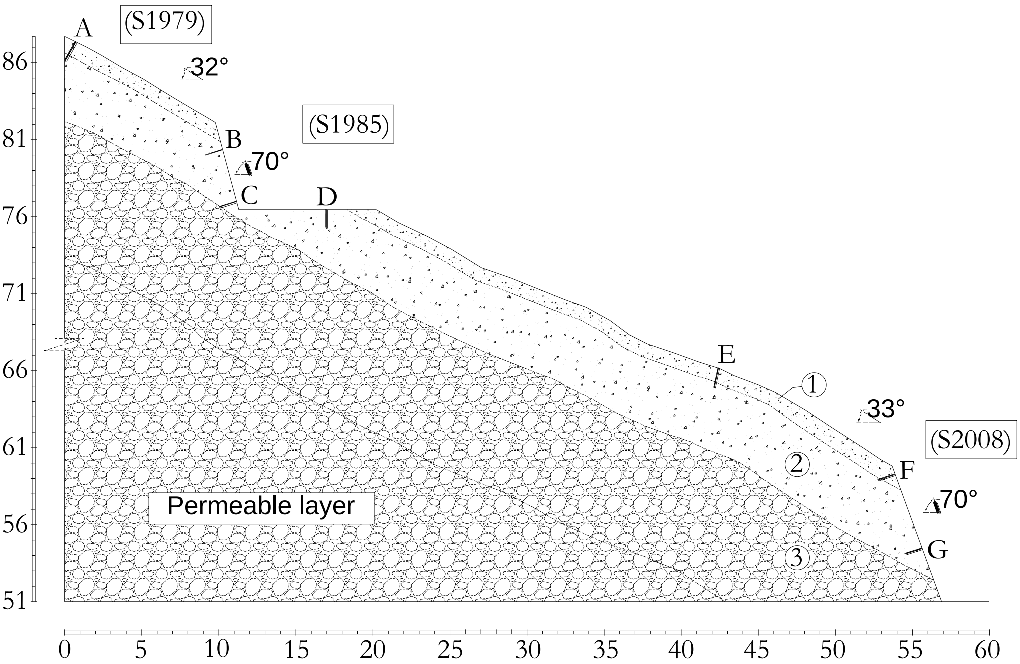

Figure 3-7: A general section cut through three study slopes

3.3.2.2. The soil profile

As highlighted in the problem statement and research objective, this research would take the soil layers that lie on the weathered rock into account. Based on the characteristics of residual soil that is quite popular in the study area and the descriptive scheme for grading the degree of weathering (Table 2-2). Also according to the results of field survey while digging soil for sampling in the three pits from the three selected slopes, and while inspecting some new cut-slopes in the study area, the typical soil profile for the research site could be drawn as in Figure 3-8.

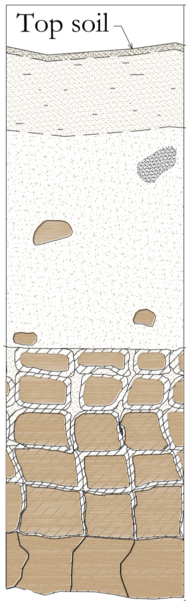

Term	Description	Grade
Residual soil 0.9m - 1.2m	Consolidated light brown silty-clay with smooth soil particle texture	VI
Completely to highly weathered 3.5m - 4.5m	Consolidated brownish to reddish silty-clay, mix with small white fractures of rock composed of kaolin, feldspar & mica, coarse texture.	V & IV
Moderately weathered 5.5m - 8m ↓ Slightly ↓ Bed-rock	> 50% is rock with main components, fresh & discolor rock is presented	III

Figure 3-8: The typical soil profile in Yen Bai city

3.3.2.3. Typical slope cross section

The cross sections were drawn base on the objective requirements; it only concentrates on the soil part and the transition layer between soil and rock. The present of the slope cross section will help to build the model for slope stability calculations. The typical cross section must representative for the whole research site. From the fact that most cut-slopes in this area have an inclination angle of $65^0 - 75^0$, and combined with the typical soil profile as shown in Figure 3-7, cut-slope cross-sections for a 70^0 when it is 2, 25 and 31 years old in Yen Bai city can be drawn as shown in figures From 3-9 to 3-11.

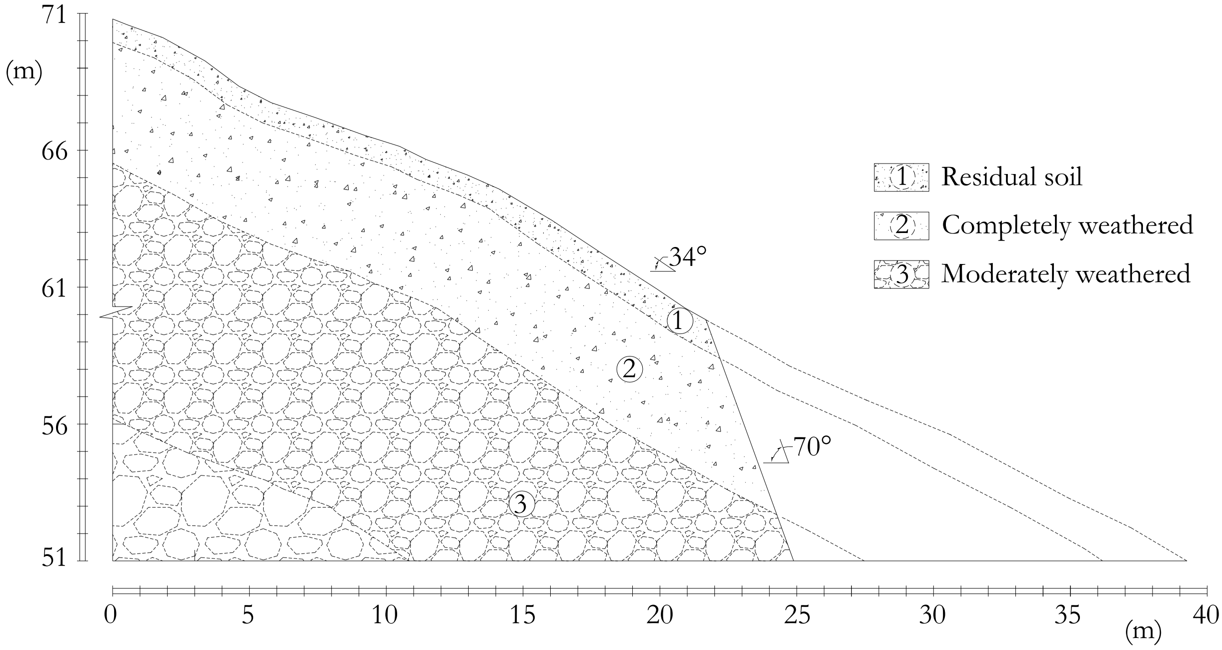

Figure 3-9: Typical cross-section for a 70^0 two year old cut-slope in the study area

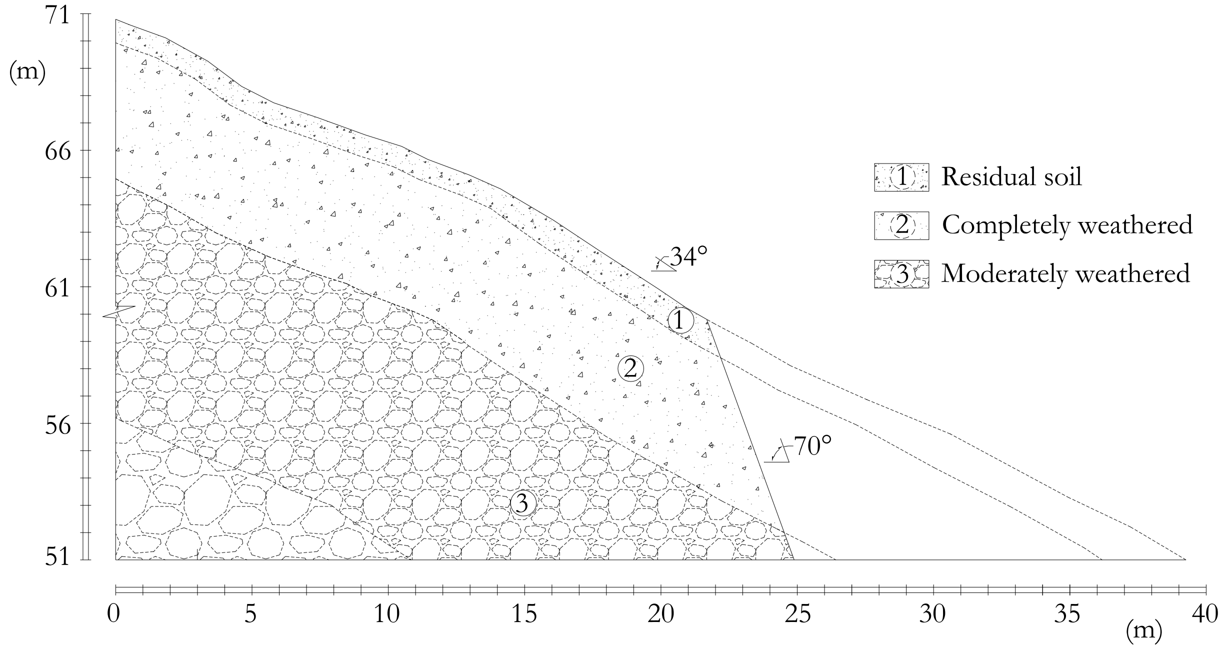

Figure 3-10: Typical cross-section for a 70^0 twenty-five years old cut-slope in the study area

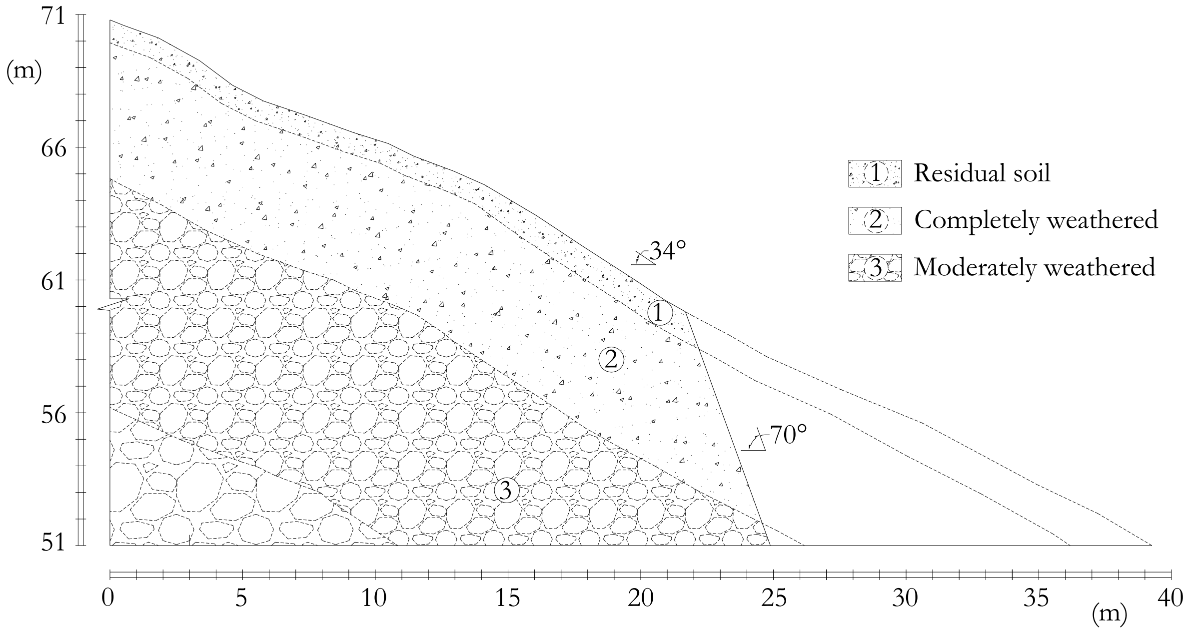

Figure 3-11: Typical cross-section for a 70^0 thirty-one years old cut-slope in the study area

In general, the only difference between these slopes is the thickness of the completely weathered as a result of weathering.

3.3.2.4. Soil sampling

Sampling was conducted to get disturbed and undisturbed samples for laboratory tests of all required soil parameters outlined in the methodology part.

- Disturbed samples are used to determine grain size distribution curves, Atterberg limits and specific gravity.
- Undisturbed samples are required for soil unit weight, permeability and shear strengths parameters

Since the study only concentrates on the soil part, the top two layers: layer 1 and layer 2 (Figure 3-8) would be taken into account. In layer 1, due to the influence of the root zone, the samples will be taken at the depth of 0.8m. For the second layer, this depth is 1.8m. Undisturbed samples were acquired by a plastic tube with the diameter or 7.6 cm and 15 cm length. The whole procedure is as in Figure 3-12 below

Figure 3-12: Soil sampling procedure

3.3.2.5. Field tests

Tests carried out in the field including: pocket penetrometer tests, pocket vane shear tests, and volumetric water content measurements.

1. Pocket penetrometer tests: The test was performed to approximate the unconfined compressive strength of soil at a certain depth which is also useful to assess the influence of weathering processes on soils. It was done using a pocket penetrometer. Five values of unconfined compressive strength were taken and their average was used for analysing. The reading values of penetrometer tests for the

slope S2008 are presented in Table 3-4, the results of slopes S1985 and S1979 are presented in Appendix A-1, analyses of the data is in Section 4.2.3

Table 3-4: Reading values of Pocket penetrometer tests in S2008

S2008	Reading value (Kg/cm^2)				
Depth	1st	2nd	3rd	4th	5th
80 cm	3.2	3.5	3	2.6	2.7
180 cm	3.4	3.9	3.2	3.7	4.1

2. Pocket vane tests: Undrained shear strength can be determined using a vane that is pushed into a flat surface of soil and rotated until the soil fails. The reading number then is converted to shear strength values based on the value of complete revolution that depends on the type of the vane. During fieldwork time, vane CL100 was used. The reading values must be converted to the soil undrained shear strength by multiplying them by 0.10936 (factor of revolution for vane CL100). In this study, five points were done for each soil layer. Table 3-5 shows the corresponding undrained shear strength of soil layers in S2008, for the other two slopes, the results are shown in Appendix A-2, the results of data analyses will be presented in Section 4.2.4.

Table 3-5: Reading values of Pocket vane tests for S2008

S2008	Undrained shear strength (Kg/cm^2)				
Depth	1st	2nd	3rd	4th	5th
80 cm	0.317144	0.371824	0.339016	0.339016	0.32808
180 cm	0.535864	0.38276	0.448376	0.415568	0.404632

3. Volumetric water content measurements: The results of volumetric water content were used to assess the effect of weathering on soil, and then they were employed as the input parameter in the SEEP/W model to calculate the in situ pore-water pressures of the study slopes. The measurement was carried on by a moisture measurement system (HH2). It is composed of some access tubes which are 1.2m length and being installed stably under the soil surface, a moisture meter, and a profile probe designed with sensors (6 sensors). To measure, first connected the probe to the meter through a cable, then it is pushed into a pre-buried tube; the volumetric moisture result is shown on the screen of the meter. Each sensor on the probe will gives one value of moisture content at the depth that it is located.

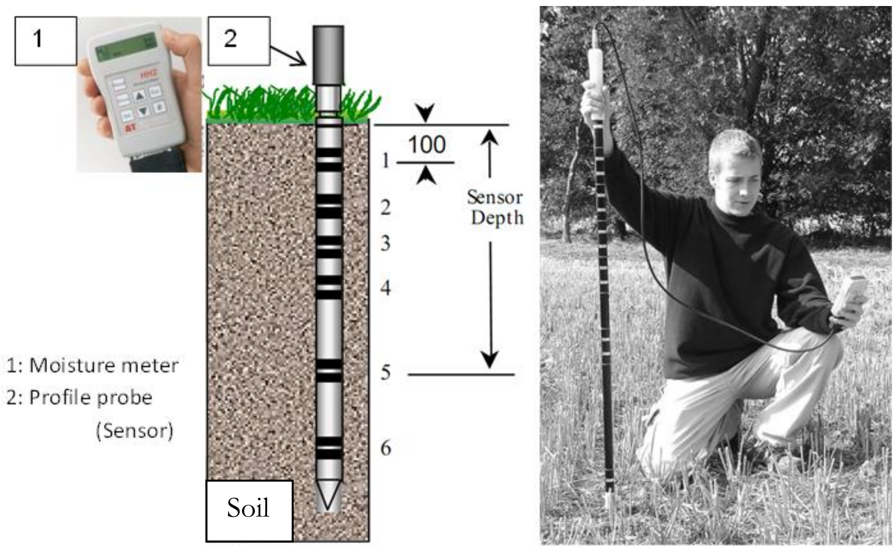

Figure 3-13: The moisture meter and the measurement of soil volumetric water content in the field (Source: Delta-T Devices Ltd, 2005)

Figure 3.7 illustrates the distribution of soil moisture measuring tubes under the notation respectively from A to F. The advantage thing about the system is that it can measure the soil moisture of multiple depths at one time days & nights continuously so the dense of the data depends on the propose of the study. However, the disadvantage thing is that it can only measure within the depth of 1m under the soil surface. All the measured results in 10/10/2010 were presented in Appendix A-5, the data analysis results are presented in Section 4.1.3.

3.3.3. Laboratory work and its results

3.3.3.1. Grain size distribution test

This test aimed to find the percentage of different grain size groups contained within the soil. It was drawn based on sieve analysis, hydrometer analysis and the Vietnamese standard of method for the determination of grain size distribution (TCVN, 1995a). In this study, 2 tests were conducted for each soil layer so with 3 different slope cross sections, 12 grain size distribution curves were drawn. All the results were shown on Appendix B-1, the analysis of the laboratory results will be presented in Section 4.1.1.

3.3.3.2. Atterberg limits

For fine grained soils, the Atterberg limits represent the soil moisture content of the soil at which it changes from one state to another state. Basically, two main types of limits are differentiated:

- Liquid limit
- Plastic limit

Each soil layer will have one value for each type of Atterberg limit. The tests were conducted based on the Vietnamese standard of methods for laboratory determination of plastic limit and liquid limit (TCVN, 1995b). All results of laboratory testing are presented in Appendix C; the conclusions of the tests are discussed in Section 4.1.4

3.3.3.3. Saturated permeability tests

The continuous void spaces in a soil permit water to flow from a point of high energy to a point of low energy. Permeability is defined as the property of a soil that allows the seepage of fluids through its interconnected void spaces (Das, 1976). There are many factors that affect the permeability of soil, such as: grain size and grain size distribution, void ratio and so on. Results of field observations showed that the two top soil layers in the study area are silty clay. Thus, the failing head test method would be used to determine the saturated coefficient of permeability (K_{sat}). To be more precise, two tests have been executed for each soil layer at the same depth then their average is calculated. The final result for each Ksat test is illustrated in Appendix. C; the conclusions are discussed in Section 4.2.1

3.3.3.4. Soil water characteristic curve (SWCC)

SWCC is a relationship between water content and the matric suction of a soil. Hydraulically and physically, it means how much equilibrium water a soil can take at a given suction originally (D. G. Fredlund et al., 2001). In a more simple way, SWCC indicates the water storage capacity of soil at various matric suction levels. Since the ability of a soil to retain water varies with matric suction. Therefore, the coefficient of permeability is not a constant in unsaturated soils but is a function of matric suction (Rahardjo et al., 2004). In this study, SWCC was used to assess the influence of weathering on soil. Furthermore, it was also applied as the input data in transient seepage problems.

The tests to define SWCC were conducted under the standard test methods for determination of SWCC (ASTM, 2003). Proposing to have more reliable results, two tests were executed for each soil layer. Doing the test, saturated undisturbed soil samples were put into a pressure chamber, and then various levels of suction were applied. For each level, after the equilibrium state is reached, a value of volumetric water content was calculated based on the weight of the sample. The relationship between soil volumetric water contents versus suction values is the soil –water characteristic curve.

In this work, two to three curves were drawn for each separated soil layer and the average of them would be the final one. The results of SWCCs for soils in the study area are illustrated in Appendix B-2. The discussions are in Section 4.2.2

3.3.3.5. Soil shear strength testing

Triaxial compression (TC) test is the most common laboratory tests used for the determination of shear strength for slope stability analysis. However, if drainage conditions are not critical, the direct shear (DS) test may be selected for its operational simplicity (Abramson, et al., 2002). In this study, as the time was too demanding, the shear strength parameters required for analyses will use the results of direct shear tests, two triaxial tests that were conducted for samples in Slope S1979 at two corresponding depths (80 cm and 180 cm) would be used to verify the direct shear test results.

1. Triaxial tests: The triaxial tests were conducted under consolidated undrained (CU) condition based on ASTM standards (ASTM, 2004). The result of triaxial tests for the completely weathered is shown in the Figure 3-14; the result for the residual soil is illustrated in Appendix B-3.

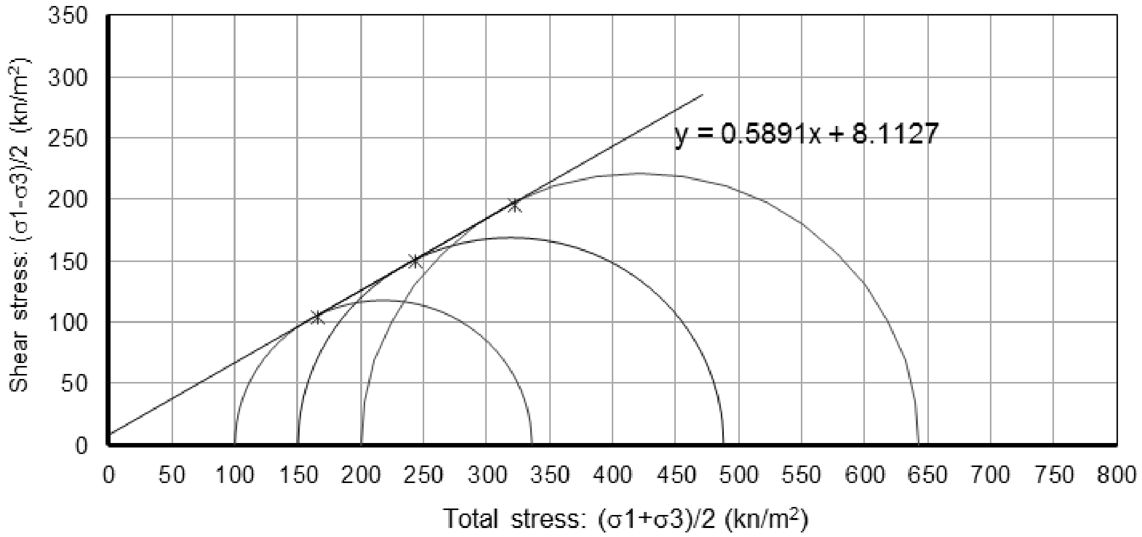

Figure 3-14: The result of triaxial test for the completely weathered layer

2. Direct shear test: Due to the thin specimen used, drained conditions can be expected to exist for most materials. Therefore, the DS results are usually reported in terms of effective stress (Abramson, et al., 2002). The tests follows the Vietnamese standard for soil-laboratory method of determination of shear resistance in a shear box apparatus (TCVN, 1995c). In the study area, cut-slopes are covered by tropical residual soils; they are expected to work in unsaturated conditions. Hence, the consolidated-drained (CD) test is required.

   The final results of direct shear test for each soil layer would be a plot of the maximum shear stresses versus the vertical confining stresses after the experiment is run for three vertical stress levels: 1 Kpa; 2 Kpa; and 3 Kpa respectively. Consequently, each relationship would need at least 3 undisturbed samples. To be sure about the testing results, for each vertical stress level, two samples have been tested, and the average between them is the final value. As mentioned in the methodology, the direct shear tests with saturated and unsaturated were conducted. Figure 3-15 presents the results of direct shear test done for the completely weathered layer in S1979. The reading numbers of all executed direct shear tests and their corresponding shear strength parameters are presented in Appendix B-4.

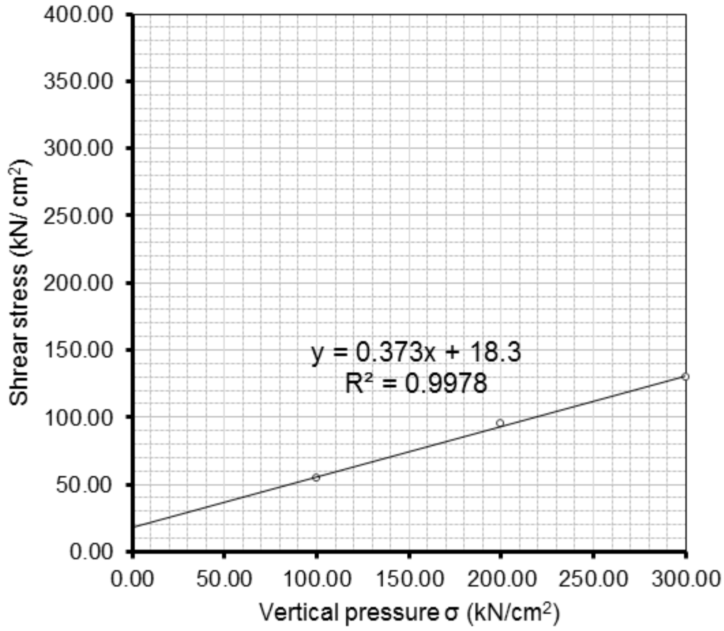

Figure 3-15: The result of direct shear test test for the completely weathered layer (saturated condition)

The results of shear parameters from triaxial tests and direct shear tests for the same layer of the same slope are quite different. Although those are two different types of tests which do not have the same applied conditions but the large difference between the results from the two is unusual. The reason may be the quality of triaxial samples, field survey and observations from the laboratory shown that there is quite large proportion of coarse sand and gravel inside the samples (Figure 3-16) so it might be broken during transporting or making. However, it is difficult to find the reason with one or two triaxial tests, so the verifying of direct shear test results using triaxial test results would be left for future researches.

Figure 3-16: Illustration of triaxial samples

3.3.3.6. Soil unit weight, specific gravity and porosity characteristics

Soil density is one of the main input parameter for slope stability calculation. In this thesis, the natural unit weight and saturated unit weight have been tested. The results of soil specific gravity were used to determine the soil porosity characteristics. The results of unit weight, specific gravity and porosity characteristics are shown in Appendix C

4. THE INFLUENCE OF WEATHERING ON SOIL ENGINEERING CHARACTERISTICS

It is clearly that the degradation of engineering characteristics of soils subjected to weathering is a function of time. The longer the time, the more significant this influence is expected. In addition, the depth of the study materials under the surface is also an important factor. A deeper layer of soil would suffer less from weathering processes than a shallower layer. However, since this study only considers two specific soil depths so any conclusions about the rate of weathering subjected to the depth factor is less reliable. Therefore, this study would concentrate more on analysing the influence of time factor on the soil index properties and soil engineering properties as mentioned in the methodology and stated in the objectives.

Besides, the results from field observation show that landslides and slope failures in the study area often occur on the top soil layer. Thus, the evaluation of weathering will concentrate on soil layer 2 (completely weathered layer) which take the most part of the possible slip surfaces in case slope failures occur, so additional analysing of weathering on soil layer 1 (residual soil) is only for referencing.

Based on the equation that show the degradation of soil parameters over time (Eq. 3.1), obtained from the data analysis part (see Section 4.1 and 4.2), the values of IR (increase rate) or DR (decrease rate) for each soil dimensional parameter will be calculated. (Eq.3.2). As the aim of this is to find an increase or decrease rate (weathering rate) in percentage which represents for the speed of changing of dimensional parameters so a certain time should be chosen to calculate this rate. In this study, as the range of the ages of study slopes are from 2 to 31 years old, the time the study slope is 15 and 16 years old will be considered.

4.1. Effect of weathering on index properties of soil

Index property test results revealed that under the influence of the time factors, there is an extensive variation in grain size distribution, porosity, Atterberg limits, coefficient of permeability, natural moisture content and soil- water characteristic relationship. Furthermore, as weathering extends to greater depths, a considerable change also was observed.

4.1.1. Grain size distribution

The degree of weathering on soil depends significantly on its available surface which is decided by the particle grain size (see Section 2.2). Therefore studying the particle size distribution of soil plays an important role in soil mechanics in general and the nature of weathering in specific. In this work, two grain size distribution curves were drawn for each different soil layer (see Appendix. B); and the average between them would be the one used in the further analyses.

The grain size distribution can be characterized by the quantities D_{60} and D_{10}. These indicate that 60 %, respectively 10 % of the particles (expressed as weights) are smaller than the diameter (Verruijt, 2006). The ratio between them is symbolized as the uniformity coefficient C_u.

$$C_u = \frac{D_{60}}{D_{10}} \quad \text{(Eq.4.1)}$$

Figure 4-1 synthetizes the grain size distributions of all six soil layers from three selected slopes. The influence of soil depth and time is clearly shown in this figure. Soil at the depth of 80 cm has much finer particle size than it does at 180 cm. In the upper layer, the fine components are dominant with about 70%. However, the story is different when it comes to the lower depth. With more that 50% sand and gravel grain sizes are the major proportions. As can be seen, all the curves are divided into two groups corresponding with two separated soil depths (80cm and 180cm), the older cut-slopes have finer grain.

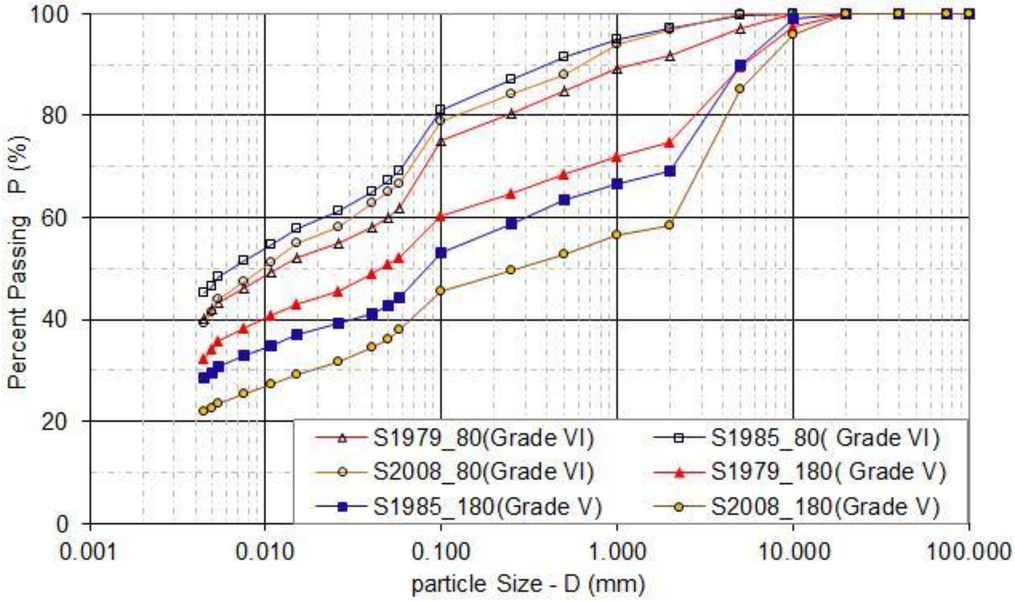

Figure 4-1: Grain size distribution curves of 6 soil layers from 3 selected slopes

Assessing the rate of weathering, the uniformity coefficients (Cu) were considered. From Figure 4-1, the values of D_{60} and D_{10} can be defined. The uniformity coefficient Cu for soil layers of all study slopes could be calculated based on (Eq.4.1). Their values are presented in Table 4-1

Table 4-1: The uniformity coefficient of particle size of three selected slopes at 16th year

Slope / Para	S1979		S1985		S2008	
	80 cm	180 cm	80 cm	180 cm	80 cm	180 cm
D10	0.0007	0.00075	0.0004	0.001	0.00058	0.0016
D60	0.04	0.095	0.023	0.3	0.0335	2.2
Cu	57	127	57	300	58	1375

From the results in Table 4-1, the trend-lines between the uniformity coefficients (Cu) overtime time were drawn using linear regression (Figure 4-2) and (Figure 4-3)

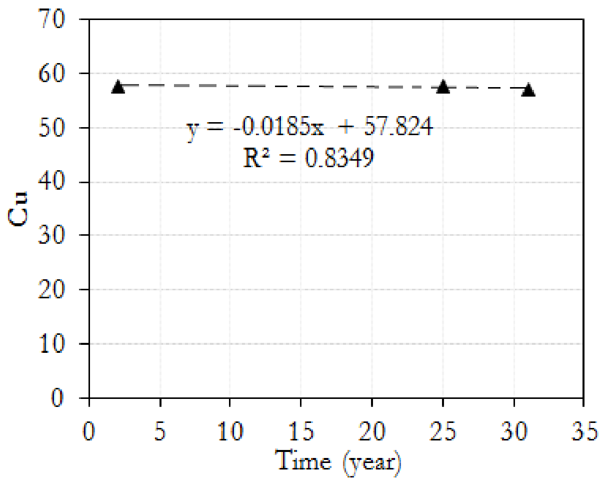

Figure 4-2: The relationship between Cu & Time of residual soil layer (layer 1)

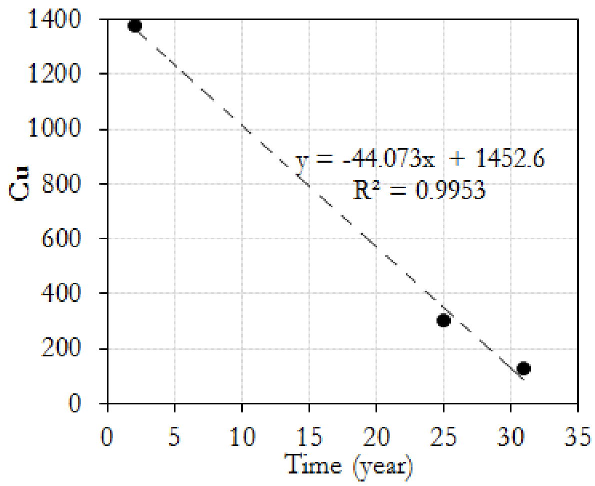

Figure 4-3: The relationship between Cu & time of completely weathered layer (layer 2)

It was found in Figures 4-2 and 4-3 that, both trend-lines illustrate a negative relationship of the uniformity coefficients over time. Furthermore, in residual soil layer (final production of weathering) this relation is nearly unchanged (Figure 4-2). However, when comes to the completely weathered layer (Figure 4-3), this change is very significant. It points out that in the second layer, the speed of the process of breaking soil particles still happens strongly.

Based on (Eq. 3.2) and the linear functions of each trend-line in Figures 4-2 and 4-3, the values of DR were calculated, their results are presented in Table 4-2.

Table 4-2: The increase rate of weathering of uniformity coefficient Cu for grain size analysis at 16th year

Depth (cm)	DR (% per year)
80	0.032
180	5.568

The table shows a decrease trend of the uniformity coefficients (Cu) in both soil layers over time. It is also can be seen that, the speed of reduction happens much quicker in 80cm depth layer than in the lower one.

4.1.2. Void ratio and porosity

Weathering leads to a porous structure due to the considerable leaching of minerals from the soil. Water and air replace the soluble minerals resulting in a porous structure (Rahardjo, et al., 2004).

The relationship between the void ratios subjected to time (Figure 4-4) and (Figure 4-5) were drawn based on linear trend-line from the laboratory testing results (see Appendix C).

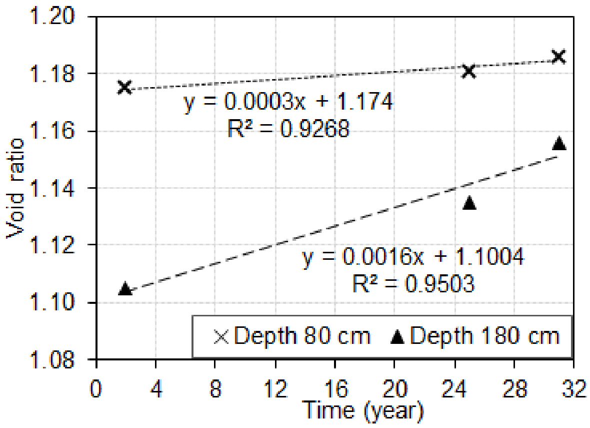

Figure 4-4: The relationship between void ratio of two soil layers on selected slopes subjected to time

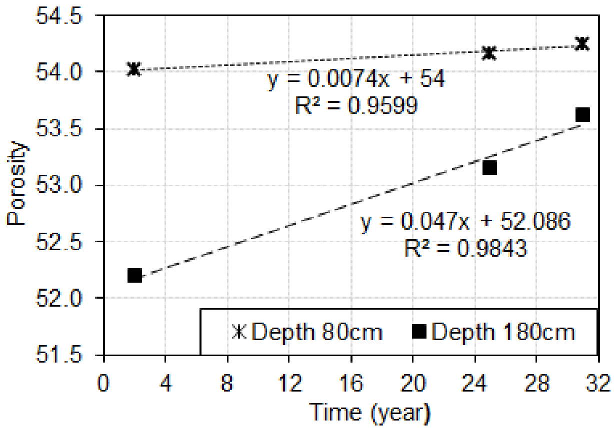

Figure 4-5: The relationship between Porosity of two soil layers on selected slopes subjected to time

The achieved figures show that Void ratio and Porosity in the top soil layer are higher and experiencing less change. While in the lower layer, this change is more considerable. This is consistent with what has been observed from the grain-size distribution analysis results when the trend-lines of void ratios and porosities subjected to time indicate an adverse relationship in compare to the trend-lines of the uniformity coefficients versus time in soil grain size. This comment is easier to see based on the IR values of void ratio and porosity which were calculated based on (Eq. 3.2). All the results are presented in the table below.

Table 4-3: The IR of soil void ratio & soil porosity of soil in the study area at 80 & 180 cm at 16th year

Depth (cm)	IR (% per year)	
	Void ratio	Porosity
80	0.03	0.01
180	0.14	0.09

4.1.3. Natural moisture content and volumetric moisture content

The natural moisture content (w_n) is the ratio of the mass of water dividing by the mass of solids in the soil (Craig., 2004) while the volumetric water content θ_v can be calculated by converting the mass of water lost on drying to a volume, and then dividing by the sample volume (IAEA, 2008). The two definitions are different but they both represent for the amount of water that distributed within the soil mass so there should not much difference in the values between them. In this study, w_n was defined by laboratory works, θ_v on the other hand was achieved throughout field measurements.

Figure 4-6 illustrates the variation of w_n (samples taken on 2/10/2010) for both soil layers of the study slopes over time. According to Gupta (2008) the optimum moisture content depends on the degree of fineness of the soil. It is likely to be true in this study since as the proportion of fine grains increase gradually over time (Section 4.1.1), the increase of moisture content with time and depth also was observed.

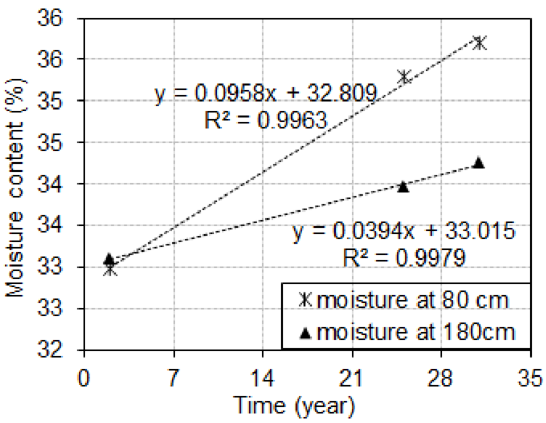

Figure 4-6: Plot of natural moisture content of study slopes & time of soil at 80 cm & 180 cm

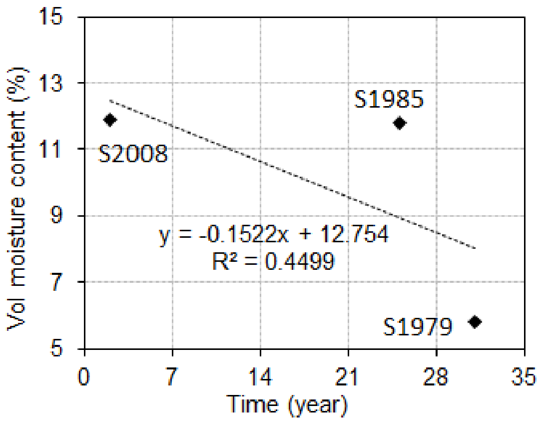

Figure 4-7: Plot of volumetric moisture content of study slopes & time of soil at 180 cm

Figure 4-7 is the θ_v (measured on 10/10/2010) over time for the soil at 80m depth. Based on the distributions of moisture tubes (see Figure 3-7), it is reasonable to say that Tube A represents for S1975, tube B represents for S1985, and the data from Tube F can be assigned for S2008.

On the day of measuring, it was cloudy, and also in the period of 7 days before that, there was no rain. Therefore, more or less the same results of the trend-line were achieved during this period. However, as can be observed, the trend-line of θ_v is scattered and totally different from the trend of w_n, the points' values are also much smaller. The problem might lie on the data of θ_v. As after the assess tubes were installed by drilling & pushing, soil around the tubes were disturbed, pores around the tubes could be created. And these pores can affect the measuring results. In this case, the reason might be the time for the tubes to be stable were not enough or the processes of installing access tubes were not successful. Therefore, assessing the rate of weathering was only conducted with the moisture content.

IR of soil moisture contents (Table 4-4) were calculated according to the linear functions in Figure 4-6, and Eq.3.2, all the results are presented in Table 4-4.

Table 4-4: Values of IR for moisture content at 80sm & 180 cm of soil in the study area at 16th year

Depth (cm)	IR (% per year)
80	0.28
180	0.12

4.1.4. Atterberg limits

The tests were carried out to find more evidence about the influence of weathering on the degradation of soils in the study area. Furthermore, the Atterberg limits can be used in soil classification. From the testing results (see Appendix C), the variation of liquid limits and plastic limits over time and depth and hence over the degree of weathering are illustrated in Figure 4-8 and Figure 4-9 respectively

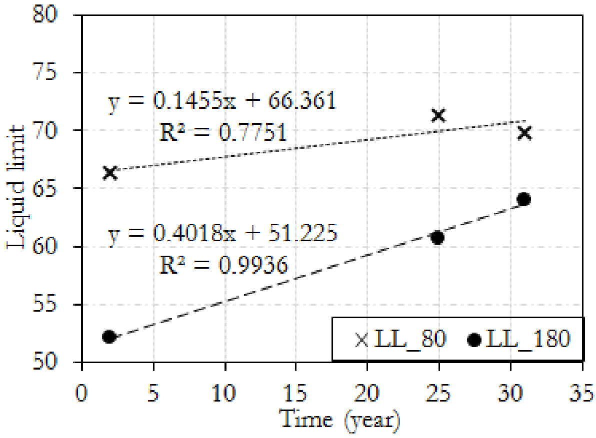

Figure 4-8: The variation of Liquid limit at 80 & 180cm over time

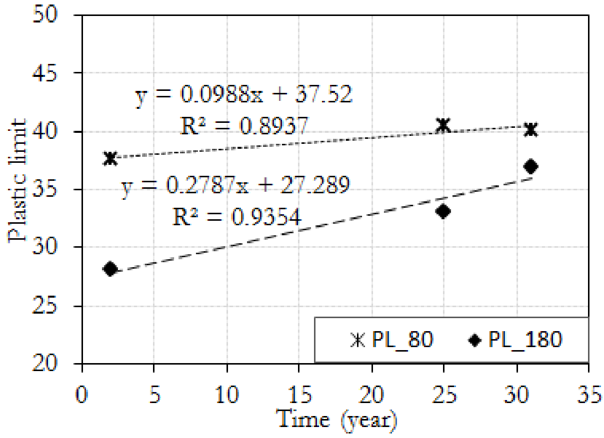

Figure 4-9: The variation of Plastic limit at 80 & 180 cm over time

In theory, it is believed that soil that has higher proportion of fine grain sizes also has high Atterberg limits since its ability to absorb water is better. This rule is indicated in the figures above. For the upper layer, with the dominant of fine grain size proportion, it has higher Atterberg limits. Also, its rate of reduction over time is less than in the lower layer.

The values of IR for Atterberg limits were calculated used (Eq. 3.2) and the linear equation shown in Figure 4-8 and 4-9, the results are in the table below

Table 4-5: Values of IR for Atterberg limits at 80cm & 180 cm of soil in the study area at 16th year

Depth (m)	IR (% per year)	
	Plastic limit	Liquid limit
80	0.25	0.21
180	0.89	0.70

Table 4-5 shows the increasing rate of Atterberg limits in residual soil layer (80cm) and completely weathered soil layer (180cm)

4.2. Effect of weathering on soil engineering properties

4.2.1. Saturated hydraulic conductivity (Ksat)

The results of saturated hydraulic conductivity are shown in Appendix C. Based on these results, a linear trend-line used to evaluate the impact of weathering as well as to predict the future of the saturated hydraulic conductivity of soils on the study slopes were drawn (Figure 4-10). From this figure, the trend of increasing permeability over depth and decreasing permeability over time can be seen. Observation from the field also shown that, the general profile of permeability is a permeable soil layer on impermeable bed rock. The permeability of soil increase significantly to a certain depth in the moderately weathered layer (Figure 3-8), then from there it starts to reduce quickly to the impermeable layer (rock head).

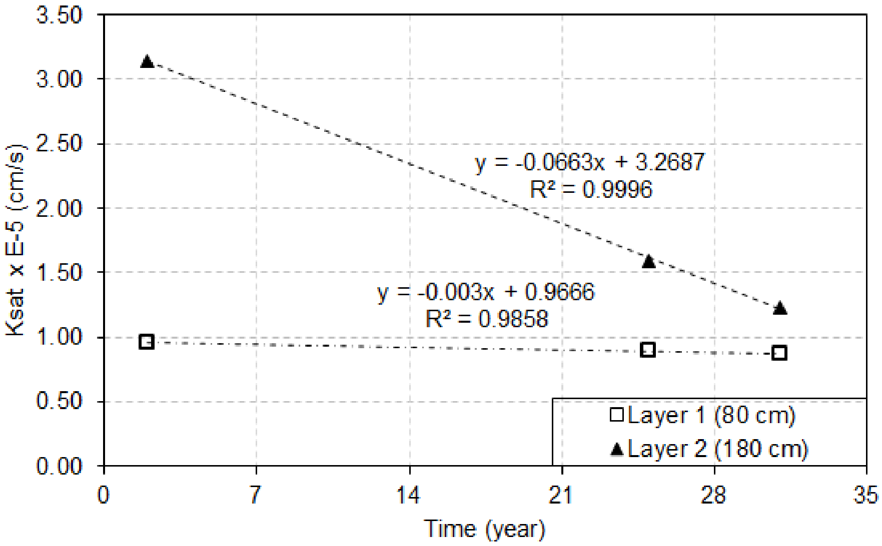

Figure 4-10: Saturated hydraulic conductivity of soil in cut-slopes of different ages

From the linear equations in the above figure and using (Eq.3.2), the DR of saturated permeability coefficient (Ksat) was defined. Its values are presented in Table 4-6

Table 4-6: Values of DR for saturated hydraulic conductivity of soil at 80sm & 180 cm in the study area at 16th year

Depth (cm)	DR (% per year)
80	0.33
180	2.92

The values of DR in Table 4-6 indicate that there is a reduction in the value saturated permeability coefficient with time. The speed of reduction is much more significant in completely weathered soil (180cm) rather than residual soil (80cm)

4.2.2. Soil – Water characteristic curve (SWCC)

The SWCC, typically the desaturation or moisture retention curve, is a continuous sigmoidal function representing the water storage capacity of a soil as it is subjected to increasing soil suction (M. D. Fredlund et al., 1996). When the soil becomes more weathered, more clay minerals are formed and the ability of the soil to retain water under high matric suction increases. Therefore, the SWCC of a soil reflects its pore-size distribution and hence the degree of weathering (Rahardjo, et al., 2004). Based on the results tested in the laboratory (see Appendix B-2), the soil-water characteristic curves for all separated soil layers are drawn as in Figure 4-11.

From Figure 4-11, it can be seen that the volumetric water content starts to decline considerably from around 40 Kpa. Here there are two groups of graphs; the first group has high matric suction values, representing for the upper layer. The second group is with much lower matric suction, stands for the lower layer. The matric suctions of the three slopes do not show much different in the upper layer (residual soil), but they do in the second layer (completely weathered soil). There is a large difference between the SWCC of S1979 and S2008 because of the higher content of fine particles and also due to the difference in saturated volumetric water content. Base on the graph in Figure 4-11, it can be concluded that the saturated volumetric water content and its corresponding matric suction decrease with depth and the age of cut-slopes.

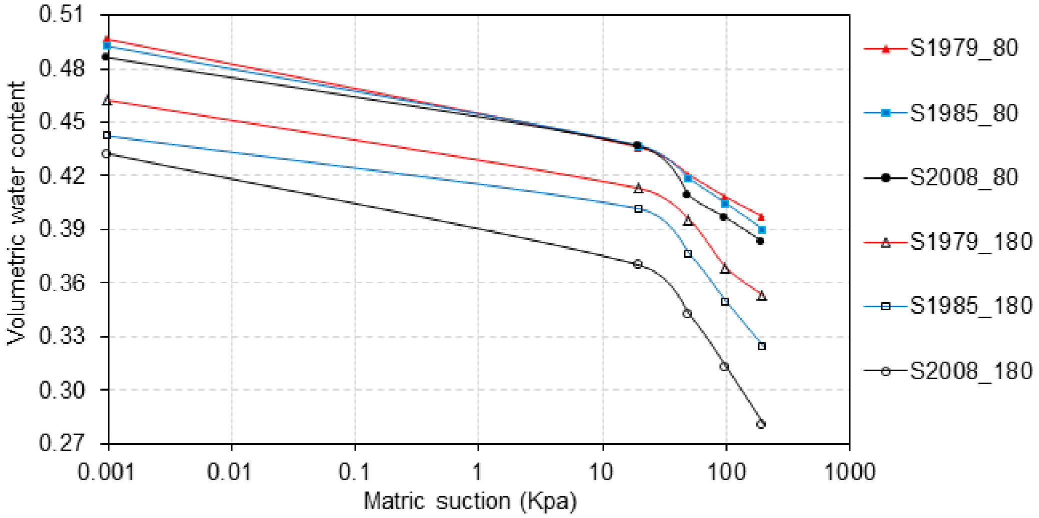

Figure 4-11: The Soil-water characteristic curves of soil in cut-slopes of different ages

The relationship between unsaturated coefficients of permeability versus matric suction (Figure 4-12) also can be drawn based on the SWCC testing results.

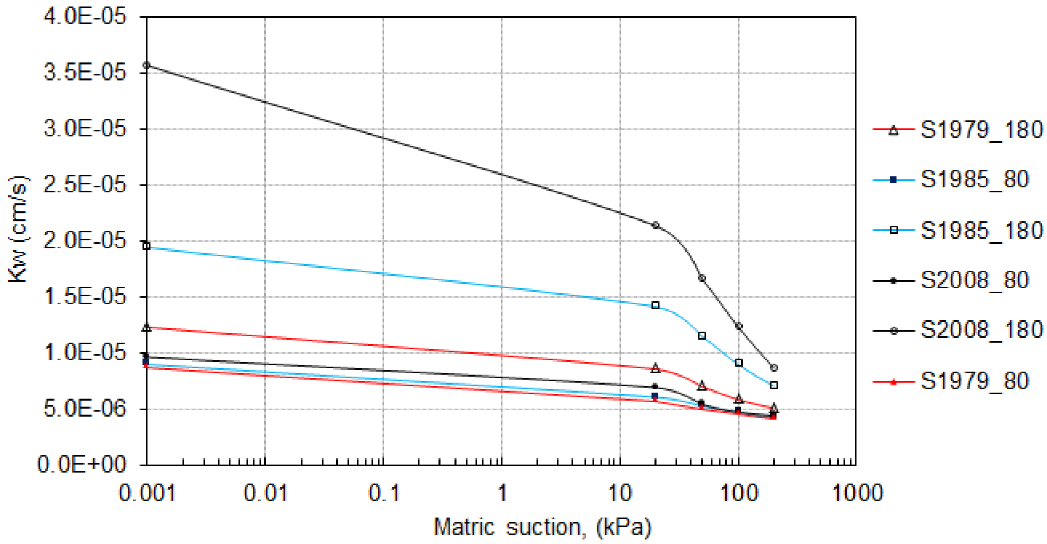

Figure 4-12: Unsaturated hydraulic conductivity & soil matric suction in cut-slopes of different ages

The above figure is the relationships between the coefficient of permeability and matric suction of six soil layers from three different cut-slopes which are 2; 25 and 31 years old. As can be seen, slopes those have different degree of weathering (different life time) show very different coefficient of permeability, especially with lower soil layers which lie on the depth of 180cm. The permeability of the new cut-slope (2 years old) is about three times larger than the 31 years old one. However, in the same conditions the permeability of all top layers (residual soil) is more or less the same.

4.2.3. Unconfined compressive strength from pocket penetrometer tester

The original testing results were presented in Appendix A-1. Figure 4-13 illustrates the relationship between the average values of unconfined compressive strength of soil layers on the selected slope subjected to time.

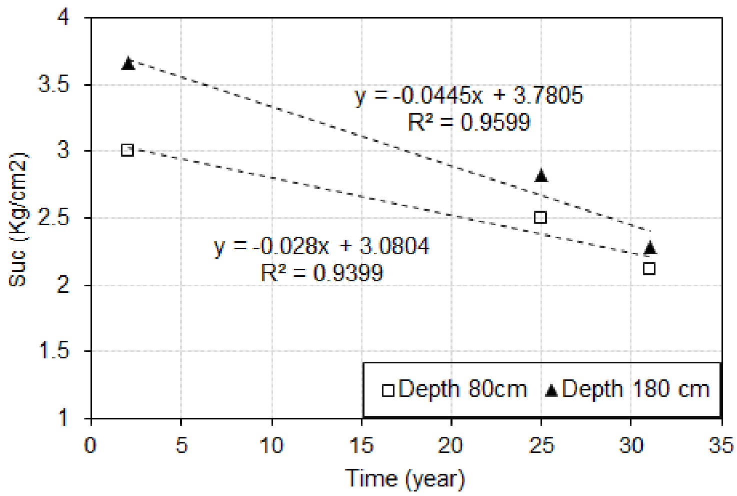

Figure 4-13: Results of pocket penetrometer tests in cut-slopes of different age at 80 cm & 180 cm

Based on the linear equations shown on the above figure and (Eq.3.2), the DR of unconfined compressive strength was defined. Its values are presented in Table 4-7

Table 4-7: DR Values for soil unconfined compressive strength at 80 & 180 cm in the study area at 16th year

Depth (cm)	DR (% per year)
80	1.051
180	1.430

The reduced trend of unconfined compressive strength over time is shown in this table, with the value of 1.051 in residual soil layer and 1.43 for the completely weathered soil, the difference of compressive strength reduction in both soil types is not significant.

4.2.4. Shear strength parameters

As indicated in Section 3.3, both field tests and laboratory tests were performed to assess the soil shear strength parameters in the study area. Among them, the pocket vane tests were used for undrained shear strength. In the laboratory, direct shear tests were executed to define effective shear strength parameters including effective cohesion c' and effective internal friction φ'.

4.2.4.1. Undrain shear strength from pocket vane shear tester

Figure 4-14 shows the result of pocket vane shear tests. The original data was presented in Appendix A-2

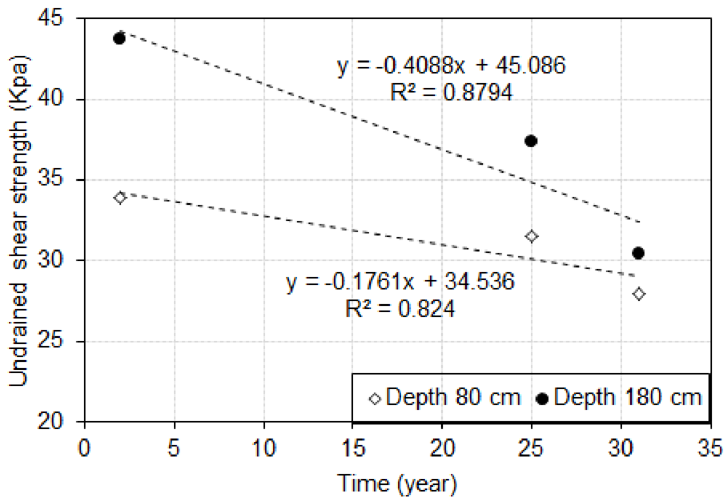

Figure 4-14: Results of pocket vane shear tests in cut-slopes of different ages at 80 cm & 180 cm

The figure illustrates a negative correlation between undrained shear strength and time. This reduction over time is quite significant especially in the layer with the depth of 180 cm. Table 4-8 with DR values those were calculated based on the linear equations in Figure 4-14 and Eq. 3.2 also shows this trend.

Table 4-8: Values of DR for undrained shear strength at 80sm & 180 cm of soil in the study area at 16th year

Depth (cm)	DR (% per year)
80	0.552
180	1.049

4.2.4.2. Shear strength parameters from direct shear tests

In this study, the effective cohesion, c', and the effective friction angle, φ' of residual soils from two different depths were calculated based on the direct shear test results (see Appendix B-4). Since the target of this thesis is to compare the influence of weathering on the shear strength parameters of soil, the shear strength parameters in saturated condition will be used as the comparative factors. The summary of average saturated shear strength parameters of residual soil in the study area at 80 cm and 180 cm are shown in Table 4-9 and Table 4-10.

Table 4-9: Shear strength parameter of residual soil (Grade VI) – 80 cm in cut-slopes of different ages

Age	c' (Kpa)	φ'(Deg)
2	18.90	19.50
25	19.10	18.50
31	21.50	17.07

Table 4-10: Shear strength parameter of residual soil (Grade VI) – 180 cm in cut-slopes of different ages

Age	c' (Kpa)	φ'(Deg)
2	17.00	28.28
25	18.00	22.38
31	18.30	20.45

Effective cohesion values for the residual soil are slightly higher than for the completely weathered soil, whereas the effective angle of internal friction is much less for the residual soil compared to the completely weathered material. In Figure 4-15 this trend is shown more clearly.

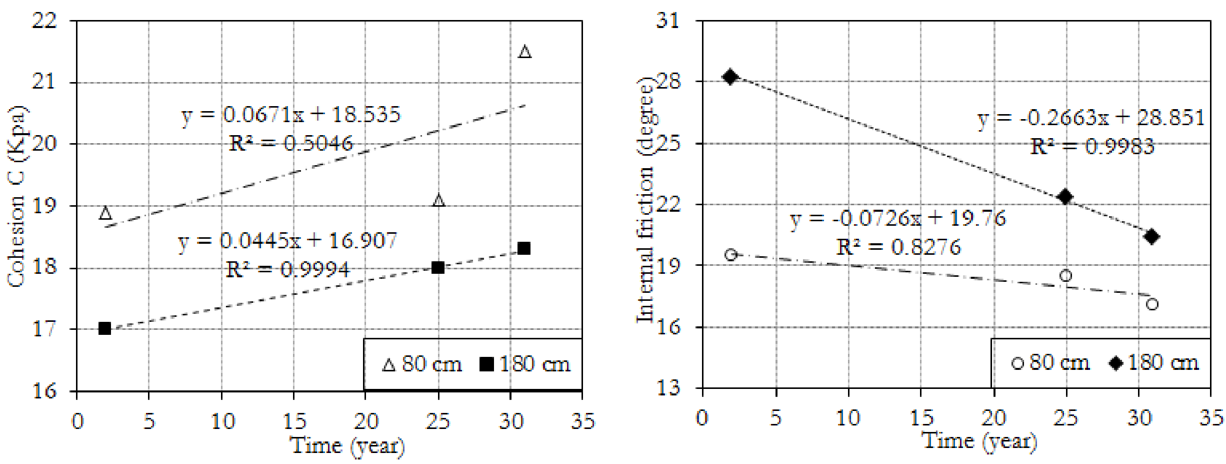

Figure 4-15: The relation between soil shear strength parameters and time in the study area

The effective cohesion c' decreases with time; soil material in older slope has larger effective cohesion than the younger one at the same depth. On the same slope, c' of soil is smaller at deeper depth (Figure 4-

15). On the other hand, the effective internal friction of soil is inversely proportional to time, hence, the internal friction decreases over time and increase with depth. Take time factor into account, at 1.8m depth in S2008, φ' is 28.28^0 while this value is 20.45^0 in S1979 with the same conditions.

Based on the linear equations shown on the above Figures and (Eq.3.2), the values of IR for the effective cohesion c' and DR for internal friction of soils in the two layers were defined. The results are presented in Table 4-11

Table 4-11: Weathering rate values of the shear strength parameters in the study area at 16^{th} year

Depth (m)	IR (% per year)	DR (% per year)
	Effective cohesion	Effective internal friction
80	0.343	0.389
180	0.253	1.071

The shear strength of soils in general show an inverse relationship with the degree of weathering (Rahardjo, et al., 2004). The shear strength parameters of residual soil from the selected slopes seem to decrease with time. This could be proved on the next Chapter which is about slope stability assessment.

4.3. Conclusion

The results of the index properties and engineering properties analysis show that under the influence of weathering, the values of important of soil parameters change over time. Together with the reduction of soil grain sizes and soil permeability, the shear strength of soil decreases. The speed of these processes seems to be inversely proportional to time. It is likely that there may be a moment that the shear strength of soil on these slopes reduces to a threshold and failures occur.

5. SLOPE STABILITY ASSESSMENT

The previous chapters showed that weathering processes change the values of slopes stability affecting parameters, both in terms of strength and in their hydrological characteristics. In this chapter the consequences of these changes on the safety factor of the slope will be demonstrated. As outlined in the methodology section Chapter 3, the software GEO-STUDIO 2004 would be used to calculate the stability of selected slopes using the method of Bishop (see Section 2.4.3)

5.1. Required data for slope stability calculation

To assess the influence of weathering on the stability of man-made slopes, three cut-slopes which have different lifetime were selected (see also Section 3.2.2). They are a 2 years old, 25 years old and 31 years old cut slopes. The conditions for selection have been mentioned in detained above (Section 3.1.1). A two-steps approach has been applied to assess the stability of the slope. Step 1: To assess the initial pore-water pressure (hydrological boundary) conditions using SEEP/W. This step is further explained in Section 5.2, and Step 2: To assess the stability of the slope, using SLOPE/W. This step will be made clear in Section 5.3.

The required data required for stability problems using SLOPE/W that intergraded with the initial pore-water pressures from a SEEP/W file has been discussed in Section 3.1.2. They includes: a slope profile, material properties as the internal factors and rainfall conditions as the external factor.

5.1.1. Material properties

The material properties required for slope stability assessment was taken from laboratory testing results. Except from the soil-water characteristics, these data are summarized in Table 5-1. In this table, the value of ϕ^b(explained in Section 2.3.2) is not mentioned but according to John Krahn (2004b), for practical purposes, ϕ^bmight be taken as half of φ'.

Table 5-1: Testing data for slope stability calculation

Testing categories	Symbol	Unit	Slope's Symbol					
			S1979		S1985		S2008	
			Depth (cm)		Depth (cm)		Depth (cm)	
			80	180	80	180	80	180
Unit weight	γ_w	T/m^3	1.695	1.697	1.687	1.700	1.662	1.710
Saturated unit weight	w_s	T/m^3	1.758	1.766	1.754	1.766	1.756	1.775
Direct shear test (Unsaturated condition)	φ'_w	Deg	18.68	20.55	19.55	23.6	20.3	30.12
	c'_w	kg/cm^2	22.00	22.500	21.6	21.9	21.500	21.200
Direct shear test (Saturated condition)	φ'_s	Deg	17.58	19.85	18.68	22.38	19.8	28.72
	c'_s	kg/cm^2	18.5	18.4	0.18	0.18	18	17.2
Permeability	K_{sat}	cm/s	8.68E-6	1.20E-5	8.97E-6	1.59E-5	9.59E-6	3.00E-5

5.1.2. Rainfall data

Rainfall data is required for pore-water pressure calculations. In this study, following types of rainfall data were used:

1. Average daily rainfall in dry seasons
2. Average daily rainfall in the wet seasons

3. Critical rainfall in the area over the past 10 years from 2000 to 2009

These types of rainfalls would be explained in a more detailed way in the next Section.

5.1.3. Slope cross-sections for stability computations

Three different slope cross-sections have been described in Section 3.2.2 representing for a 2 years old slope (S2008), a twenty five years old slope (S1985) and a thirty one years old slope (S1979) would be used. These sections should have the same high and inclination angle. Due to the influence of weathering, engineering characteristics of soil layers must be different. Observations in the field area show that the slope angles of cut-slopes in Yen Bai vary from 65^0 to 75^0. Cross-sections used in this stability assessment have a slope angle of the slope angles of cut-slopes in Yen Bai, three types of slope values which are 65^0, $70^0$and 75^0 would be taken into account. Cross-sections used for modelling having a slope of 70^0 corresponding to three different life time were shown in Figures from 3-9 to 3-11 Section 3.2.2.

5.2. Modelling the seepage conditions within the study slopes for stability calculations

A transient analysis by definition means one that is always changing. It is changing because it considers how long the soil takes to respond to the user boundary conditions (Krahn, 2004a). Before doing the calculations for the stability of slopes, models of initial conditions of pore-water pressure must be built. These initiation models are then imported into the stability models for defining the factors of safety. The negative pore water pressure distribution of the slope is simulated under the impact of rainfall in Yen Bai.

Carrying out this transient seepage modelling, first a steady- state analysis was conducted to create a hydrostatic condition. This analysis uses the average rainfall in the dry seasons. After that, the transient seepage model is built using the steady-state condition combining with the rainfall condition in rainy seasons.

5.2.1. Assumptions used in seepage analysis

SEEP/W is a powerful computer software program for seepage analyses. However, in this certain case, hypotheses are required.

1. The simulated cross-sections sketched for the seepage models are large enough so that except from the infiltrated surface, there is no connection between the left and bottom boundaries on the cross-sections with their surroundings. Therefore, the results of pore-water pressure conditions calculated from these models in the region of the predicted slope failure plane can be considered to be the same like in reality.
2. The only process that effects seepage condition within the slope is infiltration, there is no evaporation happening on the surface of the slope during computation.
3. The material within each soil layer is homogeneous; the influence of tree roots, cracks or fissures is not taken into account.
4. For rain intensities smaller than the saturated conductivity (Ksat) of the top soil, all rainfall infiltrate into the surface, else the exceeded amount will become runoff and flow down the slope and the appearance of runoff does not influence seepage conditions within the slope.

These assumptions will be discussed further in Section 7.2.1 (discussion part).

5.2.2. Assign rainfall boundary condition into a SEEP/W model

In SEEP/W 2004, the rainfall's characteristics are assigned in the form of a small "q" unit flux boundary condition which is a flux value applied along a mesh edge (Figure 5-1). SEEP/W can automatically compute and accumulate any seepage face water that comes out of the ground (Geo-Slope INTERNATIONAL, 2008a). For steady-stage analysis, rainfall is assigned as a single value for intensity. However, for transient seepage analysis, the applied rainfall in this case was assigned into SEEP/W as a function between rainfall intensity & duration. As mentioned in the hypothesis in Section 5.2.1, since there is no ponding on the surface of the slope, a value of pore-water pressure greater that zero is not permitted.

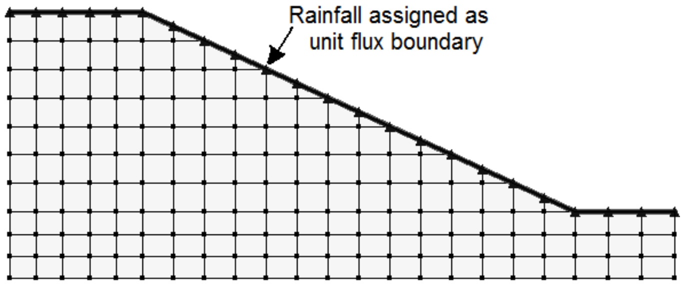

Figure 5-1: Assigned rainfall conditions on the slope surface in SEEP/W

Under the impact of the rain, there will be a redistribution of pore-water pressure inside the slope.
It is commonly believed that the first response of a slope to rainfall is an increase in saturation near the surface; followed by gradual groundwater recharge by vertical infiltration, resulting in a rise water table (Jiao et al., 2005).

5.2.3. Steady-state seepage analysis

Steady-state models were built to generate initial condition for transient seepage analysis. They were obtained by running a steady-state model with a so-called basic rainfall with an intensity of 8.21E-5 m/h. This is the mean daily rainfall during the dry seasons from January to April and November to December in the period of 1960 to 2009 (Figure 1-6).
The process to solve a seepage analysis using SEEP/W was expressed in Section 3.1.2.1. The results of steady-state analyses for the three standardized slopes were presented in Appendix D

5.2.4. Pore-water pressure of transient seepage flow under rainy seasons

The model of transient seepage flow in rainy seasons took the corresponding steady state model above and average daily rainfall in rainy seasons (Figure 1-6) as the input parameters. Based on the steps to solve a seepage analysis using SEEP/W explained in Section 3.1.2.1, the seepage models in rainy seasons were built. Their results were used later on in the assessing the influence of weathering on the stability of cut-slopes (Section 5.3.1.1).

Figure from 5-2 to 5-4 illustrate the distribution of pore-water pressure during rainy seasons within the 70^0 cuts that are two, twenty-five and thirty-one years old respectively.

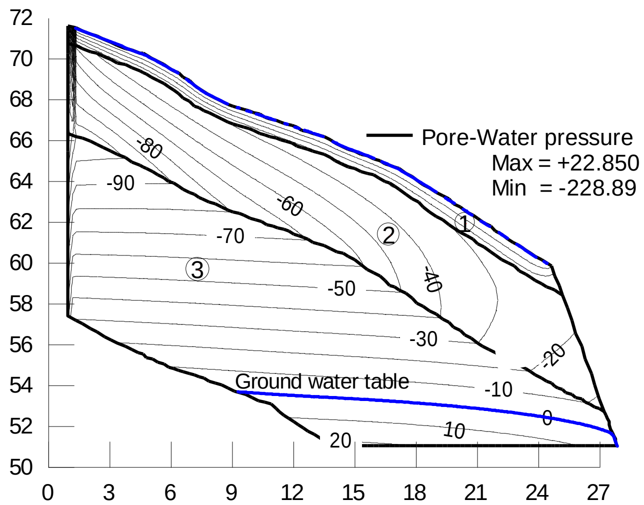

Figure 5-2: Distribution of pore-water pressure during rainy seasons within slope S2008

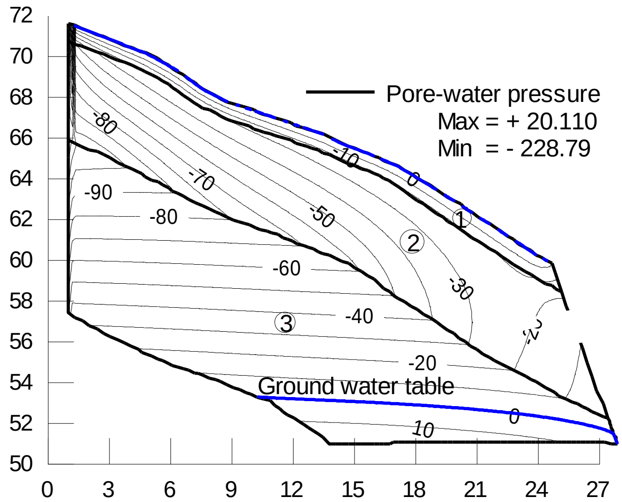

Figure 5-3: Distribution of pore-water pressure during rainy seasons within slope S1985

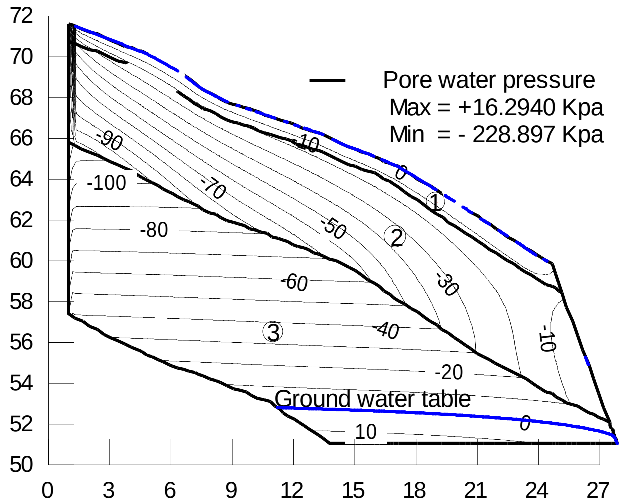

Figure 5-4: Distribution of pore-water pressure during rainy seasons within slope S1979

As can be seen in Figures 5-2 to 5-4, during rain events, when the rainfall intensity is larger than the top soil coefficient of permeability, a saturated layer is formed on the surface of the slope. The distributions of pore-pressures within the slopes are controlled by the location of ground water table and this saturated layer. This explains why there is a large difference between the pore-pressures within the top soil layers in dry and wet seasons (see Appendix D- the distribution of pore-pressures in dry seasons)

Using a vertical plane cut through the X – axis at X = 21m (Figure 5-6) (the position closes to the predicted slope failure based on the results of field observations). The difference between pore-pressure distributions within the slope during dry and rainy seasons can be clearly illustrated (Figure 5-5).

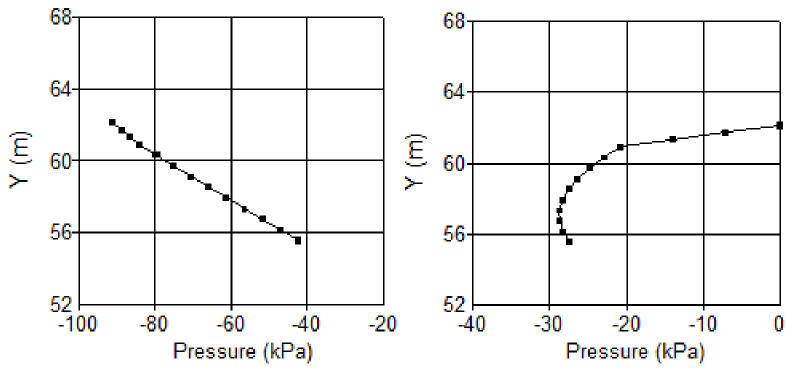

Figure 5-5: The pore -pressures in dry & wet seasons distributed with depth of 2 top layers at X =21m in S1985

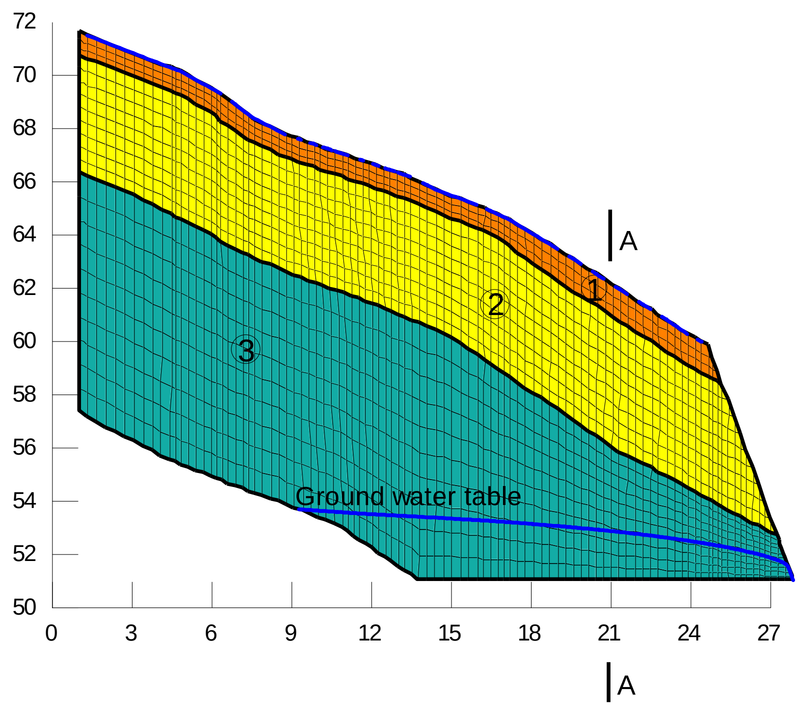

Figure 5-6: A vertical cut through X = 21m for pore-water pressure analysis

The variation of pore-pressures over the soil depth in wet seasons can be drawn (figure 5-6).

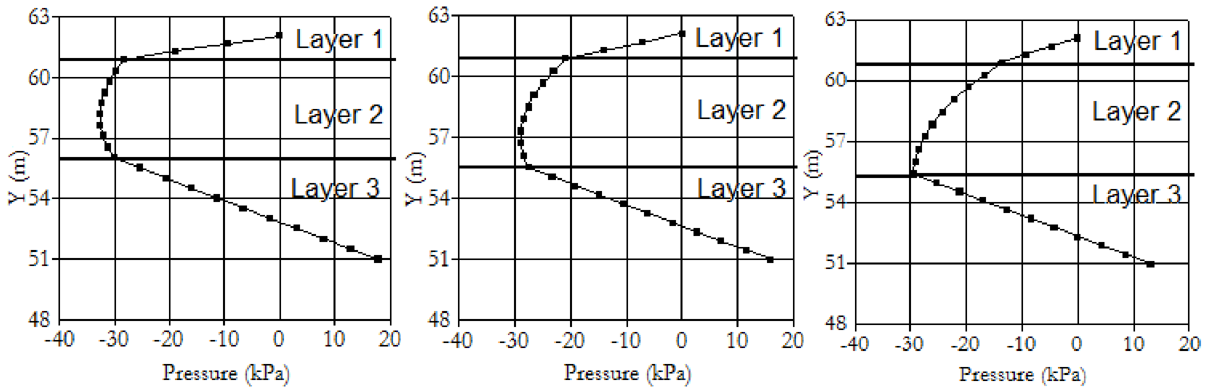

Figure 5-7: Distribution of pore-water pressures over the soil depth in wet seasons at A-A (X = 21m)

It was found in Figure 5-7 that, in all curves the pore-pressure starts from zero then it decrease significantly over depth in the top soil layer. In the second soil layer, the reduction is slightly; especially it is almost unchanged in S2008. Pore-water pressure start to increase considerably over depth until it reaches the bottom. The figure also shows that in the first two soil layers, under the same rainfall condition, the speed of pore-water dismissing decreases together with the age of the slope.

5.2.5. Pore-water pressure of transient seepage flow under critical rainfalls

The models considered the corresponding model of transient seepage flow in rainy seasons which have been simulated in the previous Section and critical daily rainfalls in the study area as the input parameters. The results of this model would be used as the input data in the stability models to calculate the stability of cut-slopes under critical conditions (Section 5.3.2)

5.2.5.1. Critical rainfall in Yen Bai

It is assumed that when the rainfall intensity is larger than the soil coefficient of permeability, the exceeded quantity will become runoff and does not have any effect on the stability of slopes (Section 5-2-1).

Therefore, the critical rainfall is believed to be the one that has long duration with the intensity larger than the top soil coefficient of permeability. Since during a rainfall, the intensity is not uniformity all the time and even short rainfalls when they meet the above requirements and happen really close to each other. These kinds of rain also have the same effect like a long one. Thus, finding a suitable critical rainfall is not an easy work. In this study, the methodology was to use old records about damages created by landslides and slope failures that happened as a result of rainstorm events to find the appropriate thresholds.

In August, 16th, 2006, a rainfall with high intensity happened continuously for three days. Followed by the failure of many cut-slopes mostly happened along the main roads around the city. Three people lived in Yen Ninh ward were killed and many houses were damaged due to this event. The other rainfall happened in August, 2008 with smaller average intensity but more or less the same duration and also this event caused massive properties damage. The intensity and duration of these two rainfalls were shown in Figure 5-8 and Figure 5-9.

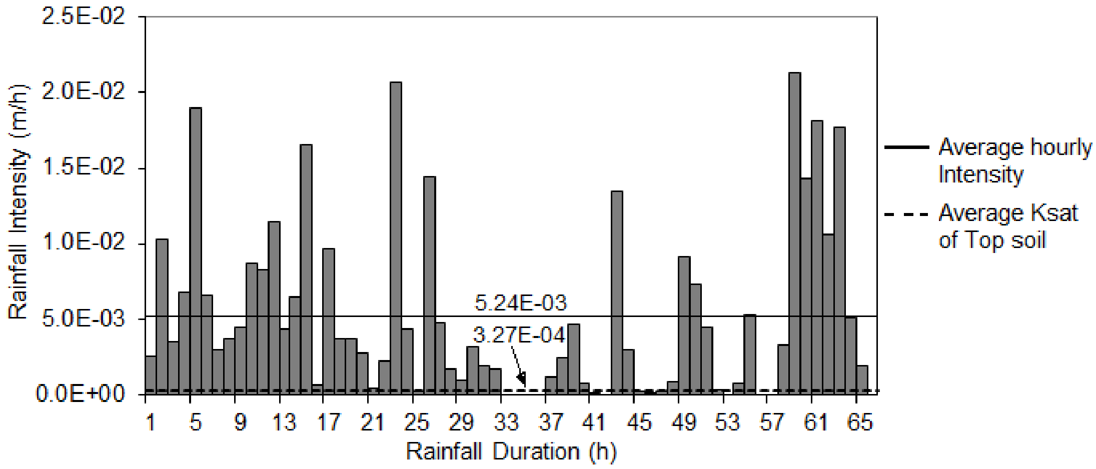

Figure 5-8: The Duration & Intensity of Aug, 2006 rainfall

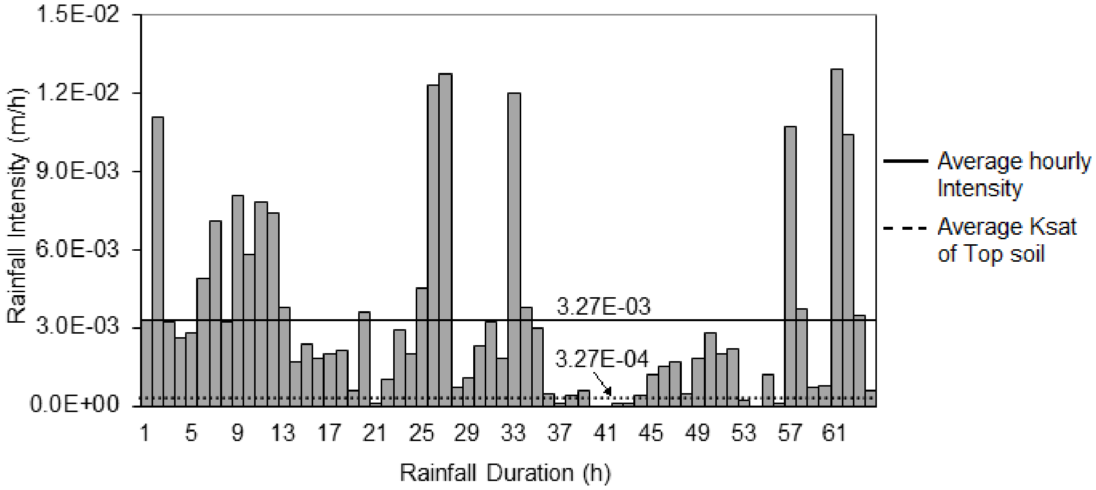

Figure 5-9: The Duration & Intensity of Aug, 2008 rainfall

5.2.5.2. Results of pore-water pressure simulation under extreme rainfalls

The results of transient seepage analysis for the 70^0slopes under the rainstorm events that happened in 2006 and 2008 are shown in Figures 5-10 to 5-15. These figures illustrate the distribution of pore-water pressure obtained with SEEP/W of the slopes which are 2 years, 25 years and 31 years old respectively.

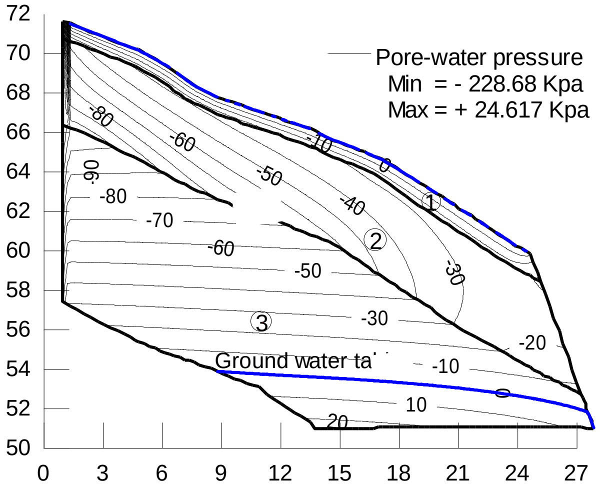

Figure 5-10: Distribution of pore-pressure within S2008 after 2006 rainfall event

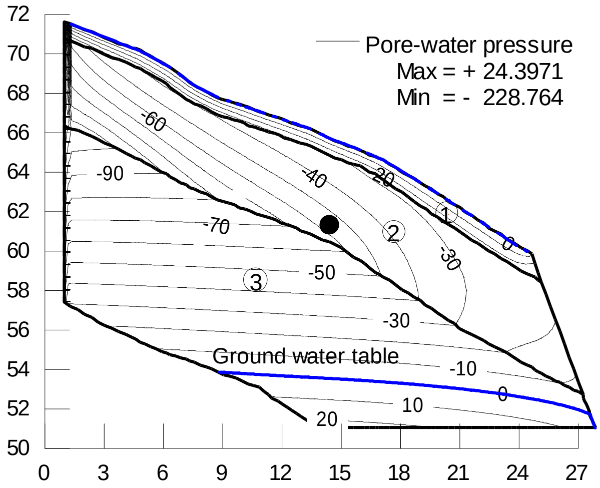

Figure 5-11: Distribution of pore-pressure within S2008 after 2008 rainfall event

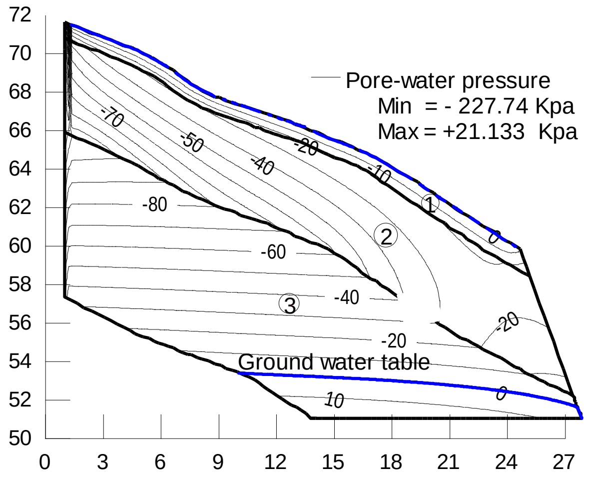

Figure 5-12: Distribution of pore-pressure within S1985 after 2006 rainfall event

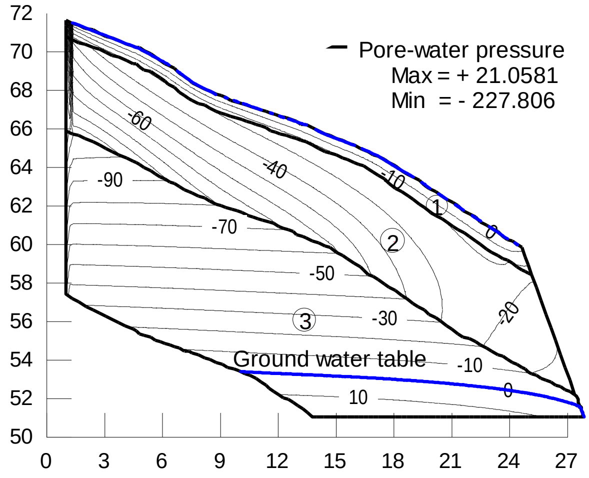

Figure 5-13: Distribution of pore-pressure within S2008 after 2008 rainfall event

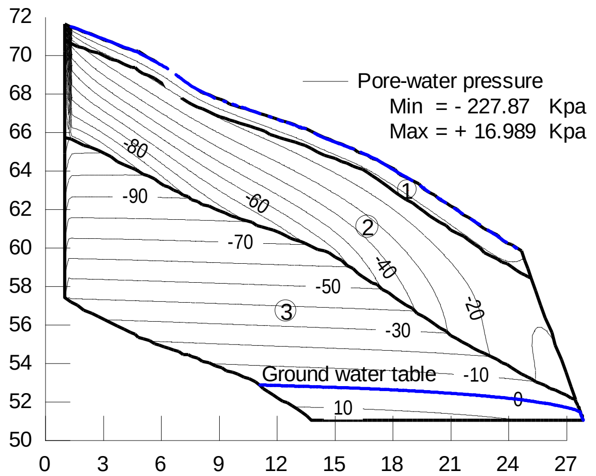

Figure 5-14: Distribution of pore-pressure within S1979 after 2006 rainfall event

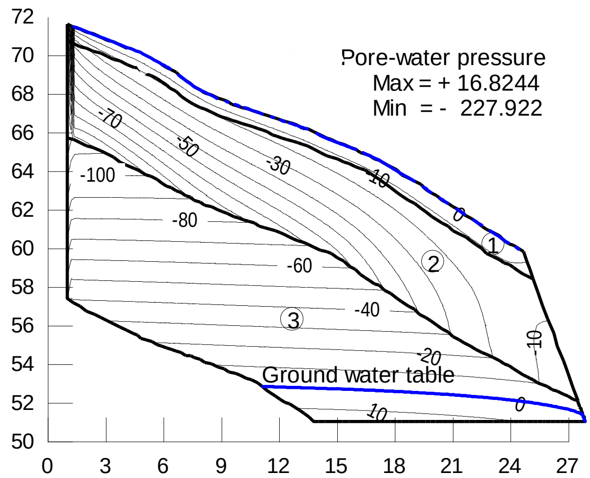

Figure 5-15: Distribution of pore-pressure within S1985 after 2008 rainfall event

It was found from these above figures that there are not many differences between the distributions of pore-water pressure inside these slopes in both critical rainfall conditions. With higher coefficient of permeability, the amount of water that infiltrates into S2008 and S1985 slopes is more than in the S1979 slope. This explains why the ground water table in the S2008 and S1975 slopes are a bit higher than in the S1979 slope as well as the positive pore-water pressure values.

The pore-pressures increase during the rainstorm as shown in Figures 5-16 to 5-18 for a) a point on the surface, b) a point in the middle of soil layer 1, and the final one in the middle of soil layer 2 (all three points are located at X = 21 m (Figure 5-6)), as shown in these figures, the deeper the point, the more significant the rate of the increase. It can be concluded that the worst pore-pressure condition is presented at the end of the storms.

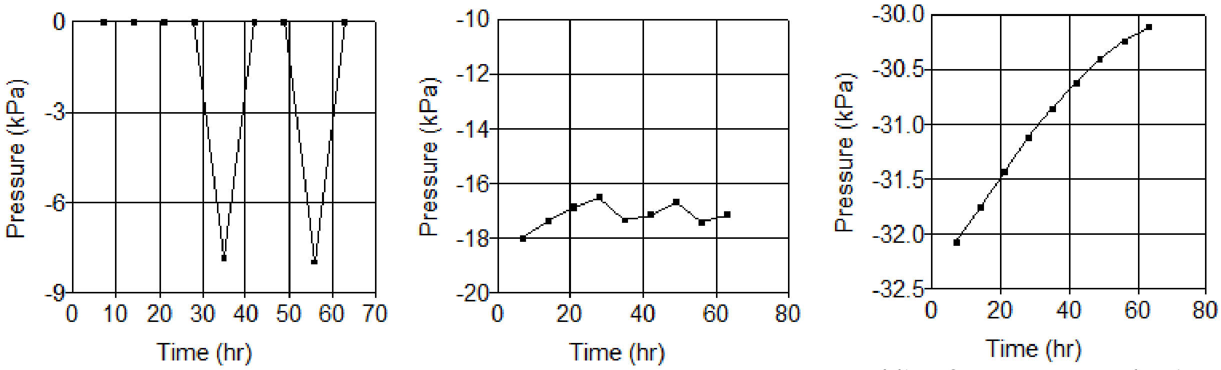

On the surface | Middle of layer 1 (0.8m depth) | Middle of Layer 2 (4.3m depth)

Figure 5-16: The change of pore-pressures during 2006 rainfall event at 3 separated depths- S2008

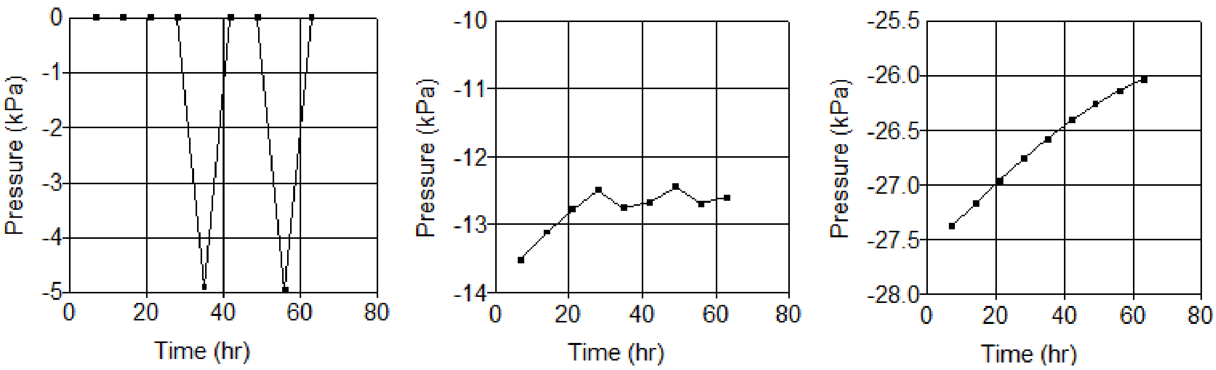

On the surface | Middle of layer 1 (0.8m depth) | Middle of Layer 2 (4.3m depth)

Figure 5-17: The change of pore-pressures during 2006 rainfall event at 3 separated depths - S1985

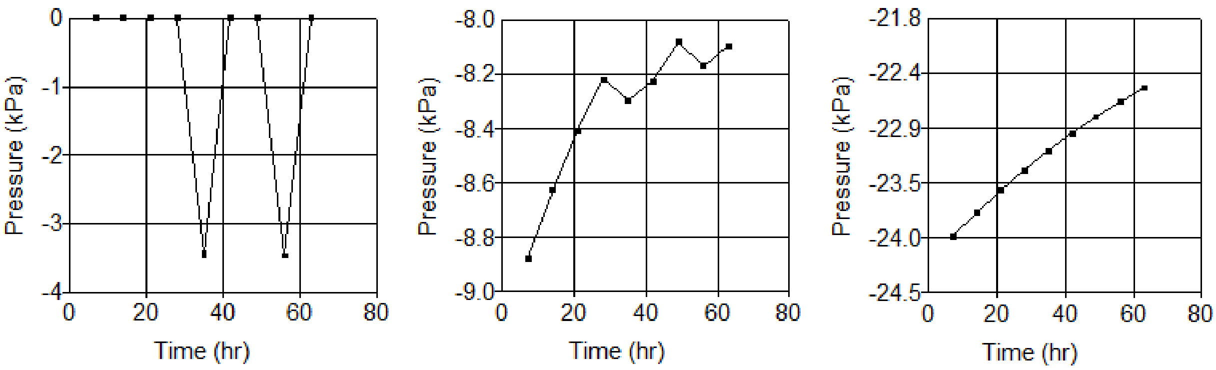

On the surface | Middle of layer 1 (0.8m depth) | Middle of Layer 2 (4.3m depth)

Figure 5-18: The change of pore-pressures during 2006 rainfall event at 3 separated depths - S1979

5.3. Slope stability calculation

As outlined in Section 3.1 and 3.2, calculations of the stability of slopes in this study aim to solve two purposes:

1. To evaluate the influence of the degradation of soil engineering properties due to weathering processes to the stability of cut-slopes.
2. To assess the stability study slopes under critical rainfall conditions.

For the first purpose, average daily rainfall in rainy seasons was considered. For the second purpose, two critical rainfall conditions corresponding to the rainfall events happened in 2006 and 2008 were considered. The reasons for choosing these rainfalls were explained in Section 5.2.5.1.

To meet the above purposes, the stability of 2 years old, 25 years old and 31 years old slopes were accessed. As observed results from the field show that the angles of cut-slopes in the study area range from 65^0 to 75^0 , so the assessment of slopes that are 2, 25 and 31 years old should cover this range. In this study, three different types of slope angles (65^0 , 70^0 and 75^0) were considered.

5.3.1. Slope stability evolution

The conclusions from Chapter 4 showed that weathering processes change the values of slopes stability affecting parameters, both in terms of strength as in their hydrological characteristics. This section will attempt to demonstrate the consequences of these changes on the safety factor of the slope.

Before building the model to calculate the stability for the study slopes, the corresponding SEEP/W models in rainy seasons which were built in Section 5.2.4 will be imported to SLOPE/W. The pore-water pressures in rainy seasons were chose in assessing the slope stability evolution as they represent for the whole rainy season. And when all study slopes suffer from the same conditions, it is more accuracy to make comparisons between their factors of safety.
The factors of safety from the stability models would be used to assess the stability evolution.

5.3.1.1. Stability modelling and its Results

Stability models were built using Bishop Method (Section 2.4.3) based on the results of corresponding SEEP/W models result (the distributions of pore-water pressures in rainy seasons) (Section 5.2.4), the required data used in slope stability calculation (Section 5.1). The modelling process was presented in Section (3.1.2.2).

The results of stability models are shown in Figures from 5-19 to 5-21 for the 70^0 slope. For the 65^0 and 75^0, the results were presented in Appendix E-1.

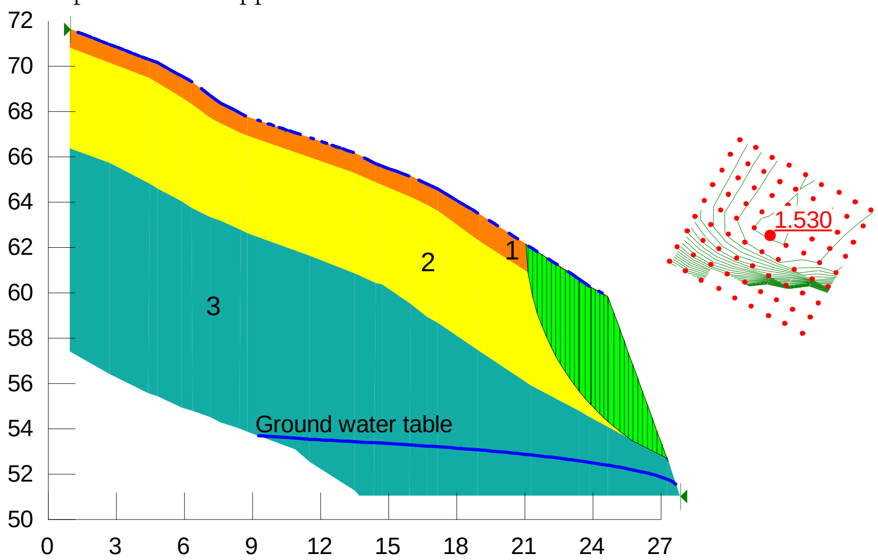

Figure 5-19: FoS of slope S2008 in wet seasons when the cut is 70^0

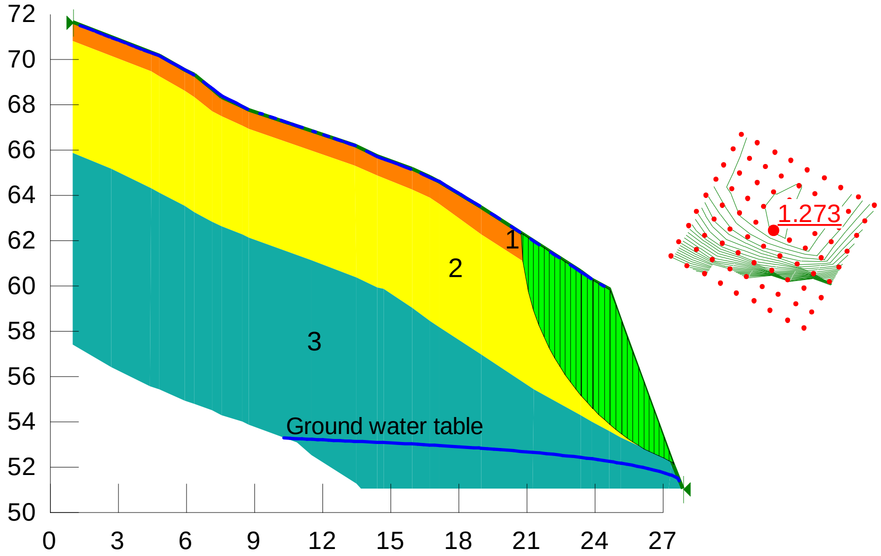

Figure 5-20: FoS of slope S1985 in wet seasons when the cut is 70^0

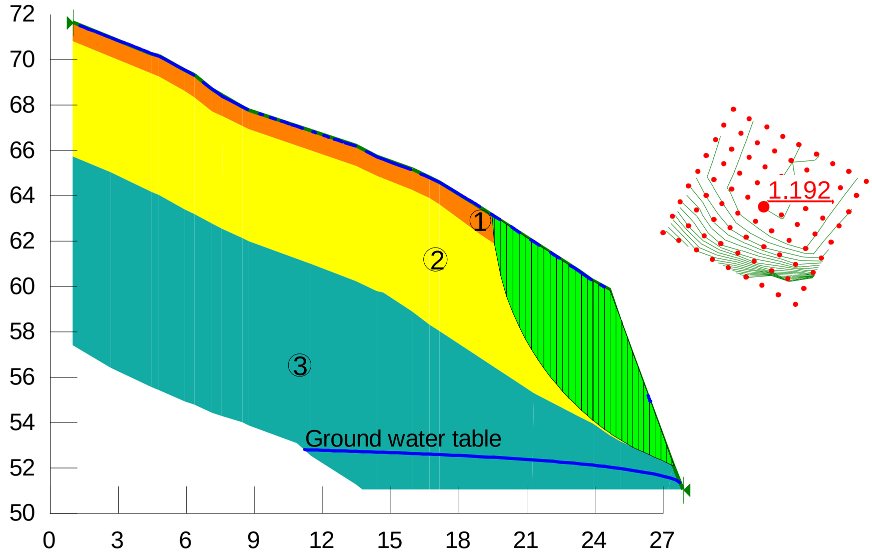

Figure 5-21: FoS of slope S1979 in wet seasons when the cut is 70^0

5.3.1.2. Slope stability evolution

All stability results in Section 5.3.1.1 were summarized in table 5-2

Table 5-2: FoS of selected slopes in rainy seasons for three different types of slope angle

Time (year)	Slope angle (degree)		
	65	70	75
2	1.602	1.53	1.484
25	1.325	1.273	1.234
31	1.243	1.192	1.149

Based on the values of factors of safety (FoS) shown in Table 5-2, the relationship between FoS ~ Time in this case were drawn as in Figure 5-22. One of the main character can be seen in this Figure is that the values of FoS decrease gradually with time, the longer the time, the lower the FoS. This is also resistance to all the conclusions have been made in Chapter 4.

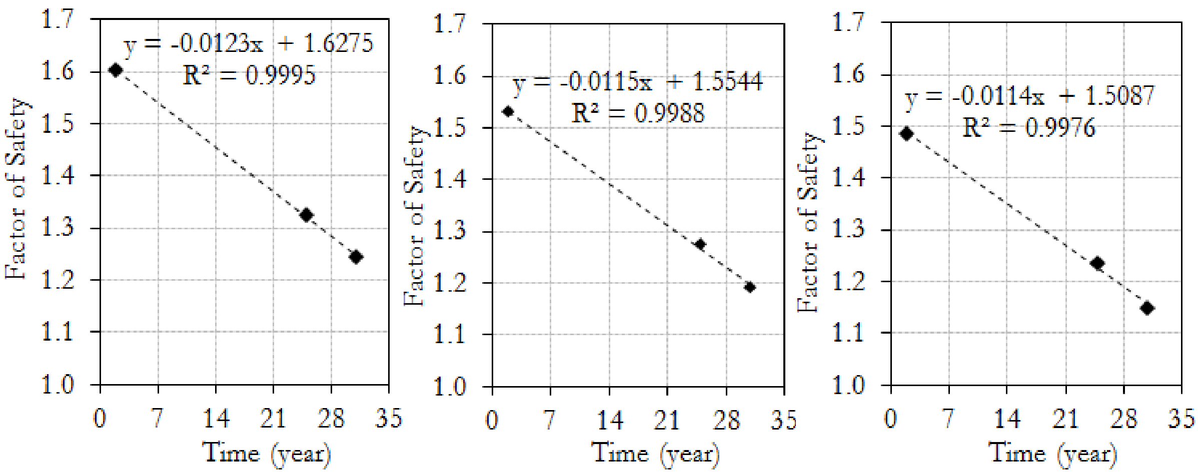

Figure 5-22: The relationship between FoS & Time of selected slopes in rainy seasons corresponding to three different study slope angles

All three trend-lines in Figure 5-22 have quite large coefficient of correlation indicating the linear regression lines that define the relationship between FoS over time of three cases study for each selected slope are reliable.

The linear regression equations in Figure 5-22 can be used: firstly to predict the future failures of selected cut-slopes in the study area. Secondly, they also help to find the reduction rate (IR) in safety factor of slopes as the consequence of the changes in effecting soil engineering parameters under the influence of weathering (see Eq. 3.2).

For the first purpose, according to the significance values of factor of safety (FoS) for design in Table 2-3, in the case of cuts, FoS = 1 would mean the slope is on the verge of collapse, while 1.2 signifies it is marginally stable, a situation should be avoided in a build-up environment. Therefore, FoS = 1.2 and FoS = 1 would be taken into account as the threshold values that need to evaluate. Based on equations shown in Figure 5-22, the estimated lifetime for cut-slopes in the study area were calculated and shown in Table 5-3.

Table 5-3: The estimated lifetime for cut-slopes in the study area

Slope angle	Years to FS = 1	Years to FS = 1.2
65	52	35
70	48	30
75	44	27

For the second purpose, Eq. 3.2 and equations on Figure 5-22 were used to calculate the DR of FOS. The results are shown in Table 5-4.

Table 5-4: The DR in safety factor of slopes as the consequence of the changes in slope stability affecting soil engineering parameters

Slope angle (Deg)	DR (% per year)
65	0.85
70	0.83
75	0.85

As can be seen, there is no rule for the variation of DR values corresponding to three different slope angle, they are around 0.85 and do not show many difference. This is likely to be true since these decrease rates in this case represent for the changing of slope stability affecting soil engineering parameters.

5.3.1.3. Conclusion

Under the influence of weathering, the lifetime of these slopes decrease gradually. The estimated times when FoS reaches 1 range from 44 years for the 75^0 slope to 52 years for the 65^0 slope respectively when no stability improvement methodologies are applied. For an engineering construction in an urban environment, this is not a long period and is also not encouraged.

5.3.2. Slope stability in extreme conditions

Observations in the field show that, cut-slopes in the study area often fall under the following situations:

- Degrading of slope's materials overtime leads to decrease in their shear strength.
- Being over cut
- Critical rainfalls

The first reason has been analysed in Section 5.3.1. Therefore, this Section only concentrates on assessing the stability of slopes under the latter two reasons. Among them, heavy rainfall is a critical factor in triggering landslides and slope failures in Yen Bai because it has the role to increase in pore-pressure in the vadose zone and may also lead to an increase in the groundwater table. In the evaluating the stability of slopes under extreme conditions in this Section, two rainfalls corresponding to the events happened in 2006 (Figure 5-8) and the other one happened 2008 (Figure 5-9) were considered. Section 5.2.5.1 explained clearly the reasons why these rainfalls were selected.

As discussed in the previous Section, man-made slopes in Yen Bai city have a range of inclination angle from 65^0 to 75^0 degree so the methodology here is still take these three types of slope angle into account.

5.3.2.1. Slope stability models under critical rainfall

The distribution of pore-pressures within the slopes at the end of the critical rainfall conditions have been calculated in Section 5.2.5.2 and it also has been proved in this Section that the worst pore-pressure condition is presented at the end of the storms. Therefore, the pore-pressure condition within the slope at the end of selected rainfall will be considered.

The stability models in this case were built using Bishop Method (Section 2.4.3). They use corresponding SEEP/W models of critical rainfalls (calculated in Section 5.2.5), the required data used in slope stability calculation (Section 5.1). The steps of modelling were expressed in Section (3.1.2.2).

5.3.2.2. Results and discussion

The factors of safety for all selected slopes were calculated based on the most extreme pore - pressures conditions which were the results of transient seepage analyses. The illustrated results for the 70^0 slope corresponding to the 2006 rainstorm event are shown in Figures from 5-23 to 5-25. Results for other case studies are demonstrated in Appendixes E-2 and E-3. Table 5-4 summaries all the calculated factors of safety for all case studies of the selected slopes in Yen Bai city

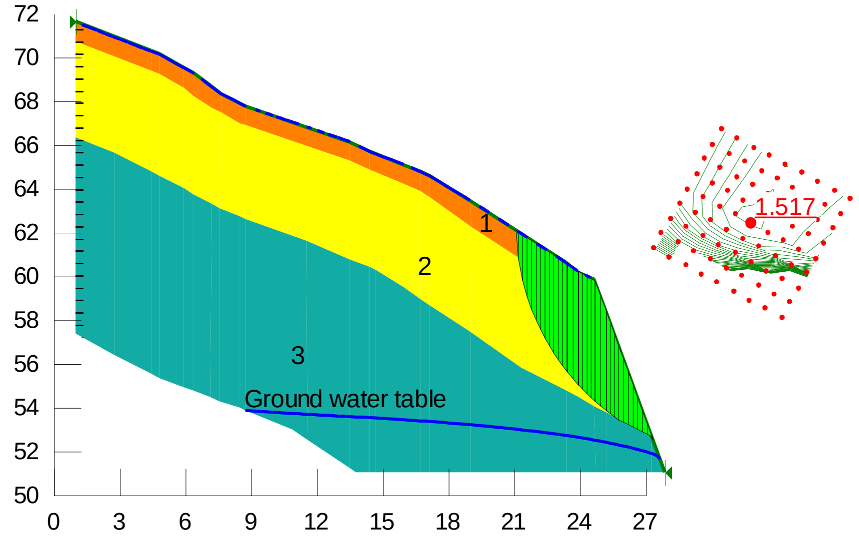

Figure 5-23: FoS of a 2 years old slope (S2008) with the slope angle of 70^0 in 2006 rainstorm event

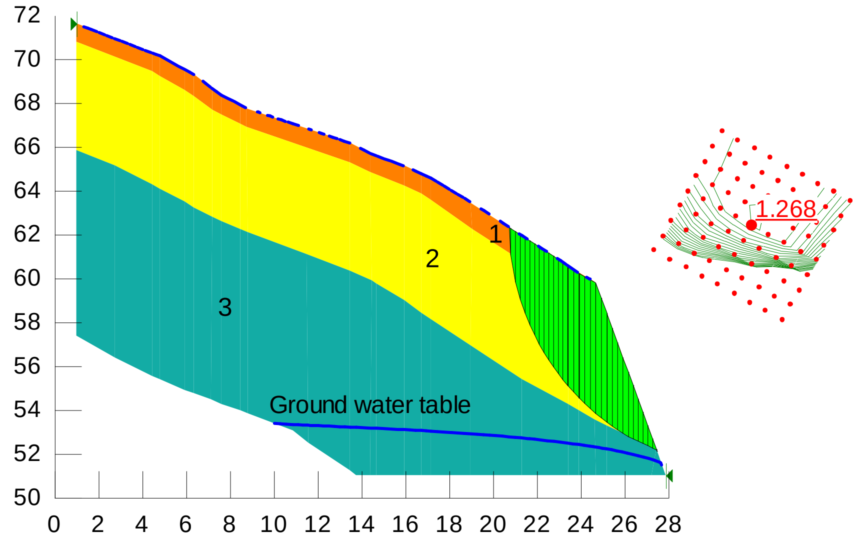

Figure 5-24: FoS of a 25 years old slope (S1985) with the slope angle of 70^0 in 2006 rainstorm event

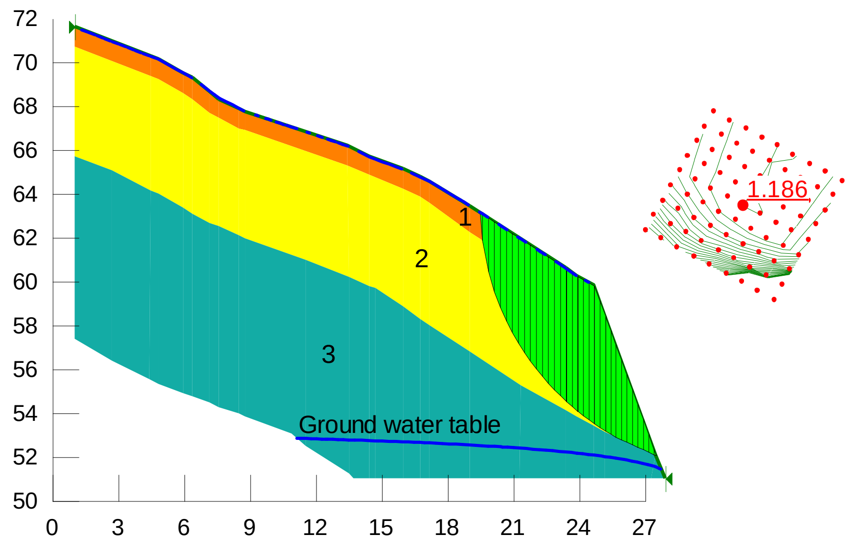

Figure 5-25: FoS of a 31 years old slope (S1985) with the slope angle of 70^0 in 2006 rainstorm event

Table 5-5: FoS after rainstorm in 2006 and 2008 for all case studies of selected slopes in Yen Bai

Rainfall event / Slope angle	2006 rainfall Event			2008 rainfall Event		
	S2008	S1985	S1979	S2008	S1985	S1979
65	1.587	1.318	1.239	1.589	1.319	1.273
70	1.517	1.268	1.186	1.519	1.269	1.187
75	1.455	1.229	1.145	1.457	1.23	1.146

Table 5-4 indicates that there is not much difference between the values of FoS calculated a result of rainstorm event in 2006 and the one in 2008. Since both of the rainstorms' intensity were larger than the coefficients of permeability of the top soil layers, the intensity of the event happened in 2006 was twice times as large as the one in 2008 but they had more or less the same duration. One conclusion can be drawn from this section is that when the intensity of the rain higher than the top soil coefficient of permeability, the rainfall duration is the deciding factor that effects the values of the slope factor of safety.

Slopes these are 2 and 25 years old show a quire safe FoS (> 1.2) in all slope angles cases. On the other hand, it is different in the 31 years old one. According the significance of factor of safety, FoS for design (Table 2-3) the FoS of slopes which are 31 years old are really low and again, for an engineering construction in an urban environment, this is not encouraged.

6. SLOPE STABILITY STABILIZATION

The methodologies in this chapter with regard to slope stability, future weathering, and remedial measures for safe slope design are conditional:

1) ***This chapter is part of a thesis being the result of a Master of Science research work and is not a report of a professional consulting project to investigate the slope stability, the future changes in geotechnical properties, nor is it an investigation to the appropriate use of remedial measures in the study area of Yen Bai in Vietnam,***
2) ***The remedial measures as proposed in this chapter are not calculated design measures, and***
3) ***The remedial measures may or may not be sufficient as measure to rule out slope instability.***

This chapter discusses some main methods for slope stabilization that can be reasonably used in Yen Bai. However, before getting into the methodologies of slope stabilization in Section 6.2, the causes of slope failures are reviewed in Section 6.1.

In Yen Bai city, cut-slopes are mostly created spontaneously by citizens for personal aims. These make them the ones who should choose optimal methods to be used for slope stabilization to protect their lives and properties. Therefore, any acceptable methods to be used should satisfy following conditions

- Have reasonable price
- Not too complicated to applied
- Easy to operate

6.1. Causes lead to the failure of man-made slopes

Understanding the causes that lead to slope failures is essential. It is not only helpful in designing and constructing but also in maintaining and repairing. In discussing the main causes of slope failures, it is important to look back to the principle of slope stability. A slope is stable if all resisting forces that act on the sliding plane are larger than all the driving forces or the shear strength of soil must larger than shear stress needed. Therefore, slope instability only occurs when, the material shear strength of the slope becomes smaller than the shear strength required for equilibrium. Look back to Section 2.5 and also according to Duncan and Wright (2005), this condition can be reached in two ways:

- Through a decrease in the shear strength of the soil
- Through an increase in the shear stress required for equilibrium

6.1.1 Decrease in shear strength

In general, there are many reasons that reduce the strength of materials inside a cut-slope. During the survey in Yen Bai, the reduction in the shear strength parameters (effective stresses) of soils on cut-slopes is as a result of three main reasons: 1) increase in pore pressure, 2) degradation of soil engineering parameters as a result of weathering processes, and 3) cracking. These causes are discussed in the next sections:

6.1.1.1 Increase in pore pressure in rainy seasons

According to Eq. 2.1 and Eq. 2.2, pore-water pressures is negatively proportion to the shear strength of soil, the increase in pore pressures will lead to the decrease in shear strength and therefore affecting the stability of slopes.

In a city with high average annual rainfall intensity, the reduction of effective stress due to the increase in pore-water pressure within slopes during heavy rainfall is the most common reason. Sections 5.2 have modelled the pore-water pressures within the study slopes for all practical cases, when the slopes in dry seasons, rainy seasons and in extreme conditions with the present of rainstorms. It has been found from this section is that there is a great difference of pore-pressures between dry and wet seasons (Figure 5-5), especially when the rainfall intensity exceeds the top soil's coefficient of permeability.

6.1.1.2 Degradation of soil engineering parameter as a result of weathering processes

Weathering which includes mechanical processes, time-dependent chemical, and geomicro-biological may result in compositional and structural changes that lead to strength loss (Mitchell & Soga, 2005). Mechanical weathering breaks down the original rock mass into smaller particles, and the chemical and biological processes change it into material with basically different properties (Duncan & Wright, 2005). When hard rocks are under the influence of weathering, their shear strength is believed to decrease with time. Experimental results of field data in Chapter 4 also demonstrate this rule as most of the values of slope stability affecting parameters in the study area show an inverse relationship with time. The analysis results taken from pocket vane shear tests point out that the undrained shear strength of soil in the completely weathered layer are predicted to reduce 1.049 % in 16th year. This value for the residual soil is 0.552 %.

6.1.1.3 Loss of strength resulting of surface cracking

Slope failures are frequently preceded by the development of cracks through the soil near the crest of the slope (Duncan & Wright, 2005). Cracks often appear on the surface of soil slopes when the soils are under tensile conditions. They often occur more on clayey slope surfaces. It is undoubtedly that all strength on the plane of the crack will be lost when this soil is cracked. In addition, when a soil slope surface is cracked, water can penetrate easier into the soils and this also leads to the strength reduction of soil.

Results of field observation (see Figure 3-8) show that the final production of weathering in the study area are silty-clay, the appearance of crack systems on cut-slope surfaces are quite popular, especially in new cuts. However, these systems are on small scale, and not so deep into the surface. Figure 6-1 illustrates the development of cracks on a new cut-slope in group 45, Yen Ninh ward.

Figure 6-1: The development of cracks on a new cut-slope in group 45, Yen Ninh ward.

6.1.2 Increase in the shear stress

Although the strength of the soils within a slope is unchanged, but the slope still can fail if for some reasons the shear stresses within the soil increase. In the study area, reasons that lead to the increase of shear stresses are discussed in the following sections:

6.1.1.1. Loads at the top of the slope

Putting loads on the top of the slopes such as building structures, parking heavy machines and so on will increase the shear stresses required for equilibrium (Duncan & Wright, 2005)

Figure 6-2: An example of putting load on the top of the slope (Khe Sen Street, Yen Bai)

The requirement for the loading value and the acceptable distance of putting loads can be calculated by slope stability analysis.

6.1.1.2. Water pressure in cracks on the surface of the slope

In case cracks on the surface of the slope is filled with water, it not only increases in the weight of the possible sliding mass, but also lead to an decrease in the shear strength of soil as pore-pressures within the slope increase.

6.1.2.2 Increase in soil weight due to increasing in water content

Infiltration and seepage not only have effect on building up the pore-water pressure within the slope but also results in an increase of the soil weight. When the unit weight of soil increased, the driving forces also increases.

6.1.2.3 Excavation at the bottom of the slope

In reality, the foot of natural slopes often are cut to create space for building roads or houses. According to Duncan & Wright (2005), excavation that makes a slope steeper or higher will increase the shear stresses in the soil within the slope and reduce stability.

In summary, when a slope fails, it is usually not possible to pinpoint a single cause that acted alone and resulted in instability (Duncan & Wright, 2005), but it is a combination of many factors these act together on the slope at the same time.

6.2. Slope stabilization methodologies

Based on the theory of slope stability, the principles of slope stabilization methods go together with the methodologies to increase resisting forces, reducing driving forces or in combination. In practice, many methods can be used in slope stabilization. However, based on the practical conditions in Yen Bai, and the literature that was highlighted in the previous section, following methodologies would be discussed.
In order to lower the driving forces:

- Excavating materials from a suitable part of the possible sliding block
- Reducing the hydrostatic pressures acting on the unstable block by using drainage method.

According to Abramson, et al. (2002), resisting forces would be increased by:

- Drainage that increases the shear strength of the ground
- Elimination of weak strata or other potential failure zones
- Provision of in situ reinforcement of the ground
- Chemical treatment to increase the ground shear strength

6.2.1. Excavating weak materials from a suitable part of the possible sliding block

Excavation is a common method for increasing the stability of a slope by reducing the driving forces that contribute to movements (Abramson, et al., 2002). In Yen Bai, excavation is a popular method for dealing with future instability. This method has been applied by the citizen; based on their daily experience. After a certain period of time they cut into the old slope to a certain depth and remove the top soil weathered layer. This part of soil contributes and increases the driving forces especially in rainy seasons when the top soil layers might be saturated.

Figure 6-3: Cut to remove weathering production in Khe Sen street - Yen Bai

Figure 6-3 demonstrates a common way to reduce the risk of slope failure in Yen Bai. The top soil layers get thicker and thicker over time, the risk of slope failure is getting higher, especially in the rainy season.

6.2.1.1. Removing the weight from the upper part of the slope

In practice, this method is often applied to slopes that are predicted to fail at present conditions or on existing failures. Removal of the material from the head of landslide will help to reduce the driving forces and tends to balance the failure (Abramson, et al., 2002) . The disadvantage of this method in Yen Bai is that most cut-slopes in this area are high and difficult to approach, so it can only be used if the problem of accessibility, safety for workers and material disposal is solved.

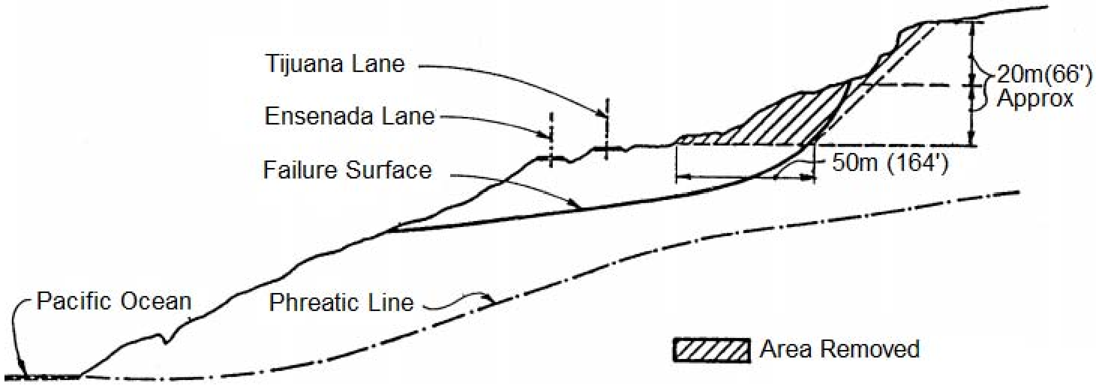

Figure 6-4: Removal of landslide head methodology
(After Abramson, et al., 2002)

6.2.1.2. Flattening of slopes

This is a very popular and economical method for improving the stability of slopes. In theory, flattening will not only reduce the sum of driving forces but also tends to force the failure surface deeper into the ground (Abramson, et al., 2002). This means in logic, the failure soil block would go through less weathered soils with higher normal effective pressure so higher strength.

Figure 6-5 illustrates the increase in slope stability that results from flattening a cut-slope. The sliding plane will move from 1 to 2 with a larger diameter.

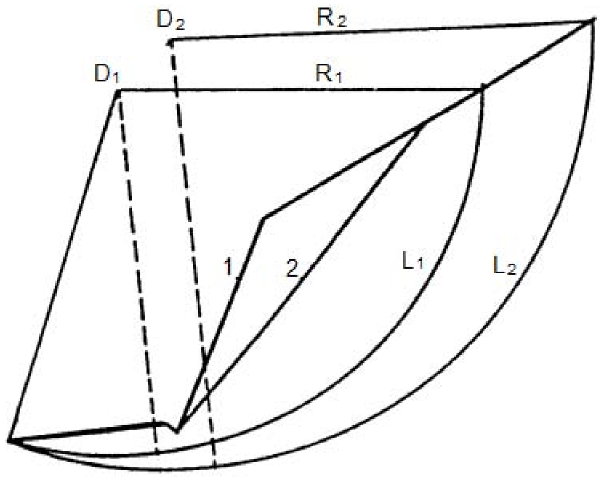

Figure 6-5: Mechanism depicting increase in stability by flattening of cut slope
(After Abramson, et al., 2002)

6.2.1.3. Benching of slopes

The purpose of benching a slope is to transform the behaviour of one high slope into several lower ones (Abramson, et al., 2002). To do so, the step after each bench should be wide enough. Basically, this method has the same principle like flattening. In high slopes, benching will result in higher overall slopes and larger quantities of excavation. However, this method will reduce subsequent maintenance costs and thereby lower the construction costs.

Except from slope stabilization, benching of slopes also help to reduce erosion since each bench should have drainage system to convey runoff to a suitable discharge outlet (Figure 6-6).

Figure 6-6 shows an example of using benching method in reality, and Figure 6-7 illustrates how this method works in Hoa Binh Street- Yen Bai

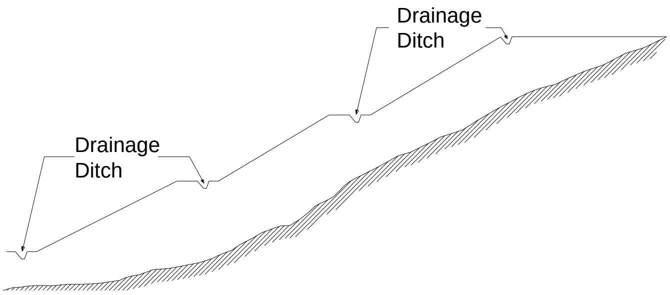

Figure 6-6: An example of slope benching in reality

Figure 6-7: Application of benching method in Hoa Binh street, Yen Bai

6.2.2. Surface slope protection

The objective of surface slope protection is to prevent infiltration by rainfall and other climatic influences to reduce the speed of weathering, the infiltration of rainfall, and the wet & dry effect (reduce cracks). This method intends to provide near impermeable surface protection to slopes, it does not aim to provide resisting forces.

6.2.2.1. Shotcrete

The main objective of shotcrete is to protect the slope from rainfall infiltration and other climatic factors that have role in increasing the rate of weathering. According to Abramson, et al. (2002), steel mesh or fiber reinforcement can be provided where necessary, admixtures and water: cement ratios need to be fine-tuned for successful shotcrete application and the mix should be tested in the laboratory for compatibility and strength and also tested in the field using test panels and field equipment. Careful consideration must be given to drying and consequent shrinkage cracking that occurs when shotcrete is used for slope surfacing (Abramson, et al., 2002). Protection of slope surfaces in Yen Bai by using shotcrete is still expensive and difficult to operate thus it is still not really commonly used here. Instead, people plaster a thin cement grout layer on the surface of the slope behind their house (Figure 6-8). This method may work in some ways, but it is not stable and not a long-term approach.

Figure 6-8: A simple type of slope surface protection in Cao Thang street, Yen Bai.

7. CONCLUSION AND RECOMMENDATION

As indicated in the title, this chapter aims to achieve three purposes:

1. Draw conclusions about the answers to the research questions and summarize the answer.
2. Discuss about the limitations of the study including the data, the applied methodology and the practical application of this study.
3. Give recommendation with suggestions for future work.

7.1. Conclusion

The purpose of this section is to discuss in detail the answer to the research questions in order to fulfil the general research objective.

7.1.1. For specific objective 1

What do the soil profiles of the selected slope look like?

The soil profile in the study area shown in Figure 3-7, it can be considered as consisting of a soil layer that lies above the rock surface. The soil layer is from 4m to 6m thick, it is subdivided into 2 separated layers: 1) residual soil (0.9 to 1.2m) on top and 2) completely weathered layer (3.5 to 4.5m). Field survey shown that the soil-profiles of the selected slopes are more or less the same like any other soil profile formed in tropical region. As they were mainly controlled by weathering processes, and the effect of these processes reduce over depth (Chapter 4). This leads to a gradual upward degradation from bed-rock at the bottom of the profile to the residual soil and layering processes starts to act on the profile.

How significant does the weathering processes affect physico-mechanical properties and engineering properties of soil on the selected slope in the study area? How can they be quantified? What parameter being influenced the most?

Based on the analysis results in Chapter 4, some conclusions were made about the influence of weathering on physico-mechanical and engineering properties of soil in the study area:

- The physico-mechanical and engineering properties of soil change over the soil depth and the lifetime of the slope. Depending on the type of the parameter, this change is small (void ratio) or significant (grain size) (see Sections 4.1 and 4.2)
- Inside the residual soil layer (layer 1), the change of soil characters under weathering processes is very small, when comes to the completely weathered layer this changing is very significant. Take grain size as an example, the decreasing rate of its uniformity in the residual soil layer over time is 0.032 % per year, however, this value in the completely weathered layer is 5.568 %.
- In this study, two factors which are called the decrease rate (DR) and the increase rate (IR) can be used to evaluate the speed of the changing over time in soil parameters under the influence of weathering. DR represents for a negative relationship with time while IR stands for a positive relationship. The larger the values of DR or IR is, the larger the change over time. These factors have unit of % per year, the detail descriptions about them were presented in section 3.1.1.
- The values of DR and IR in the 16^{th} year for all dimensional slopes stability affecting parameters have been calculated in Chapter 4, in more detailed; Tables from 4-2 to 4-5 are the values of IR for the grain size; the void ratio and porosity, the natural soil moisture content, and Atterberg limits respectively. Tables from 4-6 to 4-8 show the values of the coefficient of permeability; unconfined compressive strength; and the values of undrained shear strength. Finally, in Table 4-

11 are the rate of shear strength parameters. Base of these values, it was found that the grain sizes in the completely weathered soil layer shows the largest change over time.

What is the relationship between the shear strength of soil and rock in the study area subjected to time?

In this study, the shear strength of soil were defined by two approaches; (see Section 3.3.3.5)

- By using the results of direct shear test
- By using the field testing result from a pocket van-shear tests

The results of direct shear tests gave the values of the effective cohesion c' and effective internal friction φ'. While the field test results gave the values of undrained shear strength. Based on the results of data analyses in section 4.2.4.2, it can be concluded that the effective cohesion (c') of the residual soil are slightly higher than for the completely weathered soil, whereas an opposing story happens to the effective internal friction (φ'). The results also gave two first degree functions that can be used to estimate the values of c' and φ' over time for soil in completely weathered soil layer.

$\mathrm{C'}_{\mathrm{t}} = 0.0445\mathrm{T} + 16.907$ (Kpa) Eq. 7.1

$\varphi'_{\mathrm{t}} = -0.2663\mathrm{T} + 28.851$ (Deg) Eq.7.2

where

$\mathrm{C'}_{\mathrm{t}}$ is the effective cohesion at time T (Kpa)

φ'_{t} is the effective internal friction at time T (deg)

T is the time to be estimated (year)

The above equations show that the effective cohesion increases with time; soil material in older slope has larger effective cohesion than the younger one at the same depth. In contrast, the effective internal friction is inversely proportional to time.

In the analysing of undrained shear strength from vane shear tests (see Section 4.2.4.1), the strength also show a gradually decrease over time.

What are the factors of safety (FoS) of the study slopes? How do they change subjected to time? And when will the study slopes fail down under the same rate of weathering.

The factors of safety (FoS) for a typical profile in three cases when the cut-slope angle is 65^0, 70^0, and 75^0. The external driving force used in assessing the influence of weathering on the safety factor of the slopes is the average rainfall in rainy seasons. Table 5-2 presents the FoS of all case studies in rainy seasons. The achieved trend-lines of FoS (see Figure 5-22) in rainy seasons show a gradually decrease over time, based on these trend-lines, the estimated times when FoS reaches 1 range from 44 years for the 75^0 slope to 52 years for the 65^0 slope respectively when no stability improvement methodologies are applied. For an engineering construction in an urban environment, this is not a long period and is also not encouraged

7.1.2. For specific objective 2

What is the critical rainfall in the study area for the current physic-mechanical properties of the slope materials? What are the values of FoS when the influence of these critical rainfall are taken into account?

The selection of extreme rainfalls and their descriptions were presented in Section 5.2.5. In this study, a rainstorm event that happened in 2006 and the other one took place in 2008 were considered. Both of the rainstorms' intensity were larger than the coefficients of permeability of the top soil layers, the intensity of the event happened in 2006 was twice times as large as the one in 2008 but they had more or less the same duration

The results of cut-slope safety factor analysis in critical rainfall conditions were shown in Table 5-5. In this table, there is not much difference between the values of FoS calculated a result of rainstorm event in 2006 and the one in 2008. Therefore one conclusion can be drawn from this is that when the intensity of the rain is higher than the top soil saturated hydraulic conductivity; the rainfall duration is the deciding factor that affects the values of the slope factor of safety.

Slopes these are 2 and 25 years old show a quite safe FoS (> 1.2) in all slope angles cases. On the other hand, it is different in the 31 years old one. According the significance of factor of safety, FoS for design (Table 2-3) the FoS of slopes which are 31 years old are really low and again, for an engineering construction in an urban environment, this is not encouraged.

7.1.3. For specific objective 3

What are the main causes that lead to slope failures in the study area?
The main causes that lead to slope failure of man-made slopes can be divided into two types:

- Nature: weathering, rainfall and cracking
- Human: load surcharge on the top of the slope and excavate from the bottom of the slope.

In the above causes, Observation from the field show that the influence of weathering and over cutting of slopes are the main causes that lead to slope failures. The detailed analyses were presented in Section 6.1.

What recommendations for slope stabilization can be used?

In Yen Bai city, cut-slopes were created spontaneously by citizens for personal aims. Since they would be the one who choose which method used for slope stabilization to protect their lives and properties. Therefore, if any methods which is accepted, it must have reasonable price, not too complicated to applied and easy to operate.
When all was said and done, it can be seen that all of the main research questions were fulfilled. The practical application of the study will be discussed in the next section. However, the final conclusion can be drawn is that: the study is located in a region that suffers strongly from the influence of weathering; all cuts were steeply into the natural slopes. With this kind of conditions, the failure of these slopes will be sooner or later. As the results of slope stability analyses, a 2 year old slope with the slope angle of 75 degree is predicted to fail in 44 years.

7.2. Limitation and Recommendation

7.2.1. Limitation of the study

7.2.1.1. The method of selecting the study area and sampling

The general objective of this study is to evaluate the change the values of slopes stability affecting parameters, both in terms of strength as in their hydrological characteristics under weathering processes and the consequences of these changes on the safety factor of cut-slopes in Yen Bai. However, as the data is limited, so only the area that covers Ar-nc2 geological unit (Figure 1.5) was considered as the research site. So, the study area is in fact narrower than what was in the initial proposal.

Three sampling locations which were three cut-slopes that had different lifetime were selected in the study area. Samples which were taken from these locations were tested to extract data. As the data must be represented for the whole research site, so the selection of the sampling locations needs to be strictly consideration.

As the lack of equipment for sampling and time for laboratory testing, samples were taken from one depth or each soil layer. In this study, samples at 80 cm represented for the residual soil layer (0.9 to 1.2m thick) and 180 cm were completely weathered layer (3.5 to 4.5m thick). Therefore, data taken from these samples surely will be slightly difference from what were expected; even the sampling and laboratory work were well done.

7.2.1.2. Method of weathering evaluation

The aim of this step is to find the changing trends for slope stability affecting parameters over time. This trend-line shows a relationship between the study parameter over time and was interpolated from the values of the study parameter at different time. Based on literature, it is believed to be a curve that has a threshold value where the increase of the does not have or have very little influence on the changing of the study parameters. However, to simplify the problem, a linear relationship is used.

The trend-line was achieved by interpolating based on a numbers of known points on the coordinate axes of parameter's value versus time. Therefore, the more the values are, the more the confidence of the trend-line. In this study, as the lack of data, only three values corresponding to three different times were considered. Consequently, this will reduce the confidence of the achieved trend-line.

7.2.1.3. Method of stability analyses

As mentioned in Section 5.2.1, during stability analysing, the material within each soil layer assumed to be homogeneous; the influence of tree roots, cracks or fissures is not taken into account (see Section 5.2.1). This assumption does not reflect the reality. Furthermore, observations from the field shown that there is a gradual upward degradation from bed-rock at the bottom of the profile to the residual soil. It means that the soil's characters will change over depth. Therefore considering each soil layer to be homogeneous is not really precise.
The data of pore-water pressures were lack so fake conditions of pore-water pressures were created by using the average daily rainfall in the dry seasons.

Analysing the built up of pore-pressures under rainfall condition, the influence of runoff as heavy rain appears does not influence seepage conditions within the slope. This is also not true since in literature, the runoff on the surface does have influence on the seepage conditions within the slope.

Assuming that the only process that affects seepage condition within the slope is infiltration, there is no evaporation happening on the surface of the slope. This assumption also reduces the confidence of the achieved safety factors.

The seepage models were built based on cross-sections that were limited in size by the left and bottom boundaries (see Figures 3-9 to 3-11). This also gave more discrepancy for the overall results.

The stability models in this study were based on simplified Bishop Method. There might be another Method that is more suitable for this area.

7.2.2. Recommendation

In the view of the above discussion, these following recommendations were made:

7.2.2.1. For further studies of this topic

- Study further on the productions of weathering and their characteristics and the relationship between those weathering production to the instability of cut-slopes.
- To improve the quality of the trend-lines made in this study, more points' time-values in the range between 2 to 25 and 25 to 31 years should be quantified.
- A study on the influence of soil depth on the rate of weathering should be carried out.
- Improving the quality of the data by delineate an area for surveying, observing and sampling to find out the changing of soil's characteristics over time.
- Set up a system of measuring pore-water pressures

7.2.2.2. For the Authority

The Authority should:

- Have strict regulations to control the excavations at the bases of natural slopes for housing and road constructing
- Have a record about cut-slopes in the study area, in this record, the lifetime and geological units must be clear. So they can use this record to predict the time of failure to make the plan for evaporating people from the dangerous areas.
- Invest more on researching methodologies of slope stability stabilization to find reasonable methods reducing the risk of slope failure.
- Educate people in the city about the danger of over-steep cut-slopes and equip them necessary information about the knowledge of slope instability.

LIST OF REFERENCES

Abramson, L. W., Lee, T. S., Sharma, S., & Boyce, G. M. (2002). *Slope stability and stabilization methods* (Vol. 2). New York: John Wiley & Sons.

ASTM. (2003). Standard Test Methods for Determination of the Soil Water Characteristic Curve for Desorption Using a Hanging Column, Pressure Extractor, Chilled Mirror Hygrometer, and/ or Centrifuge, *ASTM: D6836 - 02* (pp. 20). United States: ASTM International.

ASTM. (2004). Standard test method for consolidated undrained triaxial compression test for cohesive soils, *D 4767 - 04* (pp. 13). United States: ASTM International.

Bland, W. J., & Rolls, D. (1998). *Weathering: An introduction to the scientific principles*. New York: Oxford University Press.

Chapagain, B. (2001). *Degradation of geotechnical properties of rock masses in engineering time.* Unpublished Msc Thesis, University of Twente, Enschede.

Cheng, Y. M., & Lau, C. K. (2008). *Slope stability analysis and stabilization: New methods and insight*. New York: Taylor & Francis.

Craig., R. R. (2004). *Craig's soil mechanics*. London: Taylor & Francis Group.

Das, B. M. (1976). *Advanced soil mechanics*. London: Taylor & Francis.

Delta-T Devices Ltd. (2005). *User manual for Moisture meter type HH2*. Cambridge: Delta-T Devices Ltd.

Doan, M. T. (2004). Nghiên cứu nguyên nhân và định hướng biện pháp phòng ngừa trượt đất tại các điểm dân cư vùng núi Việt Nam. Unpublished Research. Vietnamese Institute of Transport Science and Technology.

Duncan, J. M., & Wright, S. G. (2005). *Soil strength and slope stability*. New Jersey: John Wiley & Sons, Inc.

Few, R., & Tran, P. G. (2010). Climatic hazards, health risk and response in Vietnam: Case studies on social dimensions of vulnerability. *Global Environmental Change, 20*, 529-538.

Fredlund, D. G. (1996). The emergence of unsaturated soil mechanics. *Texas, A & M University Press,*, 39.

Fredlund, D. G., & Morgenstern, N. R. (1977). Stress state variables for unsaturated soils. *Journal of the Geotechnical Engineering Division, 103*(5), 447-466.

Fredlund, D. G., & Rahardjo, H. (1987). Soil mechanics principles for highway engineering in arid regions. *National Academy of Sciences*, 1-11.

Fredlund, D. G., & Rahardjo, H. (1993). *Soil mechanics for unsaturated soils*. New York: Hohn Wiley & Sons, Inc.

Fredlund, D. G., Rahardjo, H., Leong, E. C., & Charles, W. E. N. (2001). *Suggestions and recomendations for the interpretation of soil-water characteristics curves*. Paper presented at the Southeast Asian Geotechnical Conference.

Fredlund, M. D., Sillers, W. S., Fredlund, D. G., & Wilson, G. W. (1996). *Design of a knowledge-based system for unsaturated soil properties*. Paper presented at the Canadian Conference on Computing in Civil and Building Engineering.

Geo-Slope INTERNATIONAL. (2008a). Seep/W 2007. Retrieved 1/12, 2011, from http://www.geo-slope.com/products/seepw2007.aspx

Geo-Slope INTERNATIONAL. (2008b). Slope/W 2007. Retrieved 01/12, 2011, from http://www.geo-slope.com/products/slopew2007.aspx

Geo-slope INTERNATIONAL. (2008c). GeoStudio 2007- Basic edition. Retrieved 07/07, 2011, from http://www.geo-slope.com/products/geostudiobasic.aspx

Gidigasu, M. D. (1976). *Laterite soil engineering. Pedogenesis and Engineering Principles*: Elsevier Scientific Publishing Company.

Gui, M. W., & Han, K. K. (2008). A case study on rainfall infiltration effect on the stability of two slopes. *Taylor & Francis Group, London*, 7.

Gupta, K. A. (2008). *Relationship between the mean particle size, the size factor, optimum moisture content, and permeability of sandy soils*. Paper presented at the The 12th International Conference of International Association for Computer Methods and Advances in Geomechanics.

Ha, D. L. (2009). Yen Bai Portal from http://www.yenbai.gov.vn/vi/org/htt/tpyenbai/Pages/gioithieuchung.aspx

Hack, R. (1998). Slope stability probability classification (pp. 258): International Institute for Aerospace Survey and Earth Science (ITC).

Hack, R., & Price, D. (1997). Quantification of weathering. *Engineering geology and the environment*, 145-150.

Hoang, T. S., & Le, Q. H. (Cartographer). (1997). *Geological map - 1/50.000 in scale Doan Hung - Yen Binh*.
Holtz, R. D., & Kovacs, W. D. (1981). *An Introduction to geotechnical engineering*. New Jersey: Prentice Hall.
Huat, B. K., Sew, G. S., & Ali, H. F. (2004). *Tropical residual soil engineering*: Taylor & Francis Group.
Huisman, H. (2006). *Assessment of rock mass decay in artificial slopes*. Unpublished PHD thesis, Delft University of Technology, Delft.
IAEA. (2008). *Field estimation of soil water content- A practical guide to methods, instrumentation and sensor technology*. Vienna: International Atomic Energy Agency.
Jiao, J. J., Wang, X. S., & Nandy, S. (2005). Confined groundwater zone and slope instability in weathered igneous rocks in Hong Kong. *Engineering Geology*(80), 71-92.
Jumikis, A. R. (1984). *Soil mechanics*. Florida: Robert E. Krieger Publishing Company, Inc.
Krahn, J. (2004a). *Seepage modeling with SEEP/W*. Alberta: GEO-SLOPE International Ltd.
Krahn, J. (2004b). *Stability modeling with Slope/w: An engineering methodology*. Alberta: Geo-Slope/W International, Ltd.
Liu, C., & Evett, J. B. (2005). *Soils and Foundation*. Singapore: Prentice - Hall.
McLean, A. C., & Gribble, C. D. (2005). *Geology for civil engineering*. Glasgow: Taylor & Francis.
Mitchell, J. K., & Soga, K. (2005). *Fundamentals of soil behavior* (Third ed.). New Jersey: John Wiley & Sons, INC.
Nguyen (manager), T. L. (2009). *Xây dựng phương pháp đánh giá độ rủi ro do tai biến địa chất ở những khu vực đô thị miền núi phía Bắc Việt Nam bằng việc kết hợp mô hình RS & GIS. Thử nghiệm ở thành phố Yên Bái*. Hanoi: Vietnam Institute of GeoSciences and Mineral Resources Vietnam.
Ollier, C. (1969). *Weathering*. Edinburgh: Oliver & Boys.
Polynov, B. B. (1937). *Cycle of weathering* (A. Murby, Trans.). London.
Rahardjo, H., Aung. K. K., Leong, E. C., & Rezaur. R. B. (2004). Characteristics of residual soils in Singapore as formed by weathering. *Engineering Geology, 73*, 157-169.
Reiche, R. (1950). A survey of weathering processes and products. *New Mexico Univ. Publ. Geology, 3*, 95.
Ritter, M. E. (2009, 10/1/2009). The physical environment- An introduction to physical geography, 2/e. Retrieved 19/02/2011, from http://www.uwsp.edu/geo/faculty/ritter/geog101/textbook/title_page.html
Saint-Macary., C., Keil., A., Zeller., M., Heidhues., & Dung., P., T., M. (2010). Land titling and soil conservation in the northern uplands of Vietnam. *Land Use Policy, 27*, 617-627.
Selby, M. J., & Hodder, A. P. W. (1993). *Hillslope materials and processes*. Oxford: Oxford University Press, .
TCVN. (1995a). Soil-Method of laboratory determimation of grain size distribution, *TCVN 4198:1995* (pp. 16). Hanoi: Minitry of construction of socialist republic of Vietnam.
TCVN. (1995b). Soils - Methods of laboratory determination of Plastic limit and liquid limit, *TCVN 4197:1995* (pp. 7). Hanoi: Minitry of construction of socialist republic of Vietnam.
TCVN. (1995c). Soil-Laboratory method of determination of shear resistance in a shear box appratus, *TCVN 4199:1985*. Hanoi: Minitry of construction of socialist republic of Vietnam.
Terzaghi, K., Peck, R. B., & Mesri, G. (1996). *Soil mechanics in engineering practice*. New York: John Wiley & Sons, INC.
Tran., P., & Shaw., R. (2007). Towards an intergrated approach of disaster and environment management: A case study of Thua Thien Hue province, central Viet Nam. *Environmental Hazards, 7*, 271-282.
Truong, D. T., Nguyen, X. T., Vu, K., & Trinh, T. (1979). *Geology of Vietnam - Northern Part* (K. T. Tran & C. B. Truong, Trans.). Hanoi: The Research Institude of Geology and Mineral Resources of Vietnam.
Utili, S. (2004). *Evolution of natural slopes subject to weathering: An analytical and numerical study*. Politecnico di Milano, Milano.
Verruijt, A. (2006). *Soil mechanics*. Delft: Delft university of technology.
Vinh, N., Doan, K. T., Nguyen, C. L., & Phan, T. T. (Cartographer). (2005). *Geology and mineral resources map of Vietnam, Yen Bai sheets, on scale 1/200,000*.
Wolfsohn, D., & Fredlund, D. G. (1994). Unsaturated soil mechanics for agriculture conditions. *American Society of Agricultural Engineers, 38*(3), 173-181.

APPENDIX A

FIELD TESTING RESULTS

Appendix A-1: Pocket penetrometer test results for S1985

S1985	Reading value (Kg/cm^2)				
Depth	1st	2nd	3rd	4th	5th
80 cm	2	3	2.5	2.3	2.7
180 cm	2.8	2.3	3.3	3	2.7

Appendix A-2: Pocket penetrometer test results for S1979

S1979	Reading value (Kg/cm^2)				
Depth	1st	2nd	3rd	4th	5th
80 cm	2.1	2	2.4	2.2	1.9
180 cm	2.3	2	2.4	2.1	2.6

Appendix A-3: Pocket vane test results for S1985

S1985	Undrained shear strength (Kg/cm^2)				
Depth	1st	2nd	3rd	4th	5th
80 cm	0.349952	0.284336	0.295272	0.32808	0.317144
180 cm	0.339016	0.38276	0.415568	0.360888	0.371824

Appendix A-4: Pocket vane test results for S1979

S1979	Undrained shear strength (Kg/cm^2)				
Depth	1st	2nd	3rd	4th	5th
80 cm	0.262464	0.284336	0.251528	0.284336	0.317144
180 cm	0.317144	0.317144	0.295272	0.284336	0.306208

Appendix A-5: Results of volumetric water content 10/10/2010

Root Depth (mm)		50					
Sensor Depth (mm)		100	200	300	400	600	1000
Time	P	% Vol	% Vol	% Vol	% Vol	% Vol	% Vol
10/10/2010 14:26	A	5.2	10.8	7.4	8.1	18.3	5
10/10/2010 14:27	A	5.2	12.7	7.8	9	21.8	5.5
10/10/2010 14:27	A	6.1	7.9	5.8	6.9	21.9	6.9
10/10/2010 14:29	B	5.3	15.7	22	21.2	15.7	13
10/10/2010 14:29	B	7.1	20.4	18.4	19.3	20.6	11.8
10/10/2010 14:29	B	7.5	20.5	21.5	19.7	21.7	10.5
10/10/2010 14:31	C	14.9	16.9	15.9	7.2	9	13.1
10/10/2010 14:31	C	11.4	14.7	22.8	8.1	9.4	12.5
10/10/2010 14:31	C	9.3	12	24.8	8.9	5.6	12.8
10/10/2010 14:32	D	8	5.3	13.8	6.3	10.8	10.7
10/10/2010 14:33	D	10.1	6.6	13.5	4.9	13.8	10.7
10/10/2010 14:33	D	7.9	4.8	14.9	5.7	10.9	11.3
10/10/2010 14:34	E	10	14.6	15.9	14.4	26.7	21.2
10/10/2010 14:34	E	13.3	9.1	15.8	14.1	30.9	22.2
10/10/2010 14:35	E	8.9	16.2	19.9	17.6	26.9	18.5
10/10/2010 14:37	F	13.9	20.1	16.9	14.8	16.9	12.2
10/10/2010 14:37	F	15.9	21.2	17	18.4	17.8	11.8
10/10/2010 14:37	F	16.3	18	16.1	22.1	14.9	11.6
10/10/2010 14:39	G	10.7	9	5.5	6.2	14	6.6
10/10/2010 14:39	G	9.5	15.1	6.6	4.9	10.7	6
10/10/2010 14:39	G	12.1	18	7.4	6	9.4	5.9

APPENDIX B

LABORATORY TESTING RESULTS

Appendix B-1: Grain size distribution results

Appendix B-1-1: Grain size distribution results of samples in slope S2008

Depth 80cm				Depth 180cm			
Test 1		Test 2		Test 1		Test 2	
Grain size (mm)	Passing (%)	Grain size (mm)	Passing (%)	Grain size (mm)	Passing (%)	Grain size (mm)	Passing (%)
0.00448	38.73987	0.00466	39.71516	0.00449	19.48741	0.00470	24.27256
0.00500	40.38721	0.00500	42.85000	0.00500	20.43117	0.00500	24.78949
0.00545	41.79748	0.00567	45.99180	0.00547	21.31378	0.00573	26.04817
0.00766	44.85509	0.00797	50.30970	0.00770	23.14016	0.00805	27.82378
0.01077	47.91269	0.01120	54.62760	0.01082	24.96653	0.01131	29.59939
0.01514	50.97030	0.01575	58.94550	0.01521	26.79290	0.01590	31.37499
0.02607	54.02791	0.02710	62.33023	0.02619	28.61928	0.02721	34.92621
0.04071	60.14312	0.04259	65.58130	0.04092	32.27203	0.04275	36.70182
0.05702	64.72953	0.05000	68.21720	0.05715	35.92477	0.05000	40.25303
0.05000	62.75579	0.05945	67.56650	0.05000	34.31524	0.05968	38.22275
0.10000	77.59920	0.10000	80.42110	0.10000	46.22200	0.10000	44.93722
0.25000	83.11968	0.25000	85.41550	0.25000	51.19400	0.25000	48.31565
0.50000	86.80000	0.50000	89.28000	0.50000	55.00000	0.50000	50.88000
1.00000	92.08571	1.00000	95.57000	1.00000	59.07000	1.00000	54.11000
2.00000	96.54286	2.00000	97.27000	2.00000	61.22000	2.00000	55.50000
5.00000	99.82857	5.00000	100.00000	5.00000	85.84000	5.00000	84.40000
10.00000	100.00000	10.00000	100.00000	10.00000	93.92000	10.00000	97.57000
20.00000	100.00000	20.00000	100.00000	20.00000	100.00000	20.00000	100.00000
40.00000	100.00000	40.00000	100.00000	40.00000	100.00000	40.00000	100.00000
75.00000	100.00000	75.00000	100.00000	75.00000	100.00000	75.00000	100.00000
100.00000	100.00000	100.00000	100.00000	100.00000	100.00000	100.00000	100.00000

Appendix B-1-2: Grain size distribution results of samples in slope S1985

Depth 80cm				Depth 180cm			
Test 1		Test 2		Test 1		Test 2	
Grain size (mm)	Passing (%)	Grain size (mm)	Passing (%)	Grain size (mm)	Passing (%)	Grain size (mm)	Passing (%)
0.00447	41.43542	0.00463	48.88609	0.00449	26.40681	0.00467	30.89226
0.00500	43.20715	0.00500	50.04407	0.00500	27.50165	0.00500	31.57831
0.00545	44.70577	0.00563	52.00582	0.00546	28.49101	0.00568	32.99807
0.00766	47.97613	0.00792	55.12554	0.00768	30.57521	0.00799	35.10388
0.01076	51.24649	0.01113	58.24527	0.01080	32.65941	0.01123	37.20970
0.01513	54.51684	0.01564	61.36499	0.01518	34.74361	0.01579	39.31551
0.02605	57.78720	0.02692	64.48472	0.02613	36.82781	0.02718	41.42132
0.04081	62.69274	0.04229	67.60444	0.04107	38.91201	0.04270	43.52713

0.05717	67.59827	0.05000	70.72417	0.05772	40.99621	0.05000	47.73876
0.05000	65.44840	0.05942	69.00861	0.05000	40.03015	0.05961	45.34548
0.10000	83.03412	0.10000	79.20960	0.10000	52.79275	0.10000	53.34019
0.25000	89.23350	0.25000	85.09680	0.25000	57.90173	0.25000	59.41498
0.50000	93.93000	0.50000	89.20000	0.50000	62.61000	0.50000	64.08000
1.00000	96.38000	1.00000	93.39000	1.00000	66.67000	1.00000	66.51000
2.00000	97.55000	2.00000	96.53000	2.00000	70.13000	2.00000	68.44000
5.00000	99.15000	5.00000	100.00000	5.00000	91.77000	5.00000	87.72000
10.00000	100.00000	10.00000	100.00000	10.00000	100.00000	10.00000	98.05000
20.00000	100.00000	20.00000	100.00000	20.00000	100.00000	20.00000	100.00000
40.00000	100.00000	40.00000	100.00000	40.00000	100.00000	40.00000	100.00000
75.00000	100.00000	75.00000	100.00000	75.00000	100.00000	75.00000	100.00000
100.00000	100.00000	100.00000	100.00000	100.00000	100.00000	100.00000	100.00000

Appendix B-1-3: Grain size distribution results of samples in slope S1979

Depth 80cm				Depth 180cm			
Test 1		Test 2		Test 1		Test 2	
Grain size (mm)	Passing (%)	Grain size (mm)	Passing (%)	Grain size (mm)	Passing (%)	Grain size (mm)	Passing (%)
0.00446	39.67429	0.00446	41.04243	0.00444	30.43052	0.00449	33.98317
0.00500	41.29652	0.00500	42.72059	0.00500	31.63782	0.00500	36.87546
0.00543	42.57658	0.00543	44.04480	0.00540	32.50485	0.00544	39.34752
0.00763	45.47887	0.00763	47.04717	0.00760	34.57919	0.00764	42.02970
0.01073	48.38116	0.01073	50.04954	0.01068	36.65353	0.01074	44.71188
0.01508	51.28345	0.01508	53.05192	0.01501	38.72786	0.01510	47.39405
0.02596	54.18574	0.02596	56.05429	0.02583	40.80220	0.02599	50.07623
0.04078	57.08803	0.04078	59.05666	0.04059	42.87654	0.04059	55.44058
0.05731	59.99032	0.05000	63.56022	0.05703	44.95087	0.05000	59.46385
0.05000	58.70623	0.05713	61.59568	0.05000	44.06405	0.05685	57.76984
0.10000	73.84585	0.10000	76.39236	0.10000	52.72344	0.10000	68.17291
0.25000	79.06795	0.25000	81.72126	0.25000	56.19240	0.25000	73.26183
0.50000	83.68750	0.50000	85.95000	0.50000	59.40000	0.50000	77.57500
1.00000	88.97500	1.00000	89.35000	1.00000	62.45000	1.00000	81.62500
2.00000	91.66250	2.00000	92.05000	2.00000	65.77500	2.00000	84.01250
5.00000	97.01250	5.00000	97.51250	5.00000	85.75000	5.00000	93.52500
10.00000	100.00000	10.00000	100.00000	10.00000	95.12500	10.00000	100.00000
20.00000	100.00000	20.00000	100.00000	20.00000	100.00000	20.00000	100.00000
40.00000	100.00000	40.00000	100.00000	40.00000	100.00000	40.00000	100.00000
75.00000	100.00000	75.00000	100.00000	75.00000	100.00000	75.00000	100.00000
100.00000	100.00000	100.00000	100.00000	100.00000	100.00000	100.00000	100.00000

Appendix B-2: Soil- Water characteristic results (SWCC)

Appendix B-2-1: Results of SWCC tests of sample in slope S2008

Suction level (Kpa)	S2008			
	80.00		180.00	
	1(ring 56)	2(Ring 4)	1(Ring 53)	2(Ring 39)
0.00	0.49	0.49	0.44	0.43
20.00	0.43	0.44	0.37	0.37
50.00	0.41	0.41	0.35	0.34
100.00	0.40	0.40	0.32	0.31
200.00	0.38	0.39	0.28	0.28

Appendix B-2-2: Results of SWCC tests of samples in slope S1985

Suction level (Kpa)	S_1985			
	80.00		180.00	
	1(ring 45)	2(Ring 5)	1(Ring 77)	2(Ring 70)
0.00	0.49	0.49	0.44	0.45
20.00	0.44	0.43	0.40	0.41
50.00	0.42	0.42	0.37	0.38
100.00	0.41	0.40	0.35	0.35
200.00	0.39	0.39	0.32	0.33

Appendix B-2-3: Results of SWCC tests of samples in S1979

Suction level (Kpa)	S_1979			
	80.00		180.00	
	1(ring 8)	2(Ring 6	1(Ring 35)	2(Ring 7
0.00	0.50	0.49	0.47	0.45
20.00	0.44	0.43	0.43	0.40
50.00	0.42	0.42	0.41	0.38
100.00	0.41	0.40	0.37	0.37
200.00	0.40	0.40	0.36	0.35

Appendix B-3: Result of triaxial test of samples in slope S1979 at 80 cm

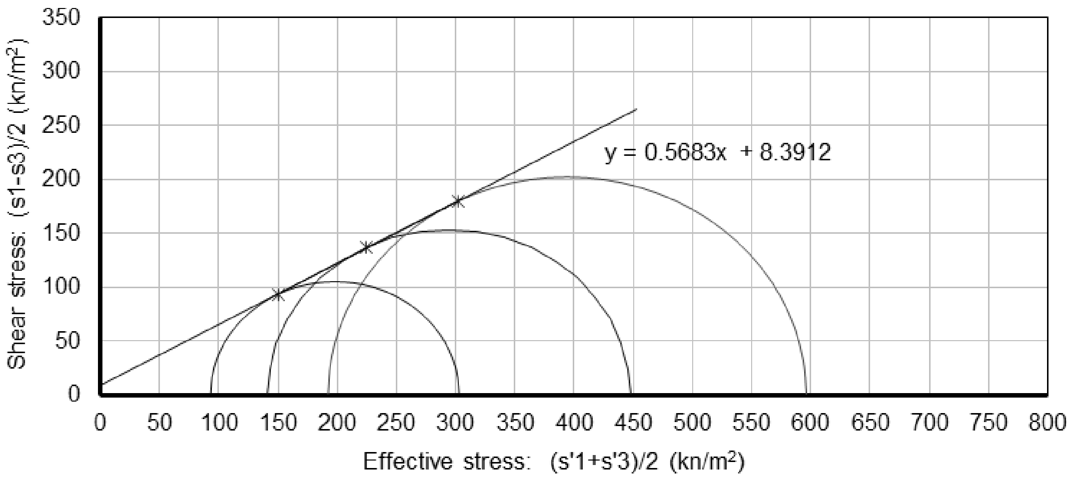

C = 8.3912 kN/cm², $\varphi = 29.61^0$

Appendix B-4: Direct shear test results

Appendix B-4-1: Reading results of unsaturated direct shear tests

Direct shear Test Reading Results (Natural condition)				
Sample symbol	Vertical pressure level			Cut type
	=1 kG/cm²	=2 kG/cm²	=3 kG/cm²	
S1979_80	32.6	49.8	64.1	Consolidated Drained Conditions
S1979_80	28.8	47.9	65.5	Consolidated Drained Conditions
S1979_80	30.7	53.2	68.1	Consolidated Drained Conditions
S1979_180	37.7	53.4	80.4	Consolidated Drained Conditions
S1979_180	32.9	56.84	74.8	Consolidated Drained Conditions
S1979_180	30.5	60.32	77.55	Consolidated Drained Conditions
S1985_80	34.2	55.8	70.2	Consolidated Drained Conditions
S1985_80	29.5	52.4	72.6	Consolidated Drained Conditions
S1985_180	33.7	58.84	81.5	Consolidated Drained Conditions
S1985_180	36.1	62.9	84.78	Consolidated Drained Conditions
S2008_80	31.3	52.5	71.8	Consolidated Drained Conditions
S2008_80	33.5	56.9	75.4	Consolidated Drained Conditions
S2008_180	37	72.9	107.5	Consolidated Drained Conditions
S2008_180	34.7	69.4	104.6	Consolidated Drained Conditions
S2008_180	39.3	67.6	101.9	Consolidated Drained Conditions

Appendix B-4-2: Reading results of saturated direct shear tests

Direct shear Test Reading Results (Cut in saturated condition)				
Sample symbol	Pressure level			Cut type
	=1 kG/cm²	=2 kG/cm²	=3 kG/cm²	
S1979_80	26.4	46.2	62.3	Consolidated Drained Conditions
S1979_80	28.2	47.2	58.7	Consolidated Drained Conditions
S1979_180	27.7	54.1	72.2	Consolidated Drained Conditions
S1979_180	31.3	48.5	67.5	Consolidated Drained Conditions
S2008_80	27.6	47.1	65.8	Consolidated Drained Conditions
S2008_80	30.2	51.1	69.1	Consolidated Drained Conditions
S2008_180	38.4	67.5	97.7	Consolidated Drained Conditions
S2008_180	35	67.9	94.1	Consolidated Drained Conditions
S2008_180	37.6	74.5	93.8	Consolidated Drained Conditions
S1985_80	29.3	49.3	61.8	Consolidated Drained Conditions
S1985_80	25.7	47.1	65.6	Consolidated Drained Conditions
S1985_180	30.1	53.7	74.3	Consolidated Drained Conditions
S1985_180	32.5	57.9	77.7	Consolidated Drained Conditions

Appendix B-4-3: Average shear strength parameters of residual soil in S2008 (Natural condition)

DIRECT SHEAR TEST

Bore hole	: S2008
Depth(cm)	: 80 cm
Description	: Brown silty clay
Testing standards	: Vietnamese

TEST RESULT (NATURAL CONDITION)

Coefficient of pressure ring

Cr = 0.0185 kG/cm2.Div.

Vertical pressure	Readed values	Shear stress
σ (KG/cm^2)	Div	kG/cm^2
0.10		
0.25		
0.50		
0.75		
1.00	32.40	0.599
1.50		
2.00	54.70	1.012
3.00	73.60	1.362
4.00		

φ =	20 ° 53 '	Deg, Min
C =	0.228	kG/cm^2

MOHR'S FAILURE ENVELOPE

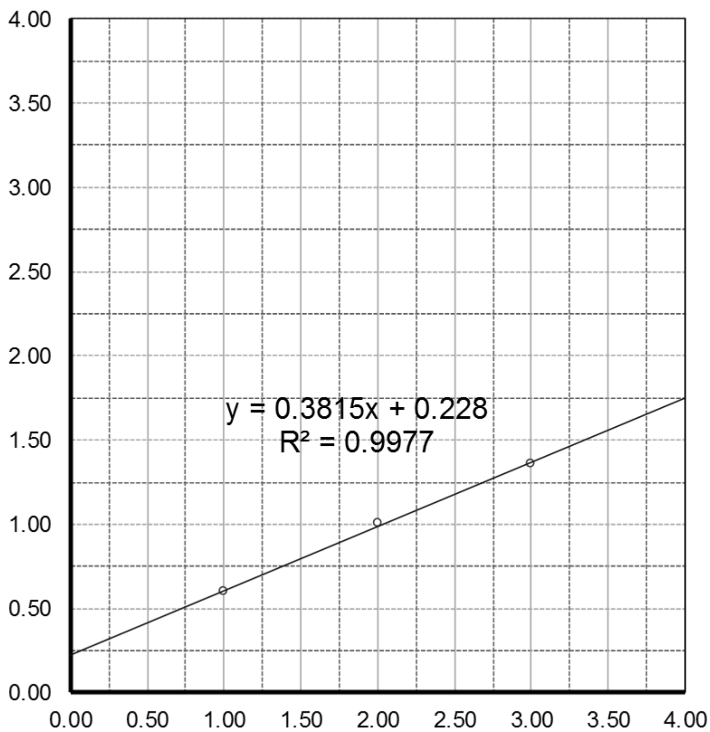

Appendix B-4-4: Average shear strength parameters of residual soil layer in S2008 (Saturated condition)

DIRECT SHEAR TEST

Bore hole	: S2008
Depth(cm)	: 80 cm
Description	: Brown silty clay
Testing standards	: Vietnamese

TEST RESULT (SATURATED CONDITION)

Coefficient of pressure ring

Cr = 0.0185 kG/cm2.Div.

Vertical pressure	Readed values	Shear stress
σ (KG/cm^2)	Div	kG/cm^2
0.10		
0.25		
0.50		
0.75		
1.00	28.90	0.535
1.50		
2.00	49.10	0.908
3.00	67.45	1.248
4.00		

φ = 19° 37 ' Deg, Min

C = 0.184 kG/cm^2

MOHR'S FAILURE ENVELOPE

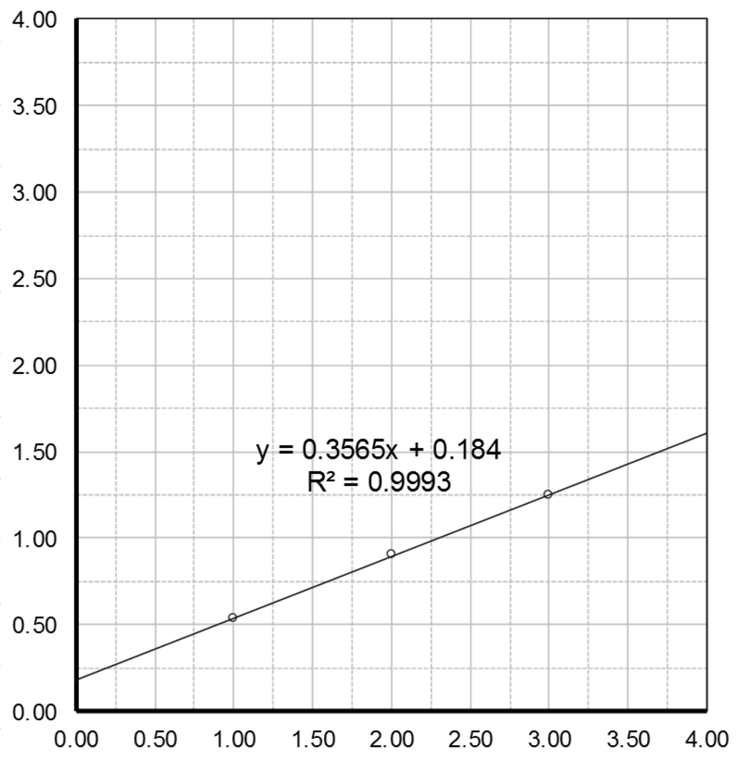

Appendix B-4-5: Average shear strength parameters of completely weathered soil layer in S2008 (Natural condition)

DIRECT SHEAR TEST

Bore hole	: S2008
Depth(cm)	: 180 cm
Description	: Browndish to reddish silty clay mixed with gravels
Testing standard	: Vietnamese

TEST RESULT (NATURAL CONDITION)

Coefficient of pressure ring		
Cr = 0.0185 kG/cm2.Div.		
Vertical pressure	Readed values	Shear stress
σ (KG/cm^2)	Div	kG/cm^2
0.10		
0.25		
0.50		
0.75		
1.00	41.27	0.763
1.50		
2.00	76.35	1.412
3.00	104.67	1.936
4.00		
φ =	30° 22 '	Deg, Min
C =	0.212	kG/cm^2

MOHR'S FAILURE ENVELOPE

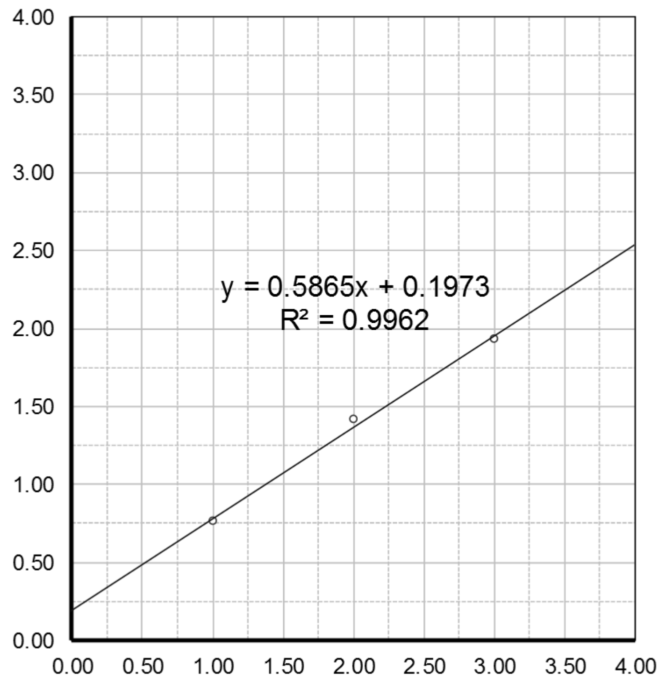

Appendix B-4-6: Average shear strength parameters of completely weathered soil layer in S2008 (Saturated condition)

DIRECT SHEAR TEST

Bore hole	: S2008
Depth(cm)	: 180 cm
Description	: Browndish to reddish silty clay mixed with gravels
Testing standards	: Vietnamese

TEST RESULT (SATURATED CONDITION)

Coefficient of pressure ring		
Cr = 0.0185 kG/cm2.Div.		
Vertical pressure	Readed values	Shear stress
σ (KG/cm^2)	Div	kG/cm^2
0.10		
0.25		
0.50		
0.75		
1.00	37.00	0.685
1.50		
2.00	69.97	1.294
3.00	95.20	1.761
4.00		
φ =	28° 17 '	Deg, Min
C =	0.172	kG/cm^2

MOHR'S FAILURE ENVELOPE

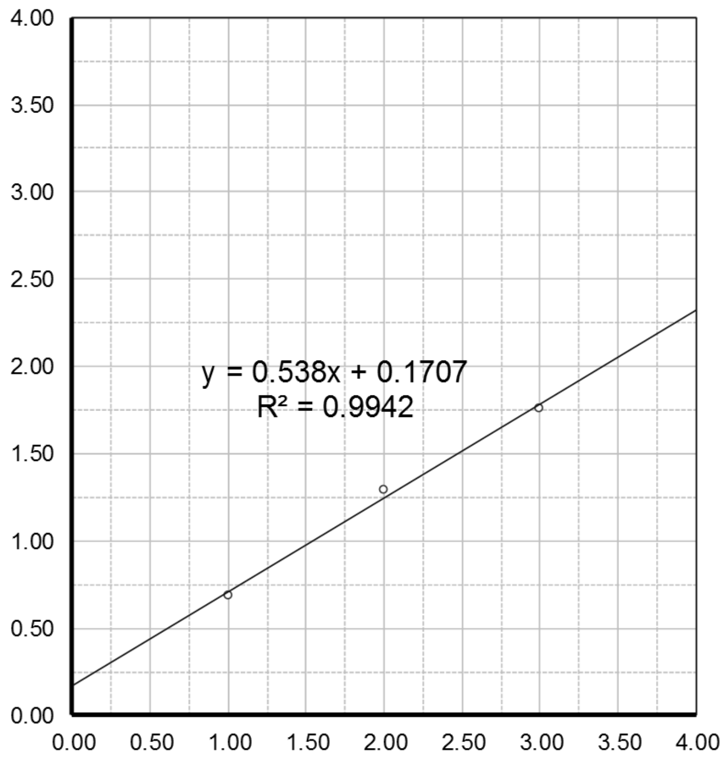

Appendix B-4-7: Average shear strength parameters of residual soil in S1985 (Natural condition)

DIRECT SHEAR TEST

Bore hole	: S1985
Depth(cm)	: 80 cm
Description	: Brown silty-clay
Testing standard	: Vietnamese

TEST RESULT (NATURAL CONDITION)

Coefficient of pressure ring

Cr = 0.0185 kG/cm2.Div.

Vertical pressure	Readed values	Shear stress
σ (KG/cm^2)	Div	kG/cm^2
0.10		
0.25		
0.50		
0.75		
1.00	31.80	0.588
1.50		
2.00	54.10	1.001
3.00	71.40	1.321
4.00		
φ =	20° 8 '	Deg, Min
C =	0.237	kG/cm^2

MOHR'S FAILURE ENVELOPE

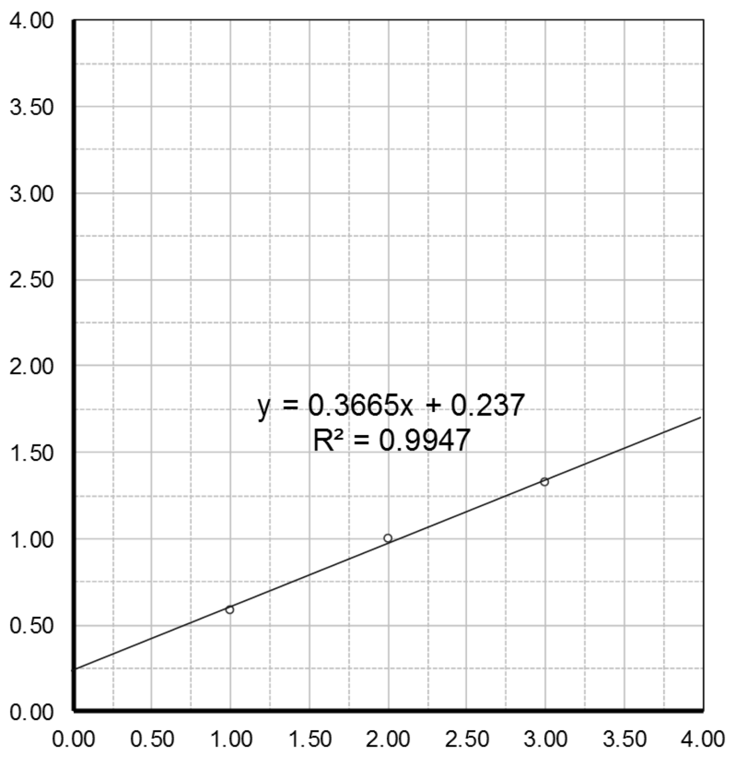

Appendix B-4-8: Average shear strength parameters of residual soil in S1985 (Saturated condition)

DIRECT SHEAR TEST

Bore hole	: S1985
Depth(cm)	: 80 cm
Description	: Brown silty-clay
Testing standards	: Vietnamese

TEST RESULT (SATURATED CONDITION)

Coefficient of pressure ring

Cr = 0.0185 kG/cm2.Div.

Vertical pressure	Readed values	Shear stress
σ (KG/cm²)	Div	kG/cm²
0.10		
0.25		
0.50		
0.75		
1.00	27.50	0.509
1.50		
2.00	48.20	0.892
3.00	63.70	1.178
4.00		
φ =	18° 30 '	Deg, Min
C =	0.191	kG/cm²

MOHR'S FAILURE ENVELOPE

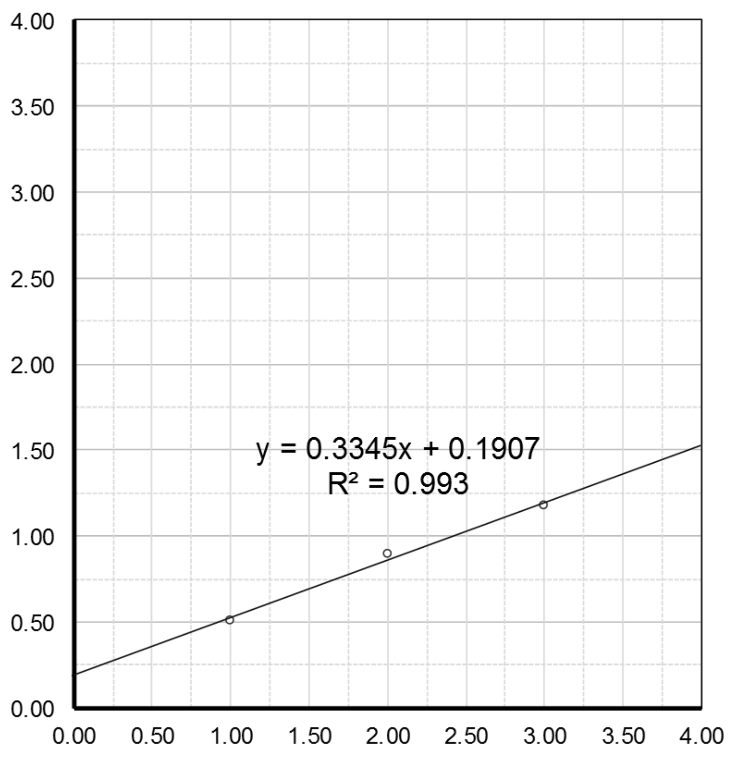

Appendix B-4-9: Average shear strength parameters of completely weathered soil layer in S1985 (Natural condition)

DIRECT SHEAR TEST

Bore hole	: S1985
Depth(cm)	: 180 cm
Description	: Browndish to reddish silty clay mixed with small amount of gravel
Testing standards	: Vietnamese

TEST RESULT (NATURAL CONDITION)

Coefficient of pressure ring

Cr = 0.0185 kG/cm2.Div.

Vertical pressure	Readed values	Shear stress
σ (KG/cm^2)	Div	kG/cm^2
0.10		
0.25		
0.50		
0.75		
1.00	34.90	0.646
1.50		
2.00	60.87	1.126
3.00	83.14	1.538
4.00		
φ =	24° 2'	Deg, Min
C =	0.219	kG/cm^2

MOHR'S FAILURE ENVELOPE

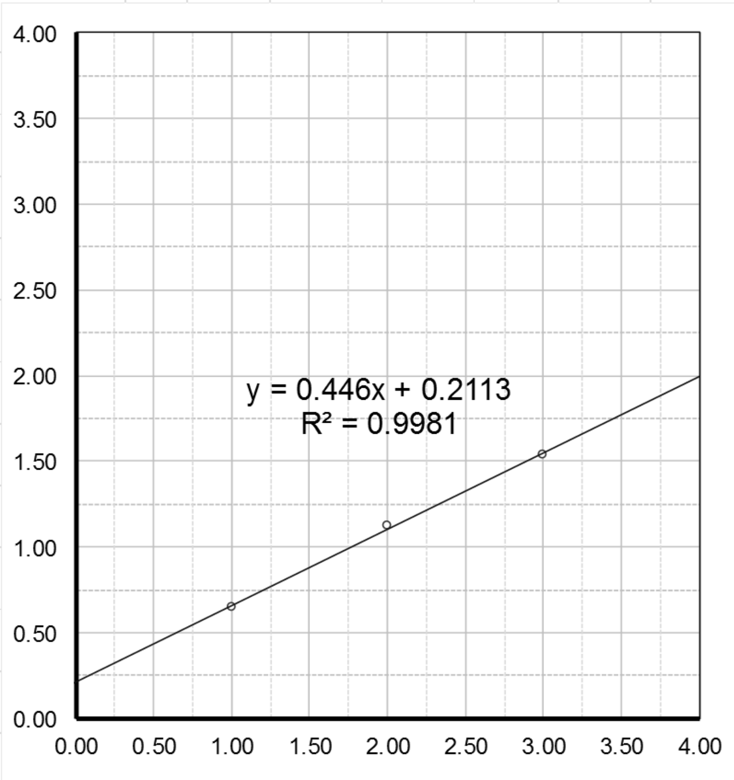

Appendix B-4-10: Average shear strength parameters of completely weathered soil layer in S1985 (Saturated condition)

DIRECT SHEAR TEST

Bore hole	: S1985
Depth(cm)	: 180 cm
Description	: Browndish to reddish silty clay mixed with small amount of gravel:
Testing standar	: Vietnamese

TEST RESULT (SATURATED CONDITION)

Coefficient of pressure ring

Cr = 0.0185 kG/cm2.Div.

Vertical pressure	Readed values	Shear stress
σ (KG/cm²)	Div	kG/cm²
0.10		
0.25		
0.50		
0.75		
1.00	31.30	0.579
1.50		
2.00	55.80	1.032
3.00	76.00	1.406
4.00		

φ =	22° 28 '	Deg, Min
C =	0.179	kG/cm²

MOHR'S FAILURE ENVELOPE

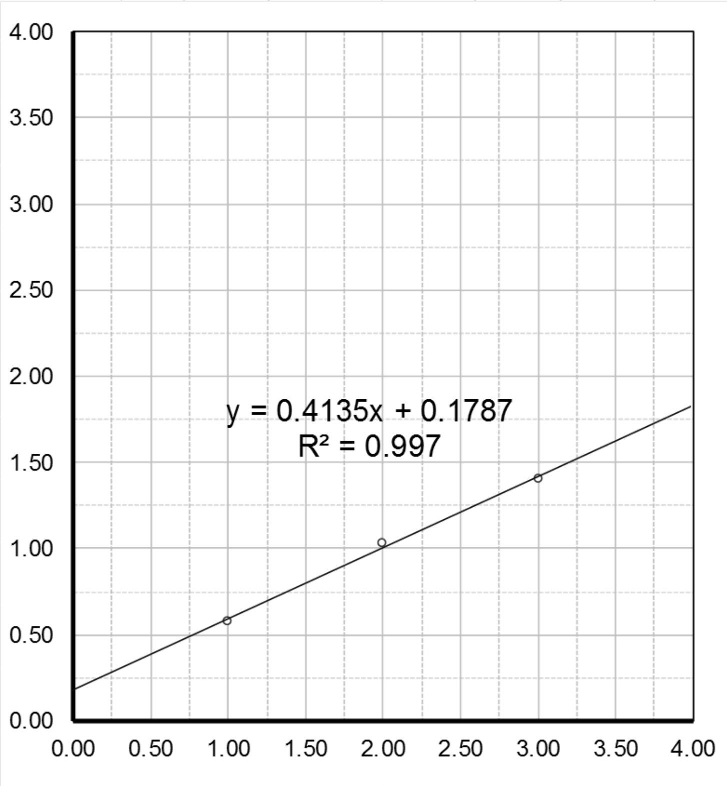

Appendix B-4-11: Average shear strength parameters of residual soil in S1979 (Natural condition)

DIRECT SHEAR TEST

Bore hole	: S1979
Depth (cm)	: 80 cm
Description	: Brown silty-clay
Testing standard	: Vietnamese

TEST RESULT (NATURAL CONDITION)

Coefficient of pressure ring

Cr = 0.0185 kG/cm2.Div.

Vertical pressure	Readed values	Shear stress
σ (KG/cm^2)	Div	kG/cm^2
0.10		
0.25		
0.50		
0.75		
1.00	30.70	0.568
1.50		
2.00	50.30	0.931
3.00	65.90	1.219
4.00		
φ =	18° 2'	Deg, Min
C =	0.255	kG/cm^2

MOHR'S FAILURE ENVELOPE

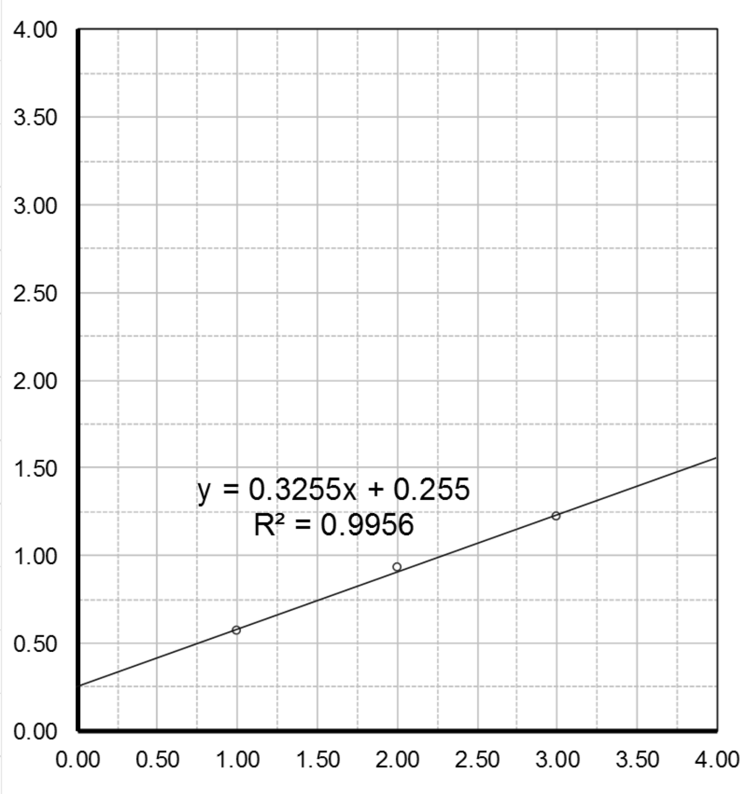

Appendix B-4-12: Average shear strength parameters of residual soil in S1979 (Saturated condition)

DIRECT SHEAR TEST

Bore hole	:	S1979
Depth(cm)	:	80 cm
Description	:	Dark brown silty clay
Testing standar	:	Vietnamese

TEST RESULT (SATURATED CONDITION)

Coefficient of pressure ring

Cr = 0.0185 kG/cm2.Div.

Vertical pressure	Readed values	Shear stress
σ (KG/cm^2)	Div	kG/cm^2
0.10		
0.25		
0.50		
0.75		
1.00	27.30	0.505
1.50		
2.00	46.70	0.864
3.00	60.50	1.119
4.00		

φ =	17° 4 '	Deg, Min
C =	0.215	kG/cm^2

MOHR'S FAILURE ENVELOPE

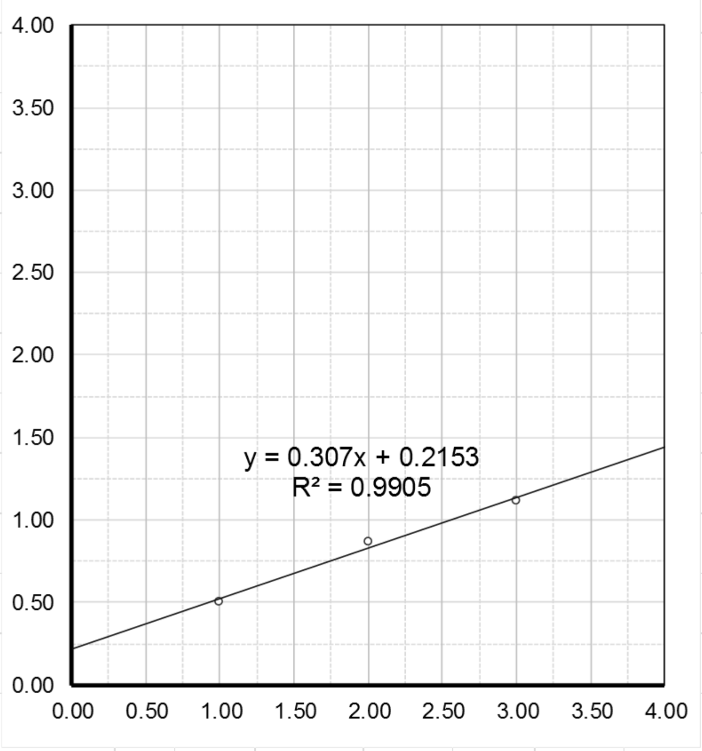

Appendix B-4-13: Average shear strength parameters of completely weathered soil layer in S1979 (Natural condition)

DIRECT SHEAR TEST

Bore hole	: S1979
Depth(cm)	: 180 cm
Description	: Browndish to reddish silty clay mixed with small amount of gravels
Testing standards	: Vietnamese

TEST RESULT (NATURAL CONDITION)

Coefficient of pressure ring

Cr = 0.0185 kG/cm2.Div.

Vertical pressure	Readed values	Shear stress
σ (KG/cm^2)	Div	kG/cm^2
0.10		
0.25		
0.50		
0.75		
1.00	33.70	0.623
1.50		
2.00	56.85	1.052
3.00	77.58	1.435
4.00		

φ =	22 ° 6 '	Deg, Min
C =	0.225	kG/cm^2

MOHR'S FAILURE ENVELOPE

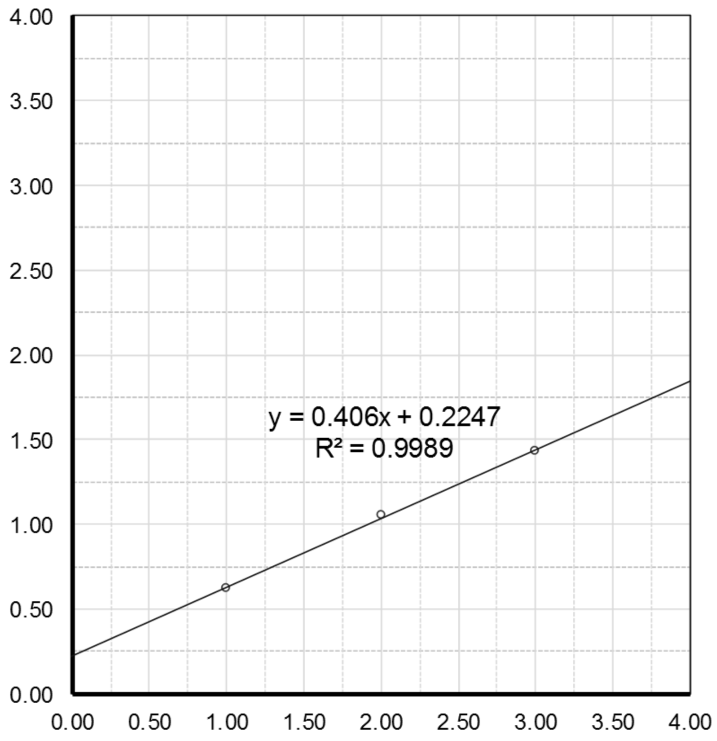

Appendix B-4-14: Average shear strength parameters of completely weathered soil layer in S1979 (Saturated condition)

DIRECT SHEAR TEST

Bore hole	: S1979
Depth(cm)	: 180 cm
Description	: Browndish to reddish silty clay mixed with small amount of gravels
Testing standards	: Vietnamese

TEST RESULT (SATURATED CONDITION)

Coefficient of pressure ring

Cr = 0.0185 kG/cm2.Div.

Vertical pressure σ (kG/cm^2)	Readed values Div	Shear stress (kG/cm^2)
0.10		
0.25		
0.50		
0.75		
1.00	29.50	0.546
1.50		
2.00	51.30	0.949
3.00	69.85	1.292
4.00		
φ =	20° 27'	Deg, Min
C =	0.184	kG/cm^2

MOHR'S FAILURE ENVELOPE

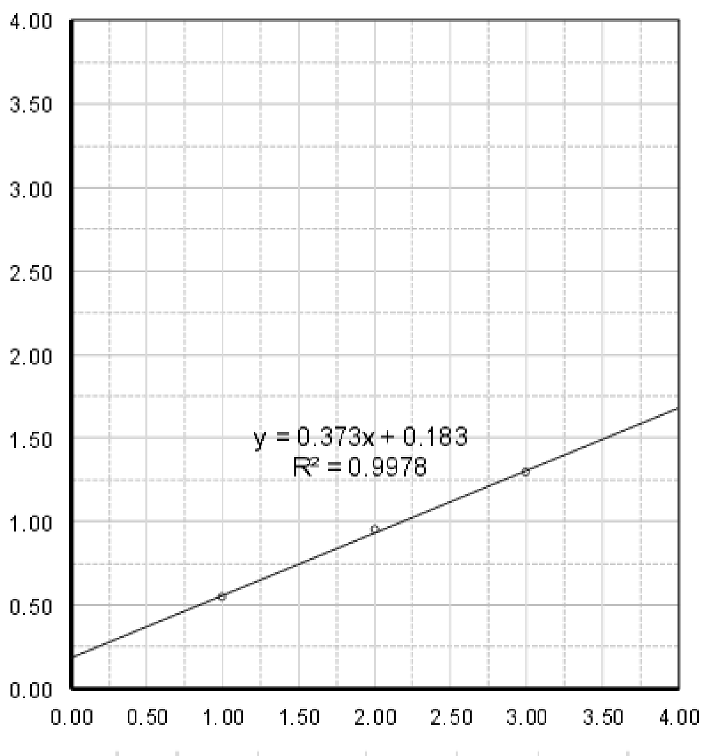

APPENDIX C

TABLE OF AVERAGE ENGINEERING CHARACTERS OF SOIL LAYERS IN THE STUDY AREA ACHIEVED BY LABORATORY TESTS

Testing categories	Symbol	Unit	Slope's Symbol					
			S1979		S1985		S2008	
			Depth		Depth		Depth	
			80 cm	180 cm	80 cm	180 cm	80 cm	180 cm
Natural moisture content	W	%	35.70	34.26	35.3	33.97	32.98	33.10
Unit weight	γ_w	T/m³	1.695	1.697	1.687	1.700	1.662	1.710
Dry unit weight	γ_d	T/m³	1.249	1.264	1.247	1.269	1.250	1.285
Specific gravity	Gs		2.730	2.725	2.720	2.709	2.718	2.705
Void ratio	e		1.186	1.156	1.181	1.135	1.175	1.105
Porosity	n	%	54.25	53.62	54.16	53.16	54.02	52.50
Degree of saturation	S	%	82.20	80.77	81.27	81.09	76.31	80.99
Liquid limit	LL	%	69.83	64.11	71.31	60.73	66.38	52.14
Plastic limit	PL	%	40.13	36.9	40.56	33.03	37.6	28.1
Plasticity index	PI	%	29.7	27.21	30.75	27.7	28.78	24.04
Saturated unit weight	Ws	T/m³	1.758	1.766	1.754	1.766	1.756	1.775
Direct shear test (Unsaturated condition)	φ	Deg	18.68	20.55	19.55	23.6	20.3	30.12
	C_w	kG/cm²	22.00	22.500	21.6	21.9	21.500	21.200
Direct shear test (Saturated condition)	φ	Deg	17.58	19.85	18.68	22.38	19.8	28.72
	Cs	kG/cm²	18.5	18.4	0.18	0.18	18	17.2
Permeability (average)	K	Cm/s	8.68E-6	1.20E-5	8.97E-6	1.59E-5	9.59E-6	3.00E-5

APPENDIX D

STEADY STATE SEEPAGE ANALYSIS

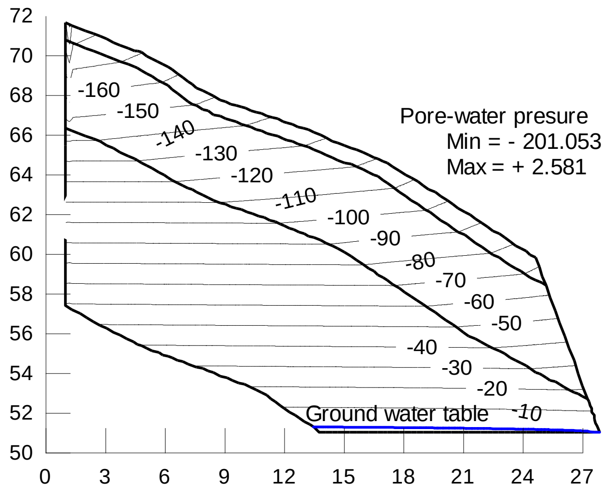

Appendix D-1: Distribution of pore-water pressures in dry seasons of S2008, slope 70^0

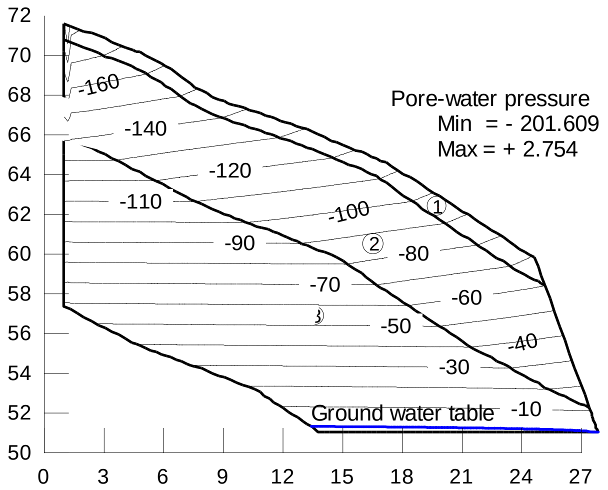

Appendix D-2: Distribution of pore-water pressures in dry seasons of S1985, slope 70^0

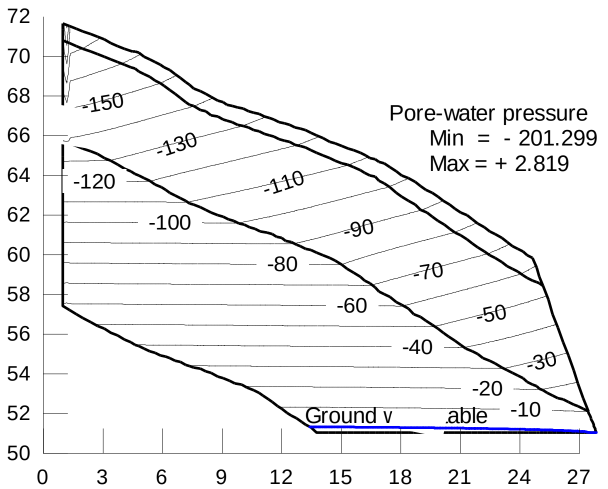

Appendix D-3: Distribution of pore-water pressures in dry seasons of S1979, slope 70^0

APPENDIX E

SLOPE STABILITY RESULT

Appendix E-1: Results of stability analysis in rainy season

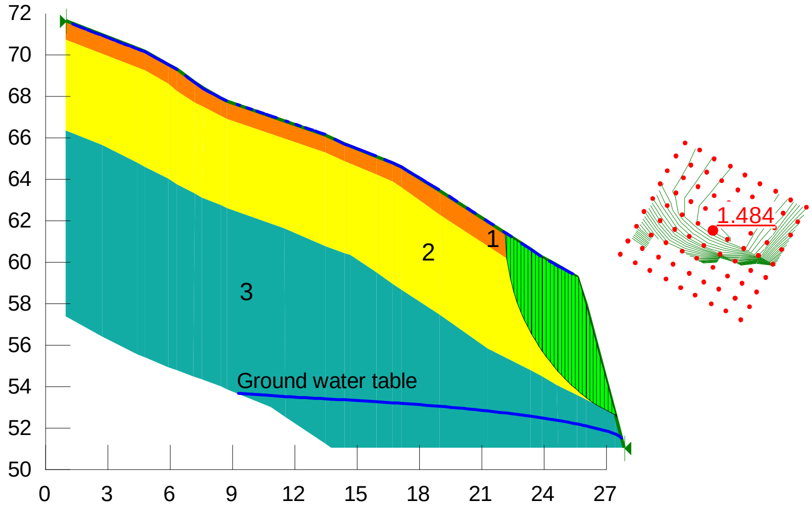

E-1-1: The factor of safety of slope S2008 when the cut is 75⁰

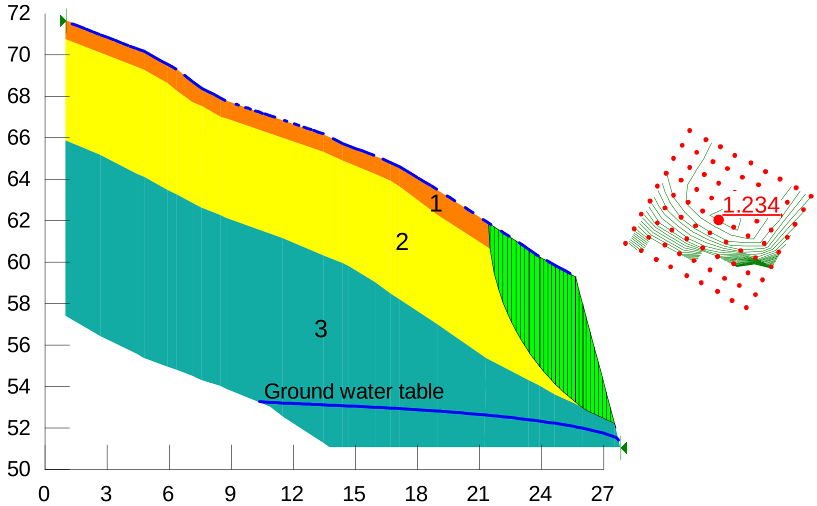

E-1-2: The factor of safety of slope S1985 when the cut is 75⁰

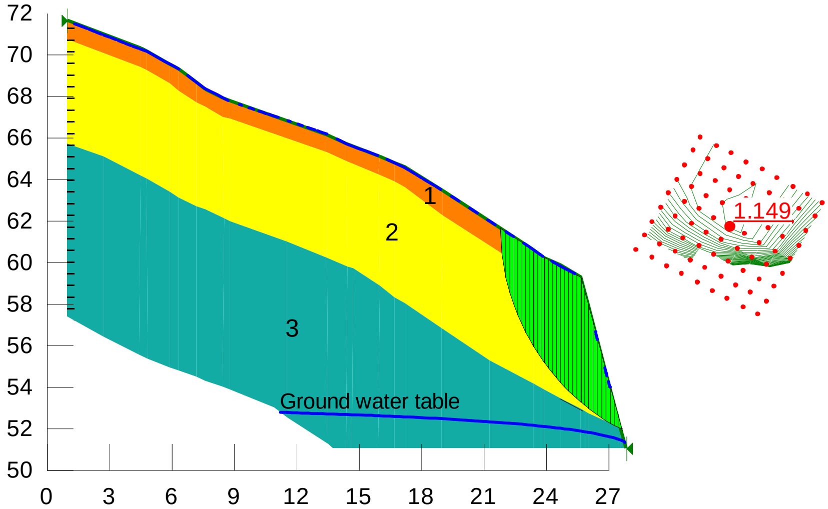

E-1-3: The factor of safety of slope S1979 when the cut is 75⁰

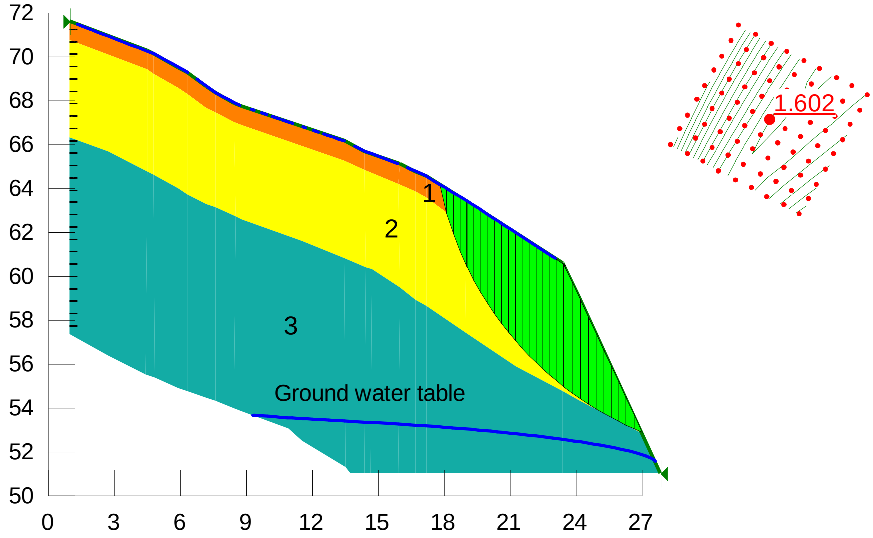

E-1-4: The factor of safety of slope S2008 when the cut is 65^0

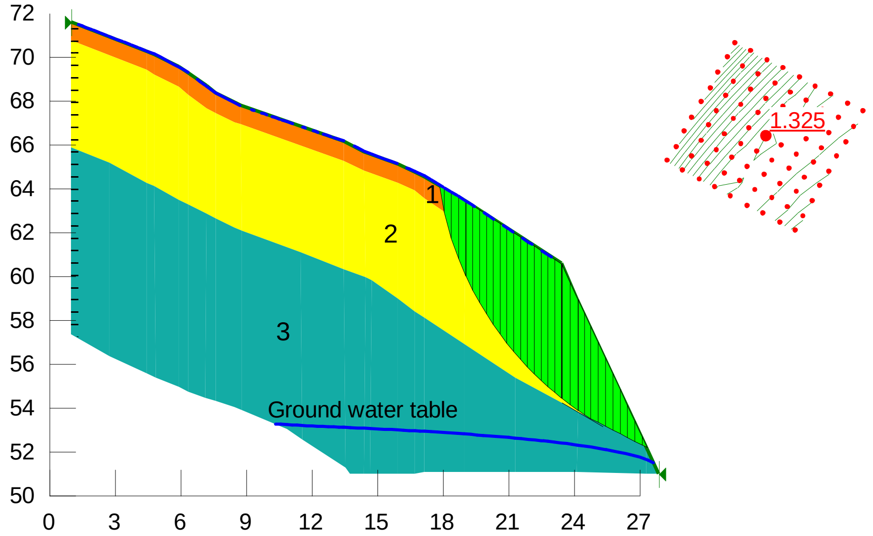

E-1-5: The factor of safety of slope S1985 when the cut is 65^0

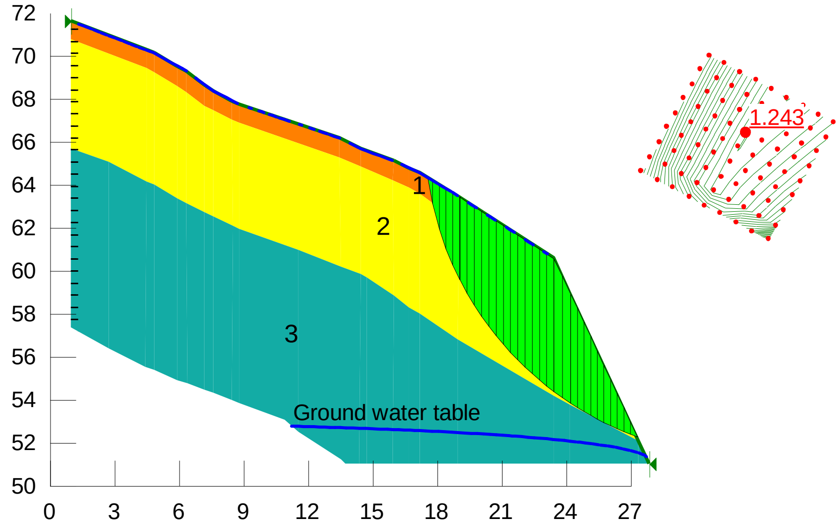

E-1-6: The factor of safety of slope S1979 when the cut is 65^0

Appendix E-2: Results of stability analysis in rainstorm event 2006

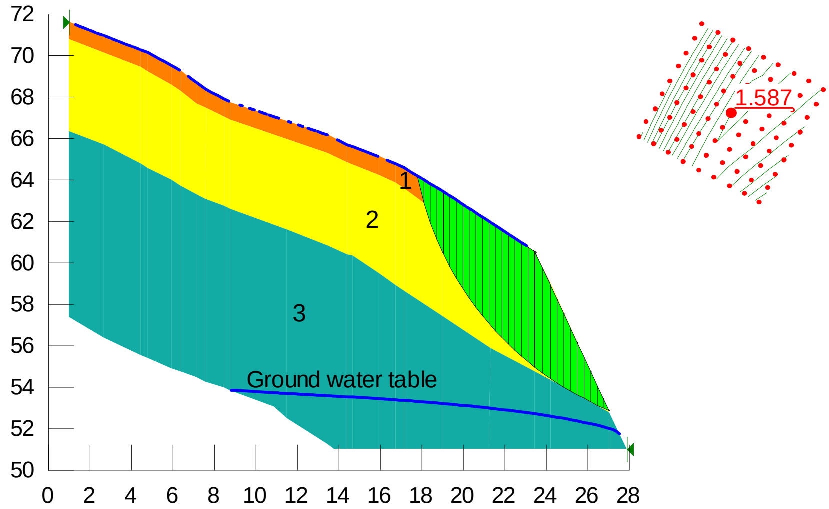

E-2-1: The factor of safety of slope S2008 in rainstorm event 2006 when the cut is 65^0

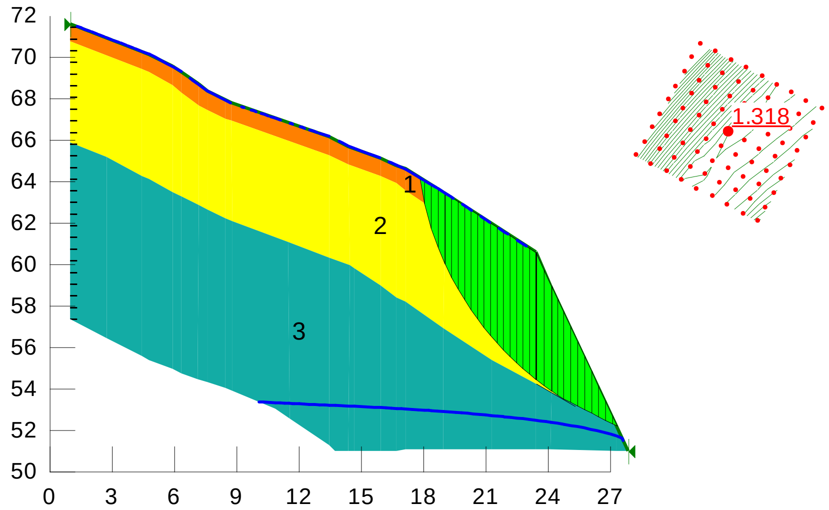

E-2-2: The factor of safety of slope S1985 in rainstorm event 2006 when the cut is 65^0

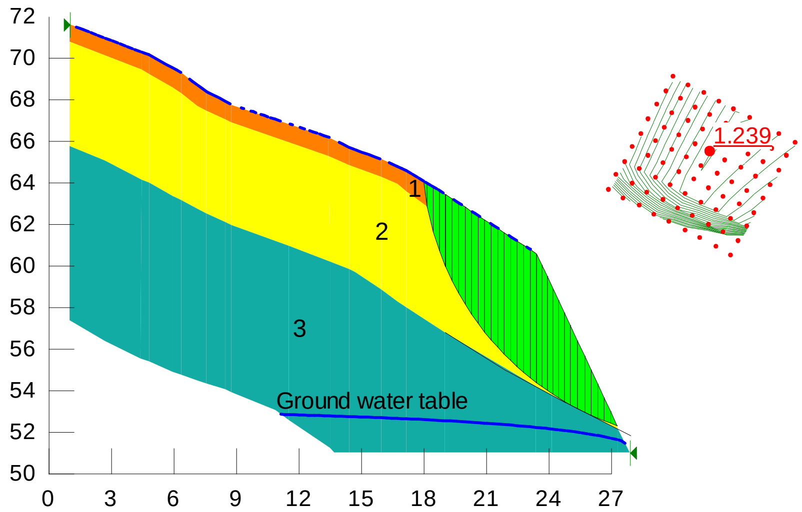

E-2-3: The factor of safety of slope S1979 in rainstorm event 2006 when the cut is 65^0

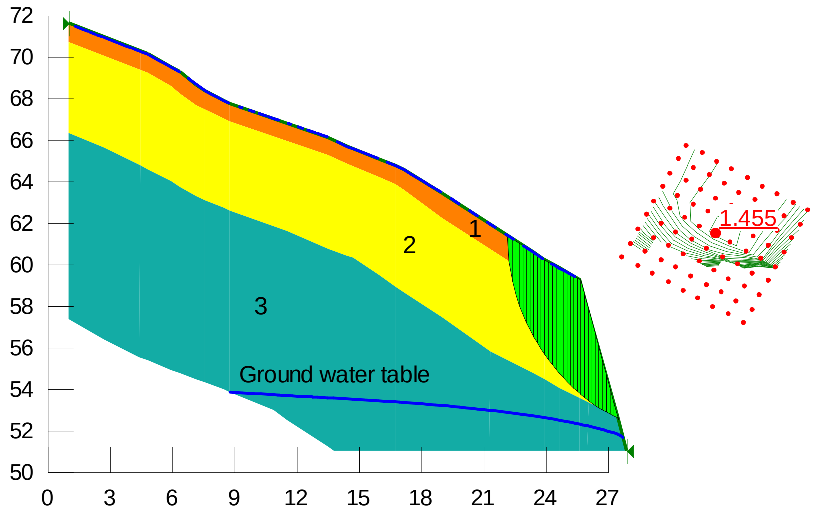

E-2-4: The factor of safety of slope S2008 in rainstorm event 2006 when the cut is 75^0

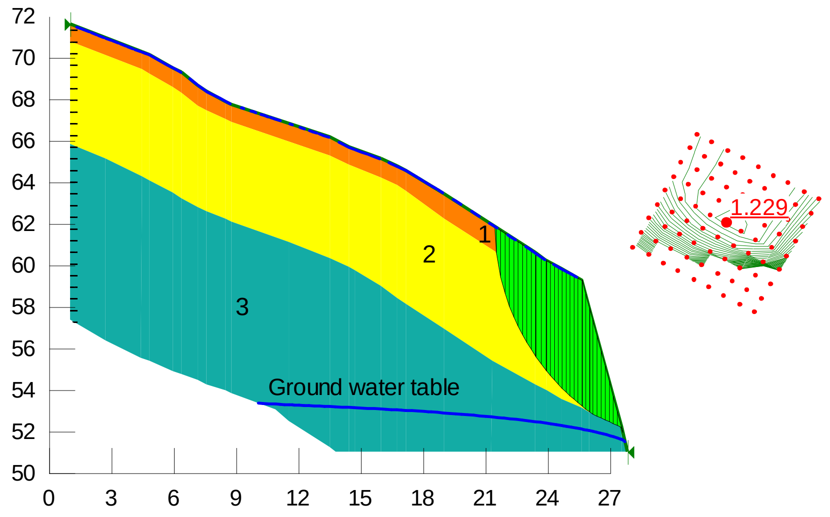

E-2-5: The factor of safety of slope S1985 in rainstorm event 2006 when the cut is 75^0

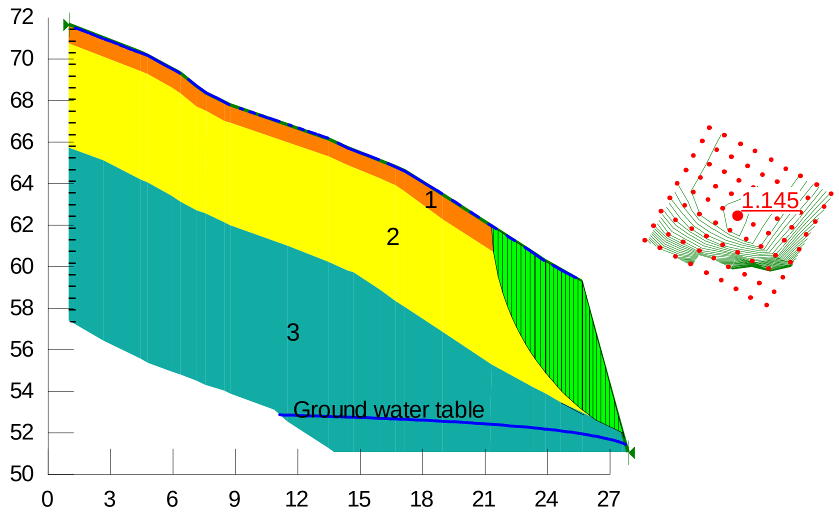

E-2-6: The factor of safety of slope S1979 in rainstorm event 2006 when the cut is 75^0

Appendix E-3: Results of stability analysis in rainstorm event 2008

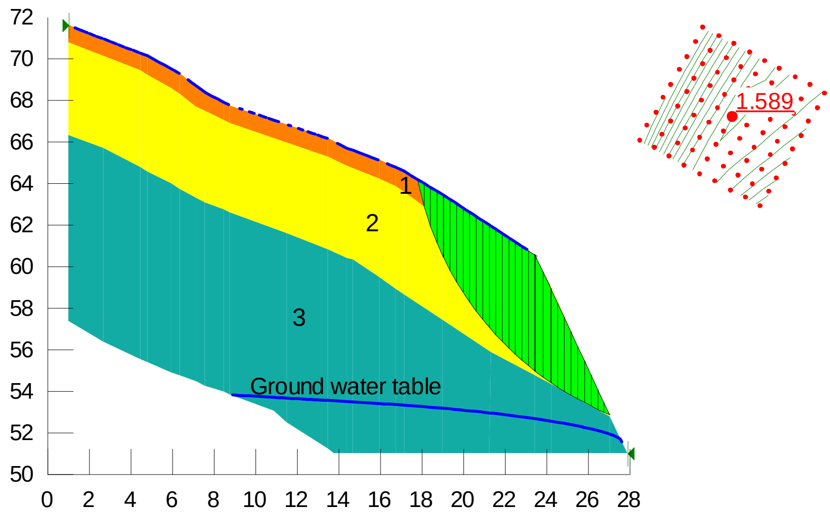

E-3-1: The factor of safety of slope S2008 in rainstorm event 2008 when the cut is 65^0

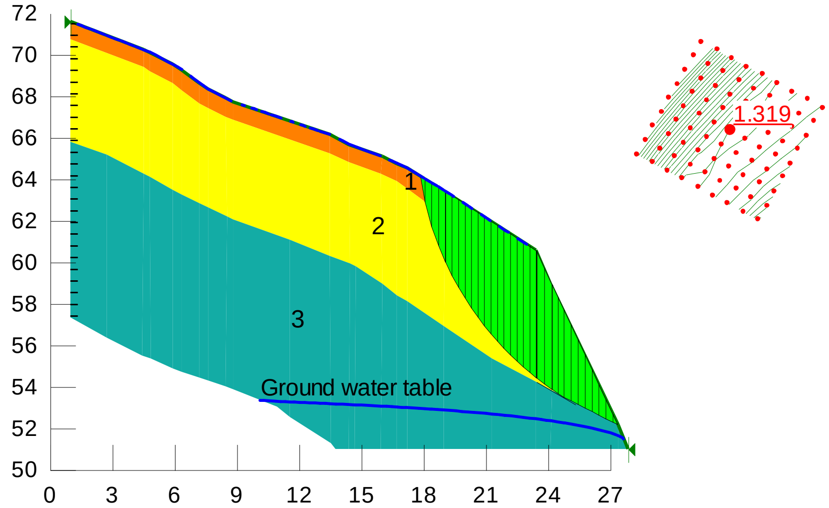

E-3-2: The factor of safety of slope S1985 in rainstorm event 2008 when the cut is 65^0

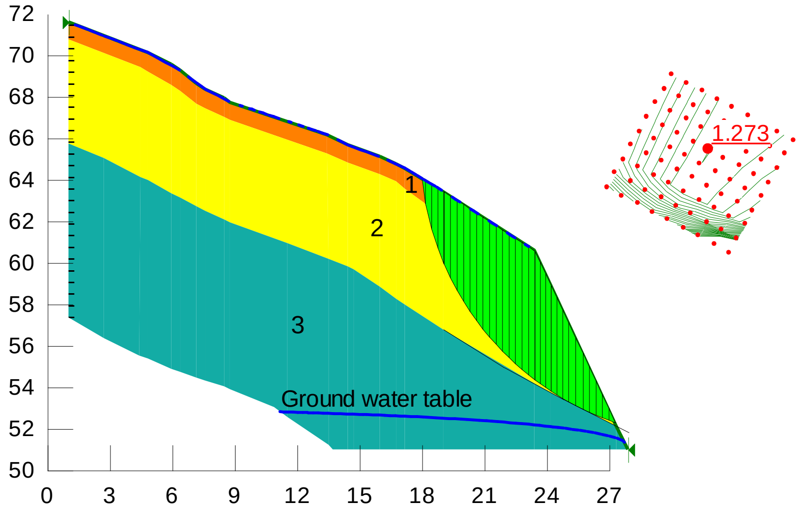

E-3-2: The factor of safety of slope S1979 in rainstorm event 2008 when the cut is 65^0

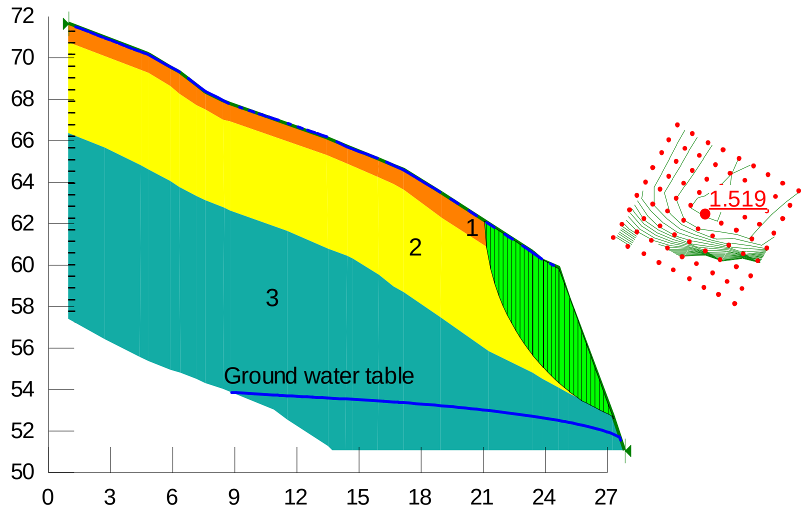

E-3-4: The factor of safety of slope S2008 in rainstorm event 2008 when the cut is 70^0

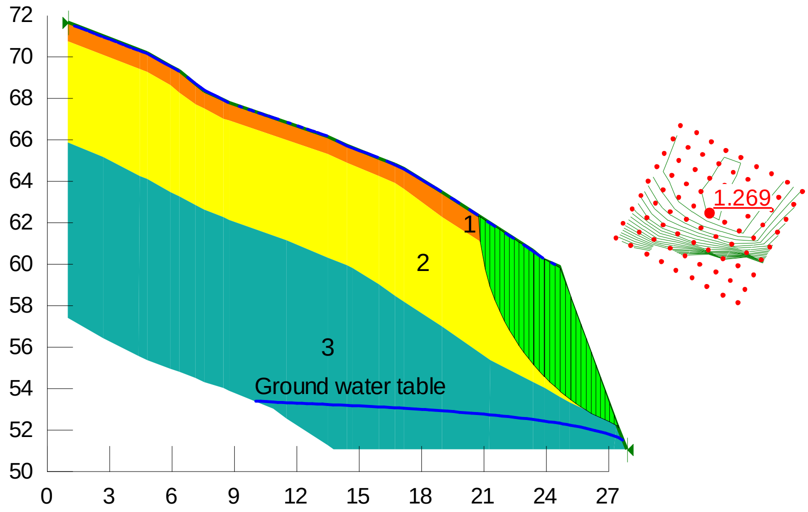

E-3-5: The factor of safety of slope S1985 in rainstorm event 2008 when the cut is 70^0

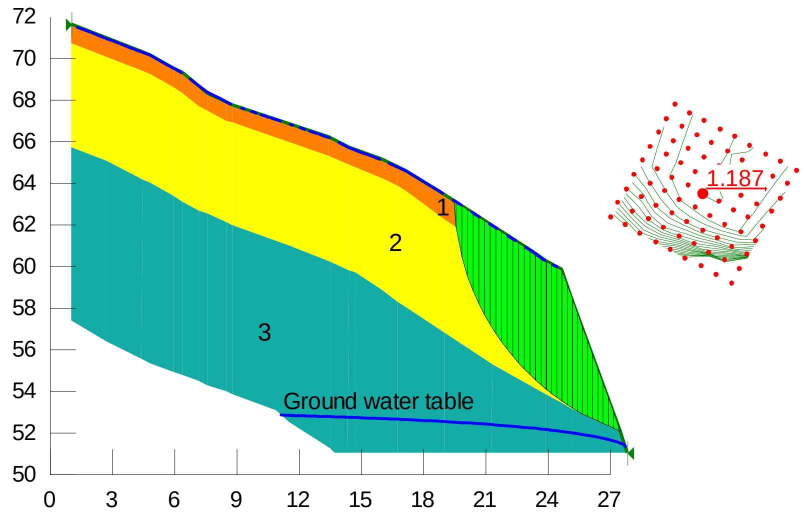

E-3-6: The factor of safety of slope S1979 in rainstorm event 2008 when the cut is 70^0

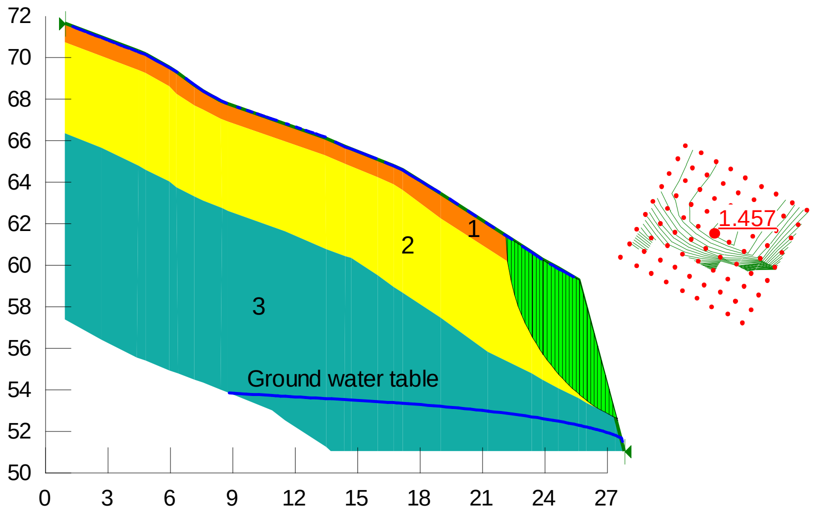

E-3-7: The factor of safety of slope S2008 in rainstorm event 2008 when the cut is 75⁰

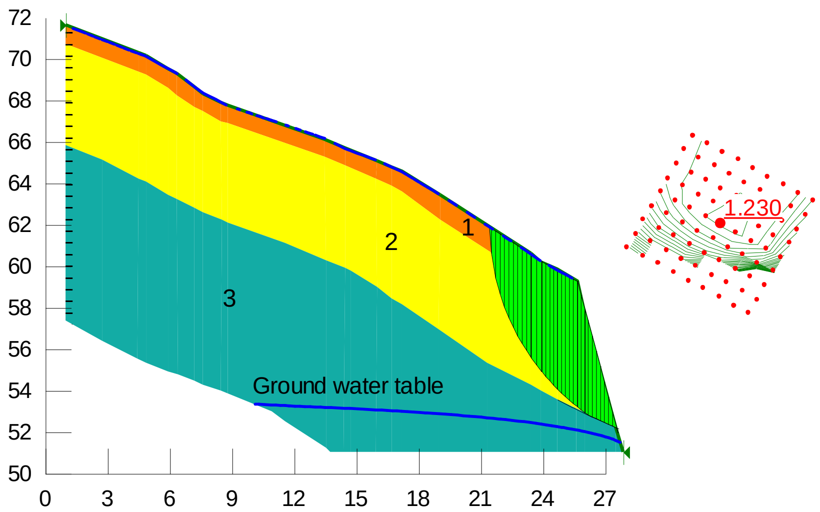

E-3-8: The factor of safety of slope S1985 in rainstorm event 2008 when the cut is 75⁰

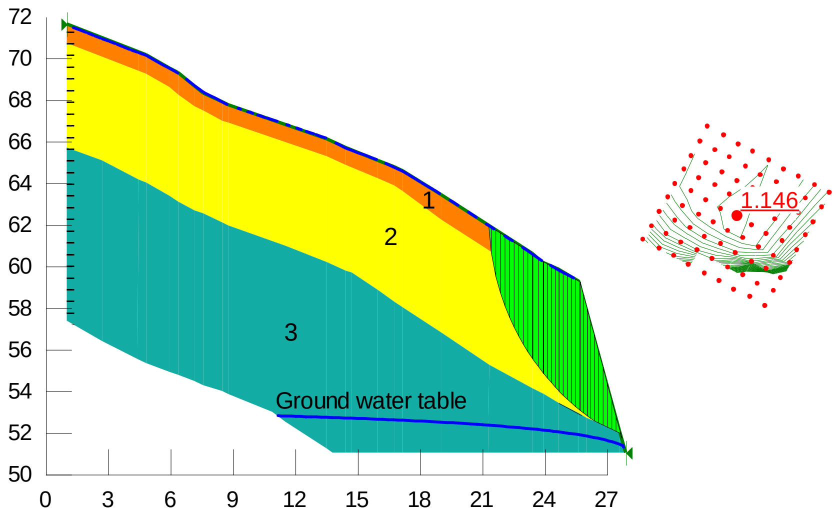

E-3-9: The factor of safety of slope S1979 in rainstorm event 2008 when the cut is 75⁰